SPECTROSCOPIC AND THERMODYNAMIC PROPERTIES OF SOME OXY-SULPHUR SPECIES

A thesis submitted by MUBARAK ELSAYED OSMAN

in candidature for the degree of

Doctor of Philosophy of the University of London

The Bourne Laboratory,
(Department of Chemistry)
Royal Holloway and Bedford New College
University of London
Egham Hill
Egham, Surrey, TW20 0EX

May 1987

Abstract

Raman and infrared activities of aqueous sulphur dioxide solution and of the sodium salts of dithionate, disulphite, sulphite, sulphate, bisulphate, thiosulphate, tetrathionate and dithionite ions have been investigated in the crystal and aqueous states. On the basis of the data obtained, the following conclusions have been derived:

(i) a gauche configuration with D_3 group symmetry satisfactorily describes the vibrational activities of the dithionate ion both in the solid and in the aqueous states (p. 47, 48).

(ii) some evidence for the existence of crystalline sodium bisulphite has been revealed (p.55). In addition to the well-known $H\text{-}SO_3^-$ form of bisulphite, the $HO\text{-}SO_2^-$ tautomer has been identified in a very significant amount in aqueous disulphite solution (p.49-56). Employing progressive dilution measurements, characteristic bands of the $S_2O_5^{2-}$, $H\text{-}SO_3^-$ and $HO\text{-}SO_2^-$ ions and of the constituent thionate and thionite units of disulphite have been assigned (p.49-55). The non-existence of the oxygen bridged disulphite ion and of the lithium, sodium and potassium salts of bisulphite have been rationalised (p.55,56). Eight bands have been identified with the $HO\text{-}SO_2^-$ isomer of bisulphite, and on the basis of C_s group symmetry they have been assigned (p.49-55).

(iii) the infrared activity of the sulphate ion has revealed that even in the free state the ion does not assume full tetrahedral symmetry (p.57). Some fundamental vibrations

of the bisulphate ion in the high frequency region have been re-assigned (p.57).

(iv) the vibrational activities of the tetrathionate ion have been analysed in terms of two thiosulphate groups held together by an S-S bond. Its fundamental modes have been assigned on the basis of C_2 group symmetry (p.70-72).

(v) the vibrational spectra of the dithionite ion in aqueous solutions strongly suggests C_2-gauche symmetry. No evidence for adoption of the trans C_{2h} or the planar D_{2h} structure has been found (p.72-75).

(vi) thiosulphate has been identified among the disproportionation products of the dithionite ion. Its formation has been confirmed by ultraviolet spectroscopy. An auto-oxidation process involving free radicals and proceeding at a low rate has been suggested to account for its formation (p.75-82).

(vii) sulphurous acid, H_2SO_3, has been detected in a significant amount in standing aqueous sulphur dioxide solutions. Both of the tautomeric forms, HO-SO-OH and H-SO_2-OH, have been identified, and in addition to the bisulphite isomers, the formations of the sulphite, sulphate, bisulphate and of the dithionate ions have been indicated in such standing systems. C_s group symmetry has been assigned to both of the sulphurous acid isomers (p.58-65).

Photographic fixation reactions have been calorimetrically investigated, and on the basis of the data derived the following points have been elucidated:

(i) fixation is an irreversible, penta-stage process which involves the following set of sequential equations (p.106-114):

$$Ag^+ + 2S_2O_3^{2-} = [Ag(S_2O_3)_2]^{-3}$$

$$Ag^+ + S_2O_3^{2-} + [Ag(S_2O_3)_2]^{-3} = [Ag_2(S_2O_3)_3]^{-4}$$

$$Ag^+ + [Ag_2(S_2O_3)_3]^{-4} = 3AgS_2O_3^-$$

$$Ag^+ + AgS_2O_3^- = Ag_2S_2O_3(aq)$$

$$Ag_2S_2O_3(aq) + H_2O = Ag_2S(c) + SO_4^{2-} + 2H^+$$

(ii) the overall reaction, ($S_2O_3^{2-} + 2Ag^+ + H_2O = Ag_2S(c) + SO_4^{2-} + 2H^+$), has been quantitatively analysed and subsequently used to re-evaluate the standard molar enthalpies of formation of $S_2O_3^{2-}(aq)$, $Na_2S_2O_3(aq)$, $Na_2S_2O_3(c)$ and $Na_2S_2O_3 \cdot 5H_2O(c)$ as -647.70 ± 0.60, -1128.30 ± 0.59, -1120.77 ± 1.21 and -1174.97 ± 0.61 kJ mol^{-1} respectively. That of $Na_2S_2O_3 \cdot 2H_2O(c)$ has been tentatively calculated to be -268.68 ± 0.86 kJ mol^{-1} (p.114-122).

(iii) using the above value for $\Delta_f H_m^\circ Na_2S_2O_3(aq)$, the standard molar enthalpies of formation of $Na_3Ag(S_2O_3)_2(aq)$, $Na_4Ag_2(S_2O_3)_3(aq)$ and $NaAgS_2O_3(aq)$ have been evaluated to

be -1989.66 ± 0.72, -2844.00 ± 3.86 and -851.79 ± 0.59 kJ mol^{-1} respectively (p.122-128).

(iv) based upon the athermal property of the reaction: $Ag_2S_2O_3(aq) + H_2O = Ag_2S(c) + SO_4^{2-} + 2H^+$, the standard molar enthalpy of formation of $Ag_2S_2O_3(aq)$ has been calculated to be -652.85 ± 0.31 kJ mol^{-1} (p.129).

(v) the structures of the above three silver-thiosulphate complexes have been elucidated on the basis of the spectral measurements performed, and that of $Ag_2S_2O_3$ has been discussed in terms of the constituent Ag_2S and SO_3 units (p.66-70).

The aqueous solubility of sodium dithionate dihydrate crystals has been determined. From the temperature coefficient of solubility, the entropy and the differential heat of solution have been evaluated to be 55.45 J $mol^{-1}T^{-1}$ and 16.48 kJ mol^{-1} respectively (p.147-151).

Table of Contents

Chapter II. Summary of previous work

Chapter III. Results and discussion (spectroscopic)

Chapter IV. Results and discussion (calorimetric)

Chapter V. Results and discussion (solubility)

Chapter VI. Experimental methods

List of Tables

List of Figures

Fig. VI-1: Calorimetric vessels:

A = Ampoule-mode reaction chamber

B = Titration-mode reaction chamber

Fig. VI-2: Thermometric titration of $Ag^+/(Br^- + Cl^-)$

Acknowledgements

I wish to express my thanks to Professor Arthur Finch and Dr. Peter N. Gates for their encouragement and advice during the course of this work. I would like to thank Mrs. Susan Cook for her excellent typing of this thesis.

To My Dear Grandfather

OSMAN

Chapter I

Introduction

I. The sulphur and the sulphoxy anions

I-A. The Sulphur:-

Sulphur in its native form has been known since early times, (16th century B.C.), and originally it was used for medicinal religious purposes and in fumigation of houses [1,2].

The first theoretical studies of sulphur and its compound were originated by the alchemists who postulated that mercury could be fixed with sulphur to form a solid compound. Further revelations were achieved by distilling many of the compounds known at that time, and identification of sulphur in the various species analysed [1]. Besides the use of sulphur in gunpowder (12th century), the most outstanding achievement of the alchemists was the synthesis of sulphuric acid from pyrites as well as from free sulphur [1,2].

It occurs in nature free and combined, and constitutes about 340 ppm, (0.048%), of the outer earth's crust [1,2]. The three most important commercial sources are: (i) elemental sulphur in the caprock salt domes in the U.S.A. and Mexico, and the sedimentary deposits in South-Eastern Poland, (ii) hydrogen sulphide in natural gas and crude oil, and organo-sulphur compounds in tar sands, oil shales and coal, and (iii) pyrites ($Fe\ S_2$) and other metal sulphide minerals[1-3].

During the first half of this century the prime method of production was the process developed by H. Frasch in 1891-94. This involves forcing superheated water and steam (160°C, 16 atm) into submerged sulphur-bearing strata and then forcing the molten element to the surface by compressed air (20-25 atm). Recovery from sour natural gas and from crude oil was first developed in the U.S.A. in 1944, and by 1970 these sources exceeded the total volume of Frasch-processed sulphur. It is rapidly becoming more important in many other countries. Recovery from natural gas involves, first, the isolation of H_2S by absorption in mono-ethanolamine and then its conversion into sulphur by a process first developed by C.F. Claus about 1880. In this process H_2S is reacted with a stoichiometric amount of oxygen in combustion chambers, (Claus vessel), to produce SO_2 and about 70% of sulphur. The SO_2 then reacts with the remaining H_2S in the presence of oxide catalysts such as Fe_2O_3 or Al_2O_3 to produce more sulphur:

$$H_2S + \tfrac{1}{2}O_2 = S + H_2O$$

$$H_2S + 1\tfrac{1}{2}O_2 = SO_2 + H_2O$$

$$2H_2S + SO_2 = 2S + 2H_2O$$

Multiple-chambered reactors have been reported to yield about 99% of sulphur [1,2]. A similar sequence of reactions is used for sulphur production from crude oil, the removal of the organo-sulphur compounds and the subsequent hydrogenation into H_2S being the prior steps. The pyrites and related sulphide minerals are

roasted to release SO_2 gas which is then used directly to prepare sulphuric acid.

Sulphur displays allotropy both in the solid and liquid phases and the sulphur atoms are characterised by a pronounced tendency to form sulphur-sulphur σ-bonds. This ability for catenation is surpassed by carbon only, and has resulted in the formation of many different chain-like elemental sulphur compounds[1,2]. The most important variety of sulphur is the orthorhombic α-form, to which all other modifications eventually revert at ordinary temperatures. It consists of S_8 molecules in the form of staggered eight-membered rings with a mean S-S bond length of 2.037A°, a mean S-S-S angle of 107°48' and a mean dihedral angle of 99°16'. At 96.5°C an enantiotropic transition into β-monoclinic sulphur occurs. Except for the presence of disordered sites the structure of the β-phase was indicated to be similar to that of the α-form[1]. While the α-phase melts if rapidly heated at 112.8°C, the β-form is stable up to its melting point at 119.6°C. The third crystalline modification, γ-monoclinic sulphur, is prepared by slow cooling of a sulphur melt that has been heated above 150°C or by chilling hot sulphur solutions in ethanol, carbon disulphide or hydrocarbons. Like α- and β-sulphur the γ-monoclinic phase comprises cyclic S_8 units, but the packing is more dense. It reverts slowly to the α-phase at room temperature and its melting point was assigned to be 106.8°C.

The use of sulphur in industrial processes is manifold. Most of

it is converted via SO_2/SO_3 into sulphuric acid which accounts, for example, for some 88% of the total sulphur consumed in the U.S.A. Apart from the sulphuric acid production, the consumption of sulphur stems from its use (i) in vulcanising rubber: this process makes rubber stronger and more able to resist wear and tear, as well as making its properties less subject to changes of temperature. When rubber is not vulcanised it is brittle in the cold and sticky in hot weather, (ii) in gunpowder, which is an intimate mixture of sodium nitrate, powdered charcoal and sulphur in the approximate ratios 75:15:10 by weight. The nitrate produces oxygen on heating, which then converts carbon and sulphur to carbon and sulphur dioxides respectively. If the gunpowder is packed into a small container, a large pressure is developed by such gases causing an explosion. About 500 cm^3 of gaseous products are released from each 1 cm^3 of the solid exploded, together with enough heat to expand them eight to ten times, and (iii) in the production of enamels, cement, matches, vermillion and ultramarine. Large quantities of sulphur are required for dyes and carbon disulphide production as well as for fine chemicals, insecticides, fungicides and pharmaceutical products. Carbon disulphide is extensively used as a solvent for the rubber industry and for artificial silk production.

Sulphur is regarded as the typical element of the VIth main group of the periodic table, the members of which are two electrons short of the inert gas configuration[1]. This property, together with some other known characteristics[1] allows the chemical activities

of sulphur to be predicted. The element will try to achieve the electronic structure of the argon atom, and thus the oxidation number -2, by either the gain of or the sharing with two electrons from other species. The very high ionisation potential for the first electron explains why positively charged sulphur ions are not involved, under ordinary conditions, in chemical reactions. Although positive oxidation states are very common in sulphur chemistry, bonding in such oxidation states is primarily covalent. The most important compounds of this type contain oxygen as partner of sulphur. Sulphur is a very reactive element, especially at slightly elevated temperatures where the rupture of the S-S bonds is greatly enhanced. It unites, under such conditions, directly with almost all elements.

I-B. The oxides of sulphur:-

Although a number of oxides are reported to exist, only two species are well defined, stable under the ordinary conditions and of technical importance, namely sulphur di and trioxide[1,2].

I-B-1. Sulphur dioxide, SO_2:-

This very important oxide is technically prepared (i) by combustion of sulphur or hydrogen sulphide, (ii) by roasting sulphide ores; particularly the pyrites (FeS_2), (iii) by reduction of calcium, magnesium and iron sulphates with coal, or via thermal decomposition, and (iv) by the reduction of sulphur trioxide with sulphur. It is

a colourless, toxic gas, easily liquefiable at -10°C. Most of the technically produced SO_2 is used in the manufacture of sulphuric acid. In addition, it is commercially used as a bleach to reduce the colouring matter in substances such as straw and wool. It also finds use as a disinfectant and food preservative. In the liquid form it is used as a refrigerant and as a non-aqueous solvent. By far the most important chemical reaction of sulphur dioxide is its further oxidation to sulphur trioxide according to the equilibrium:

$$SO_2 + \tfrac{1}{2}O_2 = SO_3 \; ; \; \Delta H^\circ = -95.6 \text{ kJ mol}^{-1}$$

The equilibrium constant, Kp, defined by:

$$Kp = \frac{P(SO_3)}{P(SO_2) \times p^{\frac{1}{2}}(O_2)}$$

decreases markedly with increasing temperature. For maximum oxidation it is thus necessary to work at low temperatures and to increase the rate of the reaction by the use of catalysts. Typical conditions are to pass a mixture of SO_2 and air over Pt gauze, or more commonly a V_2O_5/K_2O contact catalyst supported on Kieselguhr or zeolite.

Sulphur dioxide is the most important pollutant of the air in the heavily industrialised areas. Mammalian poisoning occurs mainly in the upper respiratory tract by swelling of the irritated mucous membranes and subsequent spasm of the bronchial muscles[1]. It has been suggested that the SO_2 concentration should not exceed 5 ppm in work areas[1]. In the case of plants, however, concentration

of 1-2 ppm causes acute damage within a few hours, presumably by inhibiting the process of photosynthesis.[1] Thus the steadily increasing of air pollution by sulphur dioxide threatens both man and vegetation.

I-B-2. Sulphur trioxide, SO_3:-

Sulphur trioxide is prepared technically on a huge scale by the catalytic oxidation of sulphur dioxide, and is immediately converted into sulphuric acid. It is commercially available as liquid or fuming sulphuric acid, (oleum), which is a solution of 25-65% SO_3 in H_2SO_4. In the former phase small amounts of additives such as B_2O_3, $B(OH)_3$, HBO_2 and BX_3 are added to inhibit polymerisation. It is stable in the gaseous, liquid and solid states. In the gaseous phase it is mainly monomeric and the molecules are planar with D_{3h} symmetry [1,2]. Solid sulphur trioxide exists in three modifications: (i) γ-SO_3 or ice-like SO_3. On cooling, pure liquid SO_3 solidifies at 16.86°C to this modification. The orthorhombic crystals consist of the cyclic S_3O_9 units, (ii) β-SO_3 consists of polymeric polysulphuric acids and forms glistening needle-like crystals. Polymerisation to the β-form is catalysed by traces of water and probably proceeds via an ionic mechanism, and (iii) α-SO_3 which is the most stable form under ordinary conditions. It also requires traces of moisture or other polymerising agent for its formation, and involves partial cross-linking between the chains to give a complex layer structure[1,2]. Like SO_2, gaseous SO_3 irritates the respiratory tract and mucous

membranes causing strong coughing. It dissolves spontaneously in water to yield the most important compound of sulphur, and at the same time the most important mineral acid of all, sulphuric acid. Anhydrous sulphuric acid is a colourless oily liquid, highly associated because of very strong intermolecular hydrogen-bonding. It enters into the manufacture of fertilisers such as ammonium sulphate, rayon, explosives, dyestuffs, pigments, and is also used in pickling metals and petroleum refining[1,2].

I-C. The sulphoxy anions:-

In addition to sulphuric acid, sulphur forms a number of oxoacids, though few of these can be obtained in the free state. Most are known either as aqueous solutions or as crystalline salts of the corresponding anions[1,2]. Other species such as thiosulphates, disulphites and dithionites are valuable reducing agents with a wide variety of applications.

I-C-1. The dithionate ion, $S_2O_6^{2-}$:-

In dithionic acid and the dithionates the oxidation states of the two sulphur atoms have been reduced to +5 by the formation of an S-S bond. Although the free acid is unknown in the pure state, its normal salts are well characterised. They are commonly prepared by oxidation of the corresponding metal sulphite. On a technical scale they are produced by oxidation of SO_2 by a suspension of manganese dioxide[4]:

$$MnO_2 + 2SO_2 = MnS_2O_6$$

All dithionates are readily soluble in water and can be made by standard metathesis reactions.

I-C-2. The Sulphite and the di and bisulphite ions:-

Although sulphur dioxide gas dissolves readily in water, the derivative known as sulphurous acid, H_2SO_3, has not yet been identified. However, in alkaline solutions, and depending upon the SO_2 to OH^- molar ratio, two species are known to form:

$$SO_2 + OH^- = HSO_3^-$$

$$SO_2 + 2OH^- = SO_3^{2-} + H_2O$$

Like sulphurous acid, disulphurous acid, $H_2S_2O_5$, is unknown either in the free state or in solution. However, its salts, the disulphites, are readily obtained from concentrated solutions of hydrogen sulphite:

$$2HSO_3^- = S_2O_5^{2-} + H_2O$$

They are mainly used in the paper pulp industry.

I-C-3. The thiosulphate ion, $S_2O_3^{2-}$:-

In the anhydrous state, the acid has been prepared as a dietherate by reacting sodium thiosulphate with hydrogen chloride in diethyl ether at -78° C[1,2]:

$$Na_2S_2O_3 + 2HCl + Et_2O \quad = \quad H_2S_2O_3 \cdot Et_2O + 2NaCl$$

By thiolysis of chlorosulphonic acid, anhydrous thiosulphuric acid free of any solvent at all has been synthesised[1]:

$$HO_3S\text{-}Cl + H\text{-}SH \quad = \quad HO_3SSH + HCl$$

Thiosulphate salts are best prepared by the action of sulphites on elemental sulphur according to the stoichiometry:

$$SO_3^{2-} + S \quad = \quad S_2O_3^{2-}$$

They are mainly used as 'fixing' agents in photography to eliminate the inactivated silver halides from photographic emulsions via complexation. The oxidation of thiosulphate by iodine is one of the best known reactions of thiosulphate. It is the basis of all the very many iodometric titrations in volumetric analysis:

$$S_2O_3^{2-} + I_2 \quad = \quad S_4O_6^{2-} + 2I^-$$

Strong oxidising agents take the reaction through to sulphate. A typical example for such a reaction is the oxidation of thiosulphate by chlorine, of technical importance in the use of thiosulphate as an antichlorine agent in the bleaching industry when an excess of chlorine in the fibres is destroyed by $S_2O_3^{2-}$:

$$S_2O_3^{2-} + 4Cl_2 + 5H_2O \quad = \quad 2HSO_4^- + 8H^+ + 8Cl^-$$

In addition to these species, another two groups, of much less technical importance, formulated as $H_2S_nO_3$ and $H_2S_nO_6$ ($2<n<7$), are also known[1,2,4].

I-C-4. The dithionite ion, $S_2O_4^{2-}$:-

Although the parent acid has no independent existence and has not been detected in aqueous solution either, its normal salts are well characterised. They are stable when maintained anhydrous, but solutions decompose at different rates in acidic, neutral and alkaline media[1,2,5]. Zinc dithionite is prepared by reacting sulphur dioxide with an aqueous suspension of zinc dust according to the equation:

$$2SO_2 + Zn = ZnS_2O_4$$

With restrictions on the amount of zinc allowed in plant effluents, sodium dithionite has largely displaced the zinc compound in commercial uses. It is technically prepared by either of four methods[5]: (i) from zinc dithionite by reacting with sodium carbonate solution to produce insoluble zinc carbonate:

$$ZnS_2O_4 + Na_2CO_3 = Na_2S_2O_4 + ZnCO_3$$

To produce the solid, crystalline sodium chloride and alcohol are added to salt out the sodium dithionite, which precipitates as the dihydrate, (ii) from sodium amalgam:

$$2Na\,Cl + 2Hg = 2NaHg + Cl_2$$

$$2\,NaHg + 2SO_2 = Na_2S_2O_4 + 2Hg$$

(iii) by the formate process:

$$2SO_2 + NaOH + HCO_2Na = Na_2S_2O_4 + CO_2 + H_2O$$

It is believed that this reaction involves several intermediate steps,

$$SO_2 + NaOH = NaHSO_3$$
$$SO_2 + HCO_2Na + H_2O = NaHSO_3 + HCO_2H$$
$$HCO_2H + 2NaHSO_3 = Na_2S_2O_4 + CO_2 + 2H_2O$$

The reaction is carried out in an aqueous methanol solution, in which the reactants are soluble while the product is not. The dithionite precipitates as the anhydrous salt which is then filtered and dried, and (iv) from sodium borohydride:

$$2NaH + B_2H_6 = 2NaBH_4$$
$$NaBH_4 + 8NaOH + 8SO_2 = 4Na_2S_2O_4 + NaBO_2 + 6H_2O$$

It is widely used as a reducing agent in vat dyeing and bleaching of paper pulp. Because of its ability to reduce hexavalent chromium to the trivalent state, it is used to purify waste waters containing hexavalent chromium, e.g., from plating solutions, by precipitation from alkaline solution[5]:

$$2Na_2CrO_4 + 3Na_2S_2O_4 + 4H_2O = 2Cr(OH)_3 + 4Na_2SO_3 + 2NaHSO_3$$

It has been used to investigate some biological processes[6-9], e.g., kinetics of oxyhaemoglobin dissociation, by scavenging the free oxygen in solution[7,9].

I-D. Statement of problems addressed in this thesis:-

Polyatomic ions and molecules display characteristic Raman and

infrared activities depending basically upon their constituent atomic spatial arrangements. Such phenomena are potentially useful, particularly in structural elucidations and in qualitative and quantitative analyses. It seemed therefore worthwhile to make a fairly extensive survey of the vibrational activities of appropriate ions with relevance to the following: (i) by reacting with the other atmospheric constituents, sulphur dioxide released during sulphur, coal and petroleum oil processing induces considerable environmental damage[1,2,10-13]. As a consequence the SO_2-H_2O system has received great attention in the investigation, and control, of atmospheric corrosion. The behaviour of this system has been spectroscopically monitored in order to identify the species formed. (ii) A dynamic equilibrium involving the di and bisulphite ions has been used elsewhere[14-17] to describe the composition of the aqueous disulphite solution:

$$S_2O_5^{2-} + H_2O \quad = \quad 2HSO_3^-$$

Two tautomeric forms, $H\text{-}SO_3^-$ and $HO\text{-}SO_2^-$, have been postulated to indicate the geometrical arrangements of the hydrogen atom in the bisulphite formula[14-16]. However, the existence of the $HO\text{-}SO_2^-$ isomer and the assignments of the bands observed in aqueous disulphite solution to the individual components have not yet been fully elaborated. (iii) In addition to the ordinary uses as a corrosion inhibitor, antidote in cyanide poisoning and as an analytical reagent for quantitative determinations of oxidising agents, the aqueous thiosulphate ion plays a fundamental role in silver halides-based photography as the 'fixing' agent, its complexing ability with silver ions being its basic selective

criterion for this purpose. While the photo-activated sites of the incorporated photo-tracing species constitute a permanent optical memory for the projected signals, removal of the unstimulated centres permanently eliminates further photolysis. It seemed worthwhile therefore to investigate silver-thiosulphate reactions in order to derive a proper mechanism for the fixation process. (iv) Although the dithionite ion is extensively used in vat and paper pulp processing as a reducing agent, and although a large amount of work has been done regarding the dithionite ion in aqueous solutions, some of its properties are not yet clear. It readily undergoes rupture of the strong S-O bond, forming the thiosulphate ion[1,2,5,18], while retaining the relatively weak S-S bond:

$$2O_2S{\cdot}SO_2^{2-} + H_2O \quad = \quad S{\cdot}SO_3^{2-} + 2HSO_3^-$$

The process involved in this fission is of interest.

References:-

1. Bailar, J.C., Emeleus, H.J., Nyholm, R. and Dickenson, A.F.T., "Comprehensive Inorganic Chemistry", Vol.2, Pergamon Press, 1973, P.795.

2. Greenwood, N.N. and Earnshaw, A., "Chemistry of the Elements", Pergamon Press, 1984, P.757.

3. Abbott, D., "Inorganic Chemistry", Chaucer Press, 1965, P.529.

4. Brauer, G., "Handbook of Preparative Inorganic Chemistry", Vol.1, 2nd ed., Academic Press, 1963, P.395.

5. Thompson, R., "Speciality Inorganic Chemicals", the Royal Society of Chemistry, Special Publication No 40, Whitstable Litho Ltd, 1981, P.59.

6. Kosower, E.M. and Bauer, S.W., J.Am. Chem. Soc., 82(2), 2191 (1960).

7. Morello, J.A., Craw, M.R., Constantine, H.P. and Forster, R.E., J.Appl. Physio., 19(3), 522 (1964).

8. Watt, G.D. and Burns, A., Biochem. J., 152, 33 (1975).

9. Forlani, L., Ioppolo, C., Antonini, E., Martin, C.J. and Marini,M.A., J. Inorg. Chem., 20 (2), 147 (1984).

10. Hidy, G.M., Hansen, D.A., Henry, R.C., Ganesan, K. and Collins,J., J. Air Pollu. Contr. Assoc., 34 (4), 333 (1984).

11. Moller, D., Atmos. Environ., 14, 1067 (1980).

12. Littlejohn, D. and Chang, S.G., Environ. Sci. Tech., 18, 305 (1984).

13. Kleinman, L.I., Atmos. Environ., 18, 1453 (1984).

14. Simon, A. and Schmidt, W., Z. Elektrochem., 64, 737 (1960).

15. Golding, R.M., J. Chem. Soc., 3711 (1960).

16. Connick, R.E., Tam, T.M. and Deuster, E.V., Inorg. Chem., 21, 103 (1983).

17. Herlinger, A.W. and Long, T.V., Inorg. Chem., 8, 2661 (1969).

18. Rinker, R.G., Gordon, T.P., Mason, D.M., Skaida, R.R. and Corcoran, W.H., J. Phys. Chem., 64, 573 (1960).

Chapter II

Summary of previous work

II. Summary of previous work

II-A. The structures of relevant sulphoxy anions:-

II-A-1. The solid and the aqueous state structure of the dithionate, $S_2O_6^{2-}$, ion:-

An X-ray investigation of crystalline sodium dithionate dihydrate[1] has revealed that the unit cell is orthorhombic and contains four molecules. Each sulphur atom of the dithionate ion is surrounded by the other sulphur atom and three oxygen atoms of the ion, forming an irregular tetrahedron. Recently, a re-examination by Kirfel et al.[2] has pointed out the lack of an inversion centre on the S-S bond.

Complete structural analysis of potassium dithionate crystals[3] indicated that two types of non-equivalent ions, one occupying a site symmetry of D_3, the other two a set of C_3 sites, are present in the unit cell. In both, the SO_3 groups are rotated from the eclipsed position by 23.5° and 54.5° respectively. Based upon diffraction measurements Liminga et al [4] have assigned a staggered configuration to the dithionate ion in caesium dithionate crystals.

The possible group symmetries for the dithionate ion, on the basis of X-ray studies, are the D_{3h}, D_3 and D_{3d}. From infrared, Raman and depolarisation measurements Duval and Lecomte[5], Gerding

and Eriks[6] and Palmer[7] concluded a staggered configuration with D_{3d} symmetry for the dithionate ion. The occurrence of no frequencies in common to both infrared and Raman, and the depolarisation of three bands being their evidence. Whereas Buijs[8] has explained the splitting of the S-O stretching modes in crystalline potassium dithionate in terms of the presence of two non-equivalent types of dithionate ion in the unit cell, Dawson et al.[9] have rationalised it and the number of the active modes in terms of the weak crystal field acting upon the ions. The removal of the vibrational degeneracy of the degenerate modes in crystalline sodium dithionate dihydrate has been attributed to the presence of a σXZ plane in the crystal, in which the S_6 axis lies[10]. From the available spectral data, Loewenchuss and Marcus[11] have evaluated the entropy of the gaseous dithionate ion at the standard rate.

II-A-2. The solid and the aqueous state structures of the disulphite, $S_2O_5^{2-}$, ion:-

An asymmetrical structure with C_s symmetry and containing an S-S bond has been assigned to the disulphite ion on the basis of X-ray examinations[12-15]. Simon and Kriegsman[16] suggested an oxygen bridged symmetrical configuration with C_{2v} symmetry for this ion from their Raman and infrared studies. However, their conclusion is derived from measurements in solution only and is mainly based upon the occurrence of four bands in the S-O stretching region and upon the relative intensities of the Raman active modes. A re-

investigation by Rocchiciolli[17] has indicated the same oxygen bridged symmetrical structure. Buijs[18], reporting five fundamentals in the S-O stretching region, favoured the asymetrical geometry containing the S-S bond. Using results from their Raman and infrared investigations Herlinger and Long[19] firmly concluded that the disulphite ion adopts the same structure in solution as in solid. Their evidence was based upon three facts: (i) the vibrational spectra are virtually identical for both the solution and the solid phases, (ii) the number of the polarised Raman bands are more than that predicted for the symmetrical configuration, and (iii) all the fundamentals are both Raman and infrared active. Meyer et al.[20] have improved the band assignments employing isotopic substitutions. Recently, David and Ault[21] and Peter and Meyer[22] have reported the vibrational spectra of thallous disulphite.

II-A-3. The solid and the aqueous state structure of the bisulphite, HSO_3^-, ions:-

Brosche and Schultz[23] have excluded the existence of sodium bisulphite in the crystal form. Raman spectra reported by Fadda[24] exhibit a band characteristic only of the disulphite ion, and accordingly its existence in solution has been ruled out. Using their Raman and infrared results, Simon and Schmidt[25] have assigned a pyramid structure with approximate C_{3v} group symmetry for the bisulphite ion in caesium and rubidium salts. They also suggested that the ion contains an H-S bond, the occurrence of a band in the 2530-2620 cm^{-1} region being their evidence. The existence of the

$HO-SO_2^-$ tautomer was predicted on the basis of some extra bands observed in the aqueous $H-SO_3^-$ solution[25]. Golding[26] has postulated the presence of such species in order to explain the ultra-violet absorption measurements on aqueous disulphite solutions. Using isotopic substitutions Meyer et al.[20] improved the band assignments. Johansson et al.[27] and Magnusson et al.[15] have, recently, determined the crystallographic parameters of the $H-SO_3^-$ isomer in $CsHSO_3$ and $K_5(HSO_3)_3(S_2O_5)$ crystals respectively,

II-A-4. The solid and the aqueous state structure of the sulphite, SO_3^{2-}, ion:-

Zachariasen and Buckley[28] showed by X-ray diffraction methods that the sulphite ion has a trigonal pyramidal structure in which the sulphur atom has been only slightly displaced out of the plane containing the oxygen atoms. The unit cell is hexagonal and contains two molecules. Evans and Berstein[29] have assigned its fundamental vibrations on the basis of the C_{3v} group symmetry. Herlinger and Long[19] have pointed out that the vibrational degeneracy of the degenerate modes is removed in concentrated aqueous solutions. The minor spectral deviations recognised in crystalline thallous sulphite[22] have been rationalised in terms of the greater polarising ability of the thallium (1) species. A comprehensive revision of thermogravimetric, X-ray and of Raman and infrared analyses of crystalline metal sulphites is recently presented by Verma[30].

II-A-5. The solid and the aqueous state structure of the sulphate, SO_4^{2-}, ion:-

The sulphate ion in crystalline sodium sulphate has a D_2 site symmetry and eight molecules in the orthorhombic unit cell[31]. It is tetrahedral and belongs to the high symmetry point group T_d in aqueous solution[32]. From infrared measurements Baran and Aymonino[33] have concluded that the sulphate ion in a potassium bromide matrix has a site symmetry not higher than C_{3v}. The occurrence of the ν_1 mode and the splitting of the triply degenerate ν_3 vibration into two components only, being their evidence.

II-A-6. The structure of the bisulphate, HSO_4^-, ion:-

To account for the occurrence of six bands in both Raman and infrared, and for the depolarisation of three of them, Walrafen and Dood[32] have assigned C_{3v} group symmetry to the bisulphate species in aqueous solution. Later, the difference between the spectra of the ion in solution and in molten potassium bisulphate and the occurrence of accidental degeneracy have been rationalised by Walrafen[34] and Walrafen et al.[35] in terms of C_s symmetry and hydrogen-bonding.

II-A-7. The gaseous, the liquid and the solid phase structure of sulphur dioxide, SO_2, :-

On the basis of electron diffraction and some other spectral determinations[36-40] a resonating structure has been proposed for

gaseous sulphur dioxide. Employing a low-temperature X-ray experiment Post et al.[41] have investigated the crystal geometry of this species. An orthorhombic unit cell containing four molecules has been assigned, and the interatomic and intramolecular distances and the OSO bond angle have been reported to be 1.430 ± 0.015Å, 2.46 ±0.01Å and 119 ±2° respectively.

The vibrational activities of gaseous, liquid and of solid sulphur dioxide have been extensively investigated[42-50] and using a factor group analysis, based upon the X-ray examination, the fundamental modes have been assigned. Anderson and Savoie[43] have attributed the occurrence of some additional bands in the spectra of crystalline SO_2 to imperfect crystallisation, lattice defects, partial disorder and impurities including the naturally abundant isotopic forms of SO_2. By postulating the existence of a highly ordered, crystal-like structure in the liquid phase the occurrence of a weak band on the high frequency side of the symmetrical S-O stretching vibration has been explained.[43] A plausible assignment of the lattice modes has been reported by Anderson and Campbell[45].

II-A-8. The solid and the aqueous state structure of the thiosulphate, $S_2O_3^{2-}$, ion:-

X-ray investigations[51,52] have indicated that in the thiosulphate group, one sulphur and three oxygen atoms are arranged tetrahedrally around the other sulphur atom. Siebert[53], and Freedman and Straughan[54] have assigned the fundamental vibrations of this ion on the basis of C_{3v} group symmetry.

II-A-9. The solid and the aqueous state structures of the argentothiosulphate, $[Ag_m(S_2O_3)_n]^{-2n+m}$, complexes:-

Analytical[55-57] and physiochemical[58-60] investigations of the photographic fixation reaction have indicated the existence of six coordinated species. Based upon the molar ratios of the reactants involved, they have been formulated as $Ag_2S_2O_3$, $NaAg_3(S_2O_3)_2 \cdot 2H_2O$, $NaAgS_2O_3 \cdot H_2O$, $Na_5Ag_3(S_2O_3)_4 \cdot 2H_2O$, $Na_3Ag(S_2O_3)_2 \cdot 2H_2O$ and $Na_5Ag(S_2O_3)_3$. Among them, the crystallographic parameters of the $NaAgS_2O_3 \cdot H_2O$ species only have been reported.[55] Based upon some predictions, Freedman and Straughan[54] have assigned a single sulphur to silver coordination by the thiosulphate group in the $NaAgS_2O_3 \cdot H_2O$ and $Na_3Ag(S_2O_3)_2 \cdot 2H_2O$ complexes. In addition to the postulation of an extra species, formulated as $[Ag(S_2O_3)_4]^{-7}$, El-Hinnawi et al.[61] have suggested a bridging and a non-bridging mode of bonding via sulphur in order to illustrate the mode of accommodation of the silver ion by the thiosulphate groups. The bridging mode was found[61] to be the dominant in thiosulphate deficient solutions.

II-A-10. The solid and the aqueous state structure of the tetrathionate, $S_4O_6^{2-}$, ion:-

The sulphur chain of the tetrathionate species was found to be unbranched and non-linear[62,63]. The sodium salt is monoclinic, contains two molecules in the unit cell and belongs to the C_2 point group. Buijs[18] has assigned the fundamental vibrations of potassium

tetrathionate on the basis of C_1 symmetry. Raman and depolarisation measurements by Gerding and Eriks[6] are in favour of a cis orientation of the SO_3 groups. Using Raman and infrared results Lecomte et al.[64] and Meyer et al.[65] have assigned the fundamental modes of this species.

II-A-11. The solid and the aqueous state structures of the dithionite, $S_2O_4^{2-}$, ion:-

An X-ray examination of crystalline sodium dithionite[66] has indicated that the dithionite ion consists of two SO_2^- units held together by an extraordinarily long S-S bond in an eclipsed structure of approximate C_{2v} group symmetry. It belongs to the monoclinic system and contains two molecules in the unit cell. Its solid state spectra[67,68] have been assigned on the basis of C_{2v} symmetry. Whereas Simon and Kuchler's[69] spectral measurements are in favour of a planar structure with D_{2h} symmetry for the ion in solution, Takahashi et al.[68] and Peter and Meyer[70], using results from their Raman and infrared examinations, have suggested a staggered configuration with C_{2h} symmetry. Adams et al.[71] have concluded that the solid state symmetry is maintained upon dissolution. However, their conclusion is derived from measurements in solution only.

II-B. The enthalpies of formation of thiosulphate and of the argentothiosulphate complexes:-

Bichowsky[100] has made a complete thermodynamic study of the reaction:

$$S + CaSO_3 \cdot 2H_2O = CaS_2O_3(aq) + 2H_2O$$

Based upon the experimental data obtained, he evaluated the standard free energy of formation of the thiosulphate ion to be -523.46kJ mol^{-1}. Zimmermann and Latimer[101] have re-determined the enthalpy of the reaction of thiosulphate with the triiodide ion. Based upon these measurements, the standard molar enthalpies of formation of aqueous $S_2O_3^{2-}$ and $Na_2S_2O_3$ were evaluated[102,103] to be -625.29 and -1125.50kJ mol^{-1} respectively. Those of $Na_2S_2O_3$ and $Na_2S_2O_3 \cdot 5H_2O$ crystals were calculated[103] to be -1117.13 and -2601.99kJ mol^{-1} respectively.

Gronvold and Meisingset[104] have investigated phase transitions in $Na_2S_2O_3 \cdot 5H_2O$ and reported that it melts incongruently at 321.31K forming $Na_2S_2O_3 \cdot 2H_2O$ plus aqueous solution. As the following scheme illustrates, a complete conversion into aqueous $Na_2S_2O_3$ occurs at 335K:

$$Na_2S_2O_3 \cdot 5H_2O(c) = Na_2S_2O_3 \cdot 2H_2O(c) + 3H_2O \quad (1)$$

$$Na_2S_2O_3 \cdot 2H_2O(c) = Na_2S_2O_3(aq) + 2H_2O \quad (2)$$

$$Na_2S_2O_3 \cdot 5H_2O(c) = Na_2S_2O_3(aq) + 5H_2O \quad (3)$$

The enthalpies of the first, second and of the overall transition (3) were reported[104] to be 48.8 ±0.6, 3.19 and 51.8 ± 0.4 kJ mol^{-1} respectively.

The standard molar free energy of formation of the thiosulphate ion was re-evaluated to be -522.58 kJ mol^{-1} [105], and Murray and Cubicciotti[106] have determined this parameter over the temperature range 25-300° C.

Eastman and Milner[107] have measured the heats of solution of AgCl and AgBr crystals in a thiosulphate solution. Based upon their data, the standard molar enthalpy of formation of the complex ion $[Ag(S_2O_3)_2]^{-3}$ was derived to be -1285.74kJ mol^{-1} [103,108]. Employing some mathematical treatments De Marco et al.[109,110] have identified both $[Ag(S_2O_3)_2]^{-3}$ and $AgS_2O_3^-$ species. Using potentiometric titrations, they measured the free energy, the enthalpy and the entropy changes associated with the formation of the $Ag(S_2O_3)_2^{-3}$ species as -70.66 ± 1.6, -73.04 ± 6.4 kJ mol^{-1}, and -8 ± 20J $mol^{-1}T^{-1}$ respectively. Those associated with the formation of the $AgS_2O_3^-$ species were found[109,110] to be -51.90 ± 2.0, -60.78 ± 20kJ mol^{-1} and -29.7 ± 50J $mol^{-1}T^{-1}$ respectively.

Chapter III

Results and Discussion

(Spectroscopic)

III. Results and Discussion (Spectroscopic)

III-1. The structure of the dithionate, $S_2O_6^{2-}$, ion:-

The vibrational spectra of a nearly saturated aqueous solution of sodium dithionate and of the anhydrous and dihydrate solid salts are contained in Table III-1.

Although the aqueous and the dihydrate solid salt spectra are in good agreement with those previously reported[7,10], the anhydrous salt displays a quite different activity as regard the number and the position of the bands. It can readily be recognised that there is a lowering of the sulphur-sulphur stretching and the sulphur-oxygen deformation modes in the dihydrate salt compared with their frequencies in the anhydrous salt. This is the effect of the two water molecules present in the unit cell of the dihydrate crystals, and suggests hydrogen-bonding. Similar shifts have been observed in the vibrational spectra of sodium thiosulphate pentahydrate crystals.

In view of the X-ray investigation[1-4], the dithionate ion could have an eclipsed, a gauche or a staggered configuration with D_{3h}, D_3 and D_{3d} group symmetries respectively. For the D_{3h} group the Eu modes, which are infrared active, are also allowed in the Raman effect and should appear as weak depolarised vibrations.[7] No coincidences between Raman and infrared active modes under the D_{3d} group symmetry should be observed, and the D_3 symmetry will allow the

activity of the degenerate vibrations in both Raman and infrared. Although fundamentals in the low frequency region have been predicted and theoretical values have been derived for them[7], Beattie et al.[10] have assigned all vibrations in that region to the external lattice modes.

The vibrational spectra of the dithionate ion, as presented in Table III-1, containing some fundamental vibrations in common suggest D_3 or D_{3h} group symmetry rather than the D_{3d} group previously assigned[5-7,10]. Since the eclipsed D_{3h} symmetry is energetically unfavourable, and if present should have a relatively long S-S bond in order to reduce electrostatic interactions between the SO_3 groups, then the gauche configuration with the D_3 group symmetry seems to be the most probable structure for the dithionate ion in the solid state. The splitting of the S-O stretching modes can be satisfactorily rationalised in terms of coupling between the two thionate groups. As clearly indicated by the pronounced asymmetry of the highest band around 1210cm^{-1}, and the activity of the 550cm^{-1} fundamental mode in both Raman and infrared, the same structure is maintained upon dissolution. Coordination to the metal ions in the solid state slightly affects the symmetry and allows the activity of the A_1 modes in the infrared. Assignments for the four bands at 422, 450, 602 and 638 cm^{-1}, which appear only in the infrared spectrum of the solid dihydrate, are uncertain.

III-2. The symmetries and the dilution activities of the di ($S_2O_5^{2-}$) and bisulphite (HSO_3^-) ions:-

The vibrational activities and the assignments of the fundamental modes of the di and bisulphite ions are given in Table III-2.

The vibrational spectra of the disulphite ion in the solid and aqueous states are virtually identical, indicating that the asymmetric C_s structure is largely maintained upon dissolution. The emergence of an additional strong band at 1025cm^{-1} is the most significant change occurred on passing into solution. Another striking feature is that in addition to this band some others, although closely related to those of crystalline disulphite display a concentration-dependent activity. They become more intense upon dilution, suggesting the presence of some other species in aqueous disulphite solution. Among them, those at 1080, 1055 and 1025cm^{-1} appeared to be suitable for dilution measurements.

On the basis of some additional bands observed[25] and in order to account for their dilution-dependent properties[72], the presence of the $HO-SO_2^-$ tautomer has been postulated[25,26,72] in addition to the well known $H-SO_3^-$ form of the bisulphite ion. Although most investigators[19,20,73] have indicated that the band at 1025cm^{-1} is associated with the bisulphite ion, Takahashi et al.[68] have assigned it to an impurity produced by air oxidation. No further experimental evidence for the existence of the $HO-SO_2^-$ species or vibrational assignments for this ion have been reported, except for the band at 711cm^{-1} [72].

In the present work, an attempt has been made to examine very dilute solutions. It is based upon the ultra-violet evidence of Golding[26], which suggests that in $S_2O_5^{2-}$ solutions the equilibrium shifts towards bisulphite upon dilution. Hence bands characteristic of the latter should become more intense, relative to those of $S_2O_5^{2-}$, upon dilution. In addition to this, overlapping bands from either of the bisulphite tautomers and the disulphite ion will reveal the fundamental modes associated with the constituent thionate (SO_3^-) and thionite (SO_2^-) units of the disulphite species.

As predicted above, and clearly displayed by the progressive dilution measurements presented in Fig. III-1, a complete reversion of the relative intensities of the 1080, 1055 and 1025cm^{-1} bands in the infrared occurs in fairly dilute solutions ($\leqslant$.05M). This reversion reveals that while a non-disulphite species is contributing to the band at 1025cm^{-1}, other species in addition to the disulphite ion are associated with those at 1080 and 1055cm^{-1}. The change in the relative intensities of the two bands at 1080 and 1055cm^{-1} at $\leqslant$0.05M concentrations reveals the relative contributions of the disulphite ion to these bands. It is the relatively pronounced contribution to the band at 1080cm^{-1} that accounts for the reversion, since the greater the contribution the weaker the band should be in very dilute solutions. The assignment of the above set of bands are narrowed down further by employing theoretical considerations. While a single S-O symmetrical stretching mode displaying both Raman and infrared activities is expected for the H-SO_3^- species, two vibrations associated with the SO_2^- and the S-O(-H) groups are

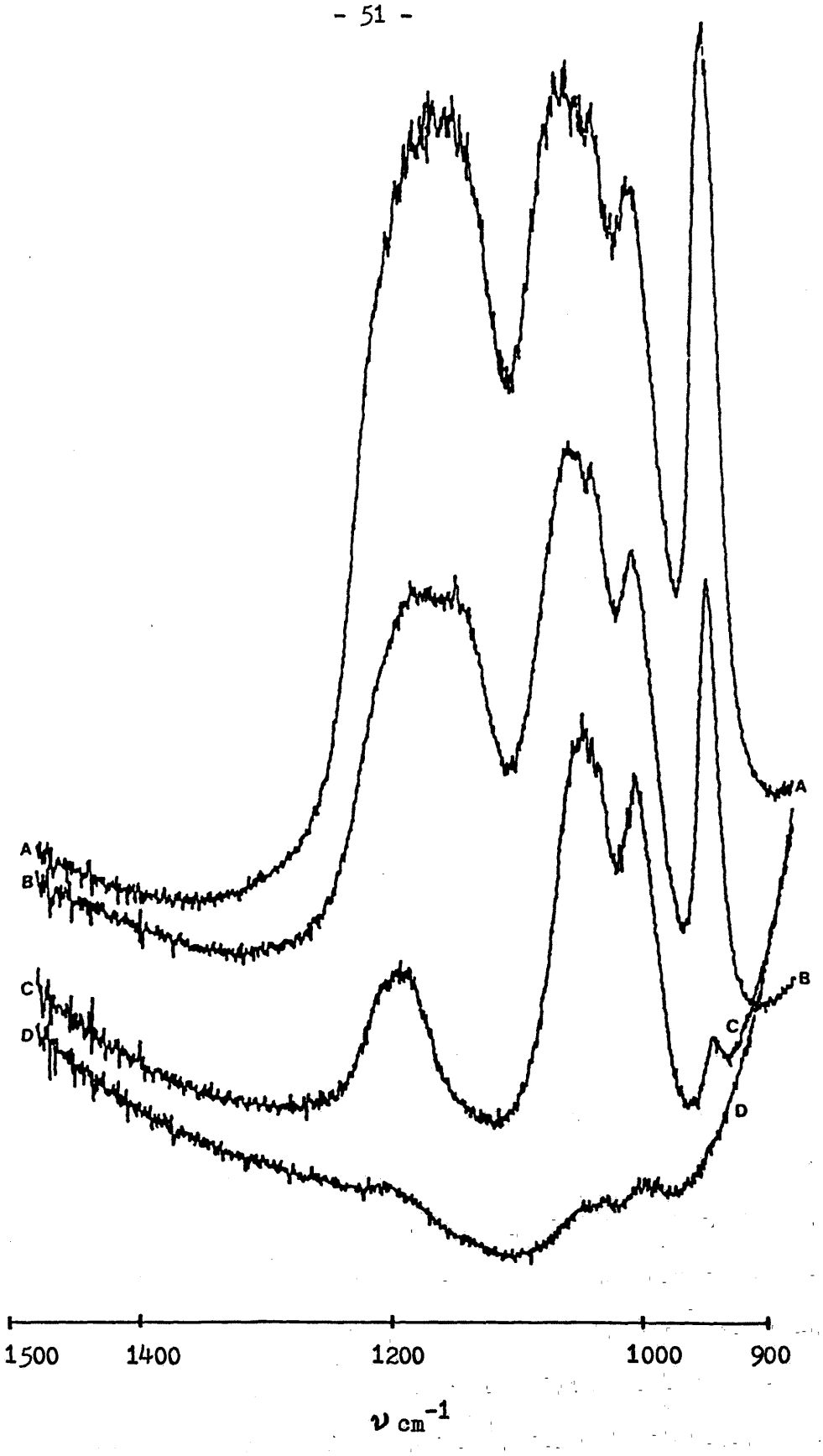

Fig.III-1. The concentration-dependence of the di-bisulphite equilibrium: A = 3.0M (saturated), B = 2.0M, C = 0.5M, D = 0.05M disulphite solution

predictable for the $HO-SO_2^-$ isomer. Being only an infrared active mode, the band at $1080cm^{-1}$ is not associated with the $H-SO_3^-$ species, and on the basis of its overlapping criterion its assignment to the thionite (SO_2^-) units of the disulphite ion and of the $HO-SO_2^-$ species is unequivocal.

An ultra-violet spectrum of a 3×10^{-2} molar aqueous sodium disulphite solution displays a weak band at 256nm and two, strong and overlapping, bands at 200 and 210 nm assigned by Golding[26] to the disulphite ion and the $HO-SO_2^-$ and the $H-SO_3^-$ tautomers of the bisulphite entity respectively. However, the concentration-dependent shifts reported by Golding[26], and which have been used to identify the two tautomers, are not observed exactly. According to Golding's explanation[26] the concentration of the $HO-SO_2^-$ species should be severely reduced in concentrated disulphite solutions. On the basis of the present investigation, and as indicated by the relative intensity of the $1025cm^{-1}$ band, the idea of a significant reduction of the $HO-SO_2^-$ concentration via hydrogen-bonding is unlikely. Upon further dilutions both of the absorption bands at 256 and 210 nm disappear, leaving that at 200 nm identified with the $HO-SO_2^-$ ion to prevail in very dilute solutions. Being the strongest band in $<0.05M$ solutions, the band at $1025cm^{-1}$ has been consequently assigned to the $HO-SO_2^-$ species. Hence it becomes clear at this stage that the band at $1055cm^{-1}$, which displays both Raman and infrared activities, is a superposition of a band from the disulphite species and a band from the $H-SO_3^-$ tautomer of the bisulphite ion. Since it is associated with the thionate (SO_3^-) group in $H-SO_3^-$,

then the overlapping criterion suggests that a similar group, (the thionate unit), from the disulphite species is also involved. Substitution by deuterium has confirmed the assignments of the 1025 and 1055cm^{-1} bands to the HO-SO$_2^-$ and the H-SO$_3^-$ species respectively. The band at 1025cm^{-1} displays the same kind of 'deuterium shift' as that observed on the 1050cm^{-1} band of the bisulphate ion[74] and assumes a value of 1036cm^{-1} in D_2O, while that at 1055cm^{-1} remains unaffected. Thus the band at 1025cm^{-1} has been assigned to the S-O(-H) stretching mode. This confirms the earlier assignment of the 1080cm^{-1} band to the SO$_2^-$ groups of the HO-SO$_2^-$ ion and the disulphite species. However, no explanation for this kind of deuterium effect has yet been found[74]. The bands at 966 and 1170cm^{-1} have been assigned to the $S_2O_5^{2-}$ group itself as their relative intensities decrease progressively with dilution. Although both bands at 427 and 659cm^{-1} behave similarly, contributions from neighbouring bands of the bisulphite ion partially compensate for the dilution effect. It is on this basis that the former two bands at 966 and 1170cm^{-1} have been assigned as characteristic of the disulphite ion. The rupture of the S-S bond upon dissolution and its reformation upon crystallisation demonstrate clearly that it is a very weak bond. Thus a low frequency vibration should be associated with it. Comparisons with the S-S stretching frequencies in some similar species, ($S_2O_4^{2-}$ = 463cm^{-1}, $S_2O_6^{2-}$ = 282cm^{-1}), in addition to the above point suggest that this mode gives rise to the band at 427cm^{-1}. Since the existence of the $S_2O_5^{2-}$ ion is characterised by the S-S bond, then the corresponding band should always be present. Thus the assignment of the band at 235cm^{-1} to the S-S stretching

mode[68] has been ignored because of its early disappearance, ($\leqslant$0.1M), upon dilution. However, the shape and the frequency of this band, in addition to the dilution effect, are very similar to those of a similar band associated with the dithionite ion. Its non-occurrence in the dithionate species indicates that it is associated with the thionite (SO_2^-) groups in the disulphite and dithionite ions. Hence the spectral changes observed below 300cm^{-1} are attributed to a detectable rotation of the thionite group round the S-S bond as indicated in the dithionite case by adoption of a slightly different symmetry upon dissolution. Assignment of the S-O deformation modes of the two tautomers are achieved by considering the solid state spectra of the H-SO_3^- species[19,22]. Comparisons of the HO-SO_2^- vibrations with those of the biselenite[75] and the bisulphate[35] ions suggest C_s group symmetry for the bisulphite tautomer. Its fundamental modes in the bending region have been identified on the basis of their polarisation properties[19] and activities in the infrared.

The relative intensities of the 1025 and 1055cm^{-1} bands in $\leqslant$0.05M solutions suggest that the HO-SO_2^- tautomer is relatively more abundant than the H-SO_3^-. Since the disulphite ion contributes also to the latter band in addition to the H-SO_3^- species, then the relative concentration of the HO-SO_2^- isomer is much greater in real terms. This has been explained by relating the stabilities of the two tautomers to their structures. An extra stability is achieved via intramolecular hydrogen-bonding, which in the HO-SO_2^- ion is enhanced by the C_s structure adopted. In H-SO_3^- it is significantly

rendered by the, approximate, C_{3v}[15,25,27] symmetry assumed.

In addition to the above discussion, thorough investigations have revealed that while the band at 1080cm^{-1} undergoes a detectable dilution shift and approaches a value of 1065cm^{-1} in very dilute solutions, that at 1206cm^{-1} resolves into two well-defined components (Fig. III-1). The relatively stronger band at 1225cm^{-1} is identified with the HO-SO_2^- ion, and to that at 1206cm^{-1} both of disulphite and the H-SO_3^- species have been assigned.

The existence of the two tautomers in solution, and their non-existence in the solid state as sodium bisulphite, suggests that both species are involved in the formation of crystalline disulphite. In solution they are separated by the water molecules and the reaction between their functional groups is thus inhibited, particularly in very dilute solutions. On this hypothesis, crystalline sodium bisulphite could be obtained in the presence of some other suitable species which can take the role of water and held the two isomer apart in the solid phase. However, a band in the H-S stretching region appeared at 2561cm^{-1}, indicating the existence of crystalline sodium bisulphite, when sodium dithionite crystals precipitated from alkaline solutions are subjected to air oxidation. This is a highly exothermic process in which a mixture of sulphate, disulphite, dithionate and of H-SO_3^- crystals is generated. Thus the inability of the lithium, sodium and potassium ions to form solid bisulphite[20] can be attributed to their small sizes being insufficient to keep the two tautomers separate.

The formation of the S-S bond-containing disulphite ion, and of an oxygen bridged species can be described by the following two equations:

$$O_2S\text{-}OH^- + H\text{-}SO_3^- \rightleftharpoons O_2S\text{-}SO_3^{2-} + H_2O \qquad (1)$$

$$O_2S\text{-}OH^- + H\text{-}O\text{-}SO_2^- = O_2S\text{-}O\text{-}SO_2^{2-} + H_2O \qquad (2)$$

Although the occurrence of both reactions appears to be possible, the existence of the $O_2S\text{-}SO_3^{2-}$ form only[12-15,19] can be attributed to a greater kinetic and/or thermodynamic feasibility of the reaction involved (1) over the other (2). The reactions of the disulphite ion are essentially those of the bisulphite species, the removal of which drives the equilibrium in such a system in the forward direction,

$$S_2O_5^{2-} + H_2O = 2HSO_3^-$$

III-3. The vibrational activities of the sulphite, SO_3^{2-}, ion:-

Table III-3 lists the vibrational frequencies and their assignments for a nearly saturated aqueous solution of sodium sulphite and for the solid salt.

Being a pyramidal molecule[28], the sulphite ion has four normal vibrations. The symmetrical modes are non-degenerate and parallel to the symmetry axis while the antisymmetrical ones are perpendicular to the axis and doubly degenerate, as observed in the aqueous state Raman spectrum. The four vibrations are both Raman and infrared

active and the band frequencies for the aqueous species are much similar in both effects in contrast to the large differences observed by Evans and Bernstein[29], and which have been attributed to strong intermolecular interactions.

III-4. The vibrational assignments of the sulphate (SO_4^{2-}) and bisulphate (HSO_4^-) ions:-

The frequencies and the assignments for the vibrational spectra of nearly saturated aqueous sodium sulphate and bisulphate solutions and of the corresponding solid salts are listed in Tables III-4 and III-5 respectively.

The activity of the totally symmetric S-O stretching mode in the infrared illustrates that the sulphate ion even in the free state does not assume full tetrahedral symmetry. On coordination to the metal ions the symmetry is lowered even more and the degeneracy of the degenerate vibrations is removed.

The presence of the hydrogen atom has a substantial effect on the vibrational activities of the bisulphate ion, and many of the spectral features observed can be rationalised in terms of hydrogen-bonding. The band at $1206cm^{-1}$ is the most intense in the infrared and has been accordingly assigned to the antisymmetric S-O stretching mode, leaving that at $1330cm^{-1}$ to the S-O-H bending vibration. The assignment of the $1054cm^{-1}$ band to the S-O(-H) fundamental is based upon the deuterium effect[74].

III-5. The behaviour of aqueous sulphur dioxide, SO_2, solution:-

On the basis of electron diffraction[36,37], X-ray[41] and some other spectral[38-40] measurements C_{2v} group symmetry has been assigned to the sulphur dioxide species. Only three fundamental frequencies associated with the symmetric and the antisymmetric S-O stretchings and with the S-O deformation mode are thus anticipated in the absence of any degeneracy. The vibrational spectra of this species have been extensively investigated[42-50].

In addition to its industrial importance and because of its significance in acidic precipitation from the atmosphere[76] much attention has been given to sulphur dioxide. Its aqueous phase behaviour has been spectroscopically investigated in the present work.

In addition to the three well known SO_2 bands at 527, 1151 and 1331cm^{-1}, a number of weak bands have been observed at 1025, 1055 and 1125cm^{-1} in fresh aqueous sulphur dioxide solution. In order to account for their appearance it has been postulated that they are either associated (i) with the hydration of the gaseous species and are a consequence of very minor alterations in structural parameters, (ii) with impurities, including the naturally abundant isotopic forms of the SO_2 species, or (iii) with some other species released upon hydrolysis, a process that may be occurring at a very low rate. Both (i) and (ii) can be eliminated by monitoring the behaviour of the additional bands on standing, when a significant portion of SO_2

has been hydrolysed.

A clearer picture on the SO_2-H_2O interactions emerged when the aqueous sulphur dioxide solution was allowed to stand for a long time, (12 months). As Table III-6 and Figs. III-2 and III-3 illustrate, the intensities of the additional bands have increased significantly on standing. In addition, another set associated with the bisulphite, sulphite, sulphate, bisulphate and with the dithionate species has emerged. Apart from others, the emergence of the three bands at 790, 1125 and 2608cm^{-1} suggests, for the first time, the existence of undissociated sulphurous acid. They have been assigned to the S-(OH), the symmetric S-O, and the H-S stretching vibrations respectively. The H-S stretching band at 2608cm^{-1} is the direct evidence for the existence of the H-SO_2-OH tautomer. Simon and Waldman[77] have reported the occurrence of a similar, but unidentified, band at 2591cm^{-1}. The existence of isomeric HO-SO-OH species which lacks a distinctive vibrational feature has been ascribed to the additional intensities of the other two bands at 790 and 1125cm^{-1}. The effects of temperature and light on such a system have been investigated by examining cooled and dark-standing samples. While ionisation of the acid should be significantly reduced at lower temperature, hydrolysis should be noticeably enhanced if photo-induced by illumination. The significant point illustrated in Fig. III-3 is that the intensity of the 1025cm^{-1} band has been greatly reduced in the low temperature (0° C) standing solution, suggesting repression of ionisation and also contribution of the acid to the succeeding band at 1055cm^{-1}, otherwise it should suffer

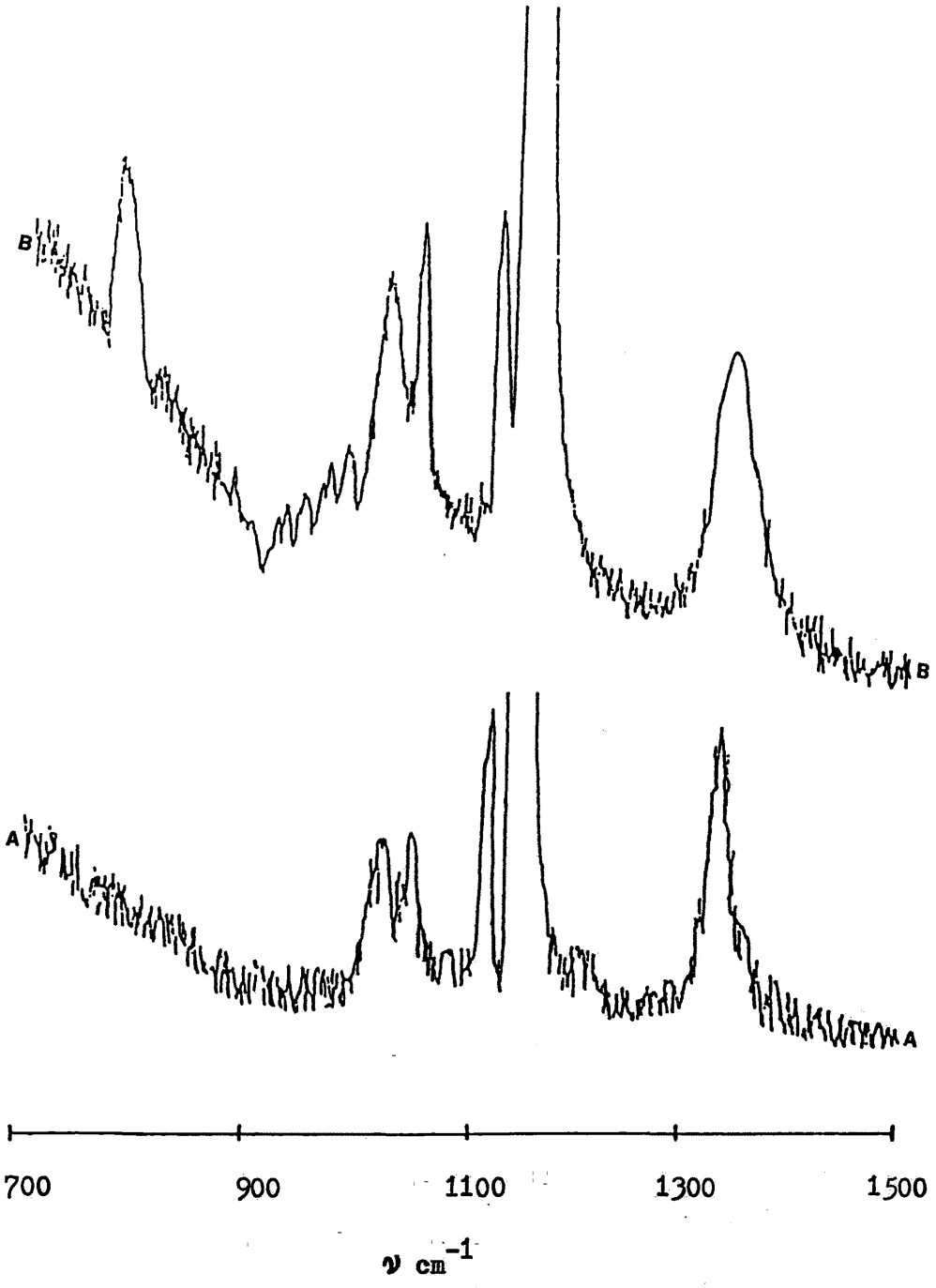

Fig. III-2. Raman spectra of:
A = Fresh aqueous sulphur dioxide solution
B = Standing, (25°C), aqueous sulphur dioxide solution

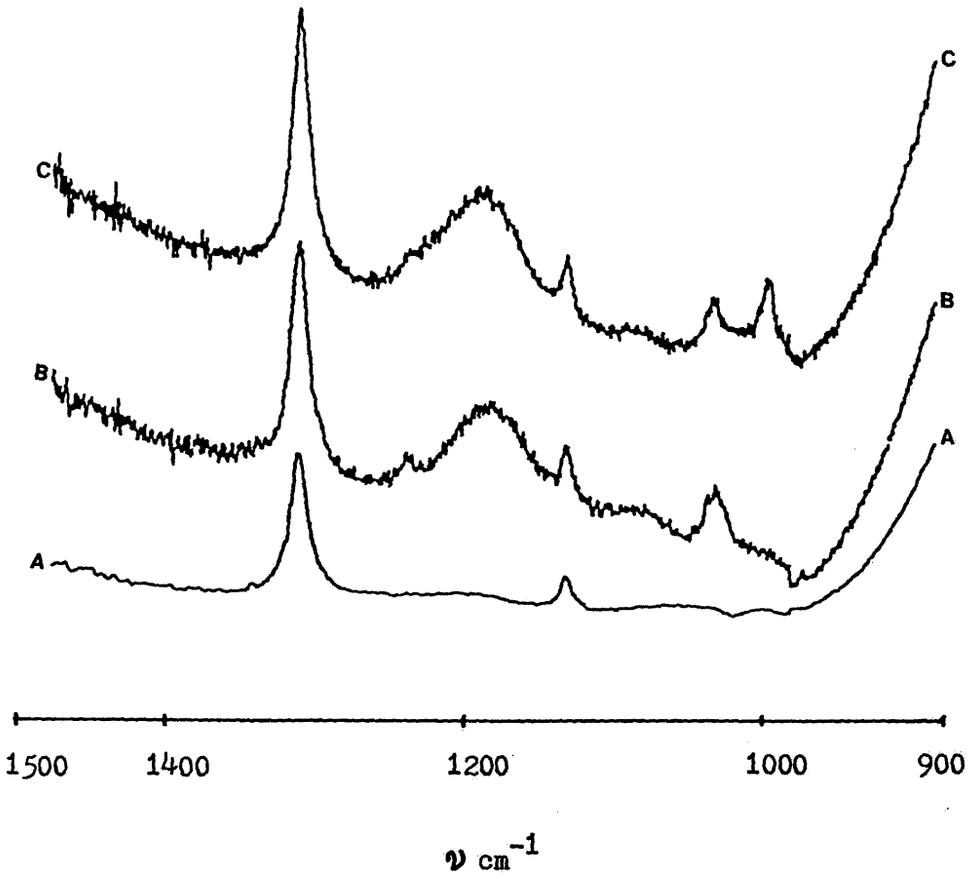

Fig. III-3. Infrared spectra of:
A = Fresh aqueous sulphur dioxide solution
B = Standing, (0°C), aqueous sulphur dioxide solution
C = Standing, (25°C), aqueous sulphur dioxide solution

from the same effect. By inspection of closely related vibrations in some relevant species, $HO-SO_2^-$ and $HO-SO_3^-$, the bands at 1055 and 1125 cm^{-1} have been assigned to the S-O(-H) and the symmetric S-O stretching vibrations respectively. Both of the $\nu_9 A''$ and $\nu_5 A''$ fundamentals associated with the H-S deformation modes in $H-SO_2-OH$ and $H-SO_3^-$ species respectively should be contributing to the latter band also. Together with some other incorrect assignments, Meyer et al.[65] have assigned the band at 1125cm^{-1} in a multi-component system to the SO_2 species. The characteristic disulphite bands at 966 and 1170cm^{-1} have not been revealed, and accordingly its formation has been excluded. Its non-existence in such a system has been attributed to the stronger acidity of the resultant solution, and can be represented by:

$$2H^+ + S_2O_5^{2-} = 2SO_2 + H_2O$$

The SO_2-H_2O system has been extensively investigated[77-82], and based upon the emergence of some additional bands at 1049 and 1013cm^{-1}. Simon and Waldmann[77] have identified the di and bisulphite ions in very low concentrations. However, the occurrence of the band at 1049cm^{-1} does not confirm the presence of the disulphite ion in the absence of the two characteristic, (infrared active), modes at 966 and 1170cm^{-1} as stated earlier. It is on this basis that the equilibrium: $SO_2 + HSO_3^- = HS_2O_5^-$ suggested by Falk and Giguere[81] in order to account for the disulphite formation is discounted. If the disulphite ion is present, then it should have been generated from the bisulphite tautomers according to the equation:

$$H\text{-}SO_3^- + HO\text{-}SO_2^- = S_2O_5^{2-} + H_2O$$

In order to account for the formation of the dithionate ion, the following two reactions have been suggested:

$$2H\text{-}SO_3^- = S_2O_6^{2-} + H_2$$

$$H\text{-}SO_3^- + HO\text{-}SO_3^- = S_2O_6^{2-} + H_2O$$

Although the first reaction is believed to be hypothetical only, since its occurrence will certainly rule out the existence of the di and bisulphite ions (see III-2), the second one seems more likely. The very low concentration of the dithionate species suggests, however, a low kinetic and/or thermodynamic feasibility for the reaction involved.

Although samples have been prepared in de-aerated, deionised distilled water, the presence of sulphate and bisulphate ions can only be attributed to the oxidation of the sulphite and bisulphite species, which are the resultant ions of the sulphurous acid ionisations. All of the above points, and consequently the behaviour of the standing aqueous sulphur dioxide solution, can be summarised by the following scheme:

$$SO_2 + H_2O = O_2S\text{---}OH_2$$

$$O_2S\text{---}OH_2 = HO\text{-}SO\text{-}OH = H\text{-}SO_2\text{-}OH$$

$$H_2SO_3 = HSO_3^- + H^+$$

$$HSO_3^- = SO_3^{2-} + H^+$$

$$SO_3^{2-} + \tfrac{1}{2}O_2 = SO_4^{2-}$$

$$SO_4^{2-} + H^+ = HSO_4^-$$

$$HSO_3^- + \tfrac{1}{2}O_2 = HSO_4^-$$

Since hydrolysis of sulphur dioxide is found to be extremely slow and reversible, then other processes of considerable rates should be postulated in order to account for the elevated sulphur precipitations[76].

The reaction between sulphur dioxide and the hydroxide ion is extremely fast, producing the bisulphite and the sulphite ions depending upon the reacted molar ratios:

$$SO_2 + OH^- = HSO_3^-$$

$$HSO_3^- + OH^- = SO_3^{2-} + H_2O$$

Accordingly it is concluded that strong nucleophiles and Lewis bases will react with sulphur dioxide, and the rates will be dependent upon the nucleophilicity or the basicity of the species involved. The slowness of the reaction involving water has been attributed to its weak basicity. PH_3, NH_3, NH_2^-, H_2NNH_2, HOO^- and the other strong basic atmospheric constituents can thus play a major role in the SO_2-induced atmospheric corrosion by generating the OH^- ion according to the following reaction:

$$Nu: + H_2O = Nu^+H + OH^-$$

On the basis of the above arguments it appears more likely that the

formation of the sulphoxy anions in cloud-waters arises from alkaline hydrolysis of the SO_2 species and from a subsequent oxidation as the following reactions imply:

$$OH^- + SO_2 = HSO_3^-$$

$$HSO_3^- + \tfrac{1}{2}O_2 = HSO_4^-$$

Other reactions of considerable significance could involve the naturally occurring amines, the alkaloids, and subsequently account for the damaging effects of SO_2 on vegetation. Its physiological effects on man can be accordingly removed by using alkaloid-rich species.

III-6. The vibrational activities of the thiosulphate, $S_2O_3^{2-}$, ion:-

Table III-7 lists the frequencies and assignments of the vibrational spectra of a nearly saturated thiosulphate solution and of the solid salts.

The crystal structure of sodium thiosulphate pentahydrate[51] shows the presence of hydrated sodium ions, and the effect of hydrogen-bonding can readily be recognised by a lowering of the S-S stretching frequency and a corresponding increase in the symmetrical S-O stretching mode compared with their frequencies in the anhydrous salt.

The thiosulphate ion can be pictured as a sulphate species in which one of the oxygen atoms has been replaced by sulphur. This

replacement lowers the symmetry of the thiosulphate species to C_{3v} and causes splitting of the degenerate vibrations and activates the infrared inactive modes.

III-7. The symmetries of the argentothiosulphate, $[Ag_m(S_2O_3)_n]^{-2n+m}$, complexes:-

In the present thermochemical investigations, (see IV-A), only four compounds involving thiosulphate and silver ions have been identified. On the basis of the molar ratios of the reactants involved they have been formulated as $[Ag(S_2O_3)_2]^{-3}$, $[Ag_2(S_2O_3)_3]^{-4}$, $AgS_2O_3^-$ and $Ag_2S_2O_3$. Based upon the stoichiometries of the individual steps involved and upon the sequential and the irreversible nature of the overall reaction the following mechanism has been derived:

$$Ag^+ + 2S_2O_3^{2-} = [Ag(S_2O_3)_2]^{-3}$$

$$Ag^+ + S_2O_3^{2-} + [Ag(S_2O_3)_2]^{-3} = [Ag_2(S_2O_3)_3]^{-4}$$

$$Ag^+ + [Ag_2(S_2O_3)_3]^{-4} = 3AgS_2O_3^-$$

$$Ag^+ + AgS_2O_3^- = Ag_2S_2O_3(aq)$$

$$Ag_2S_2O_3(aq) + H_2O = Ag_2S(c) + SO_4^{2-} + 2H^+$$

No evidence suggesting the existence of the $[Ag(S_2O_3)_3]^{-5}$ has been found. Of the above four species, only the first three have been isolated, in the present work, by alcoholic precipitation after titrating 1.50M thiosulphate solutions with 1.00M silver nitrate to

exact molar ratios. Being sparingly soluble, they separate out even while titration proceeds. Such precipitates have been removed prior to isolation, in order to eliminate contamination by the decomposition product Ag_2S. To avoid immediate formation, and instantaneous decomposition, of the $Ag_2S_2O_3$ species the silver solution was added drop by drop to the thiosulphate solution while stirring very effectively. Even with thorough stirring the reverse addition yields the inevitable Ag_2S species only. However, by using ampoule-mode calorimetry and sweeping the reaction at different molar ratios the existence of the $[Ag_2(S_2O_3)_3]^{-4}$ compound has been indicated in the reverse additions. Among these species the compound $Ag_2S_2O_3$, having the greatest silver to thiosulphate ratio, exhibits greatest sensitivity to light and darkens instantaneously. Its instability renders its isolation and spectroscopic investigation difficult. However, its structure can be satisfactorily described by considering its formation and decomposition processes:

$$Ag^+ + S_2O_3^{2-} = AgS_2O_3^-$$

$$Ag^+ + AgS_2O_3^- = Ag_2S_2O_3(aq)$$

$$Ag_2S_2O_3(aq) = Ag_2S(c) + SO_3(g)$$

$$SO_3(g) + H_2O = SO_4^{2-} + 2H^+$$

The negative charge already present on the thiosulphate ion is used to accommodate the first silver ion via the sulphur atom, forming the $Ag\,S_2O_3^-$ species. The coordination via sulphur is indicated by the lowering of the S-S stretching frequency in

$AgS_2O_3^-$ and relevant species with respect to its value in $S_2O_3^{2-}$, (see Tables III-7 and III-8). Then the second silver ion reacts with the $AgS_2O_3^-$ complex ion to yield the short-lived $Ag_2S_2O_3$ species. The electron-density on the S-S bond is continuously pulled over during this reaction in order to coordinate the second silver ion via another Ag-S bond. The cessation of the electron-density drift marks the completion of the second Ag-S bond formation and subsequently synchronises with the separation of the Ag_2S precipitate. Hence the duration of the Ag^+ and $AgS_2O_3^-$ reaction is believed to be the life-time of the $Ag_2S_2O_3$ compound.

On the basis of the above points, the $Ag_2S_2O_3$ species can be usefully discussed in terms of the constituent Ag_2S and SO_3 units loosely held together by the S-S bond. Thus its structural parameters are believed to be similar to those of the constituent units. It is on the basis of these descriptions that C_{2v} group symmetry has been suggested for the $Ag_2S_2O_3$ species.

In Table III-8, the vibrational activities of the other species are given with their assignments. The sites of coordination are deduced from the lowering of the S-S stretching frequency and the corresponding increase in the S-O stretching frequencies compared to their values in the free $S_2O_3^{2-}$ ion as postulated by Freedman and Straughan[54]. An unidentified weak band reported by El-Hinnawi et al.[61] at 242cm^{-1} has been assigned to the Ag-S stretching mode. Except for the appearance of this band and for the splitting and the frequency shifts observed, the spectral features of the $AgS_2O_3^-$

species are basically similar to those of the $S_2O_3^{2-}$ ion. It is on this basis that C_{3v} group symmetry has been assigned to the $AgS_2O_3^-$ complex ion. In both $\left[Ag(S_2O_3)_2\right]^{-3}$ and $\left[Ag_2(S_2O_3)_3\right]^{-4}$, apart from the frequencies associated with the $AgS_2O_3^-$ compound, an additional band has been observed at $1020cm^{-1}$ in the Raman. This is taken to illustrate the mode of bonding of the additional thiosulphate groups in those species to the silver ion. Loose bonding, via the sulphur atom, will reduce the lowering of the S-S stretching frequency, compared to its value in the $AgS_2O_3^-$ species, where strong Ag-S bonding occurs as the high frequency shifts in the S-O stretching modes indicate. Although the broadness of the S-S band obscures detailed observations, the occurrence of the band at $1020cm^{-1}$ suggests that a relatively weak Ag-S bond is associated with the additional thiosulphate groups in $\left[Ag(S_2O_3)_2\right]^{-3}$ and $\left[Ag_2(S_2O_3)_3\right]^{-4}$. Based upon the occurrence of some typical $AgS_2O_3^-$ bands in the spectra of these species, their compositions can be satisfactorily analysed in terms of fundamental $AgS_2O_3^-$ units to which the additional thiosulphate groups are loosely held. The existence of such structures is strongly supported by the reactions of both $\left[Ag(S_2O_3)_2\right]^{-3}$ and $\left[Ag_2(S_2O_3)_3\right]^{-4}$ with excess silver ions to form the intermediate $AgS_2O_3^-$ species and eventually the transitory $Ag_2S_2O_3$ compound as the mechanism proposed illustrates. The loosely held thiosulphate groups are involved in these reactions, since the firmly bonded ones will undergo decomposition only via formation of the $Ag_2S_2O_3$ species. The above postulations account thus for the sequential nature of the silver-thiosulphate reactions, and the existence of the strong Ag-S bond in the fundamental $AgS_2O_3^-$

unit explains the irreversibility. The following structures and group symmetries have been suggested on the basis of the above arguments to describe the argentothiosulphates:

$Ag_2S_2O_3$ C_{2v}

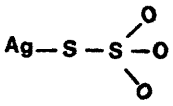

$AgS_2O_3^-$ C_{3v}

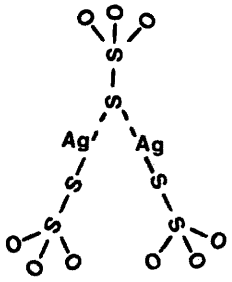

$[Ag_2(S_2O_3)_3]^{-4}$ C_{2v}

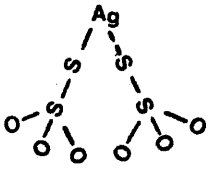

$[Ag(S_2O_3)_2]^{-3}$ C_{2v}

On standing, the aqueous solutions of the $AgS_2O_3^-$, $[Ag_2(S_2O_3)_3]^{-4}$ and $[Ag(S_2O_3)_2]^{-3}$ complex ions gradually decompose into Ag_2S, the resultant solutions being acidic. The non-existence of the $[Ag(S_2O_3)_3]^{-5}$ and other highly thiosulphated complexes is more likely due to steric effects exerted by the additional thiosulphate units.

III-8. The symmetry of the tetrathionate, $S_4O_6^{2-}$, ion:-

The vibrational spectra of a nearly saturated sodium tetrathionate solution and of the anhydrous salt are given in Table III-9.

The chain of the sulphur atoms in the tetrathionate ion is non-planar, and the ion adopts a C_2^3-C_2 space group in the sodium salt[63]. The activity of all fundamentals in both Raman and infrared supports a C_2 point group assignment for this ion. The degeneracy of most vibrations and the small separation between the two absorption bands observed imply a very weak coupling between the fundamentals of the two SO_3 groups.

If the molecule is regarded as being composed of two thiosulphate groups held together via an S-S bond in the definite mode described[63,83], then in addition to the normal vibrations of the thiosulphate ion the tetrathionate species should display some additional bands associated with the $S-S_2O_3$ stretching and the $SO_3 \cdot S \cdot S_2O_3$ deformation modes. On the basis of Freedman and Straughan postulations[54] comparison of the vibrational frequencies of the tetrathionate ion with those of the thiosulphate species will reveal the coordination site and the proper geometry can be accordingly deduced.

As Table III-9 illustrates, and except for the emergence of two additional bands at 262 and 139cm^{-1} assigned on the basis of the above points to the $S-S_2O_3$ stretching and the $SO_3 \cdot S \cdot S_2O_3$ deformation modes respectively, the vibrational spectra of the tetrathionate ion are basically similar to those associated with coordinated thiosulphate species, (see III-7). Thus they can be satisfactorily discussed in terms of two coupled thiosulphate units. As postulated by Freedman and Straughan[54], coordination via the sulphur atoms

should lower the S-S stretching frequency and correspondingly increase the S-O stretching ones. Both kinds of shifts have been observed. On coupling to form the tetrathionate ion, the S-S stretching frequency in $S_2O_3^{2-}$ is lowered from 450 to 393cm^{-1}, and the symmetrical and the asymmetrical S-O stretchings are increased from 1000 and 1122 to 1046 and 1225cm^{-1} respectively. Based upon these analyses the vibrational modes of the tetrathionate species have been fully assigned and C_2 group symmetry has been suggested. Decreasing more pronouncedly with the increase in mass of the coordinated species, ($Na_2S_2O_3.5H_2O$ = 437, $NaAgS_2O_3$ = 420 and $Na_2S_4O_6$ = 393cm^{-1}), the lowering of the S-S stretching frequency appears to be dependent upon the mass of the accomodated entity. Coupling, of two thiosulphate groups, via sulphur eliminates hydrogen-bonding, thus an additional lowering of the S-S stretching frequency in the dihydrate salt, $Na_2S_4O_6.2H_2O$, is not anticipated. Assignment of the band at 262 cm^{-1} to the S-S_2O_3 stretching mode agrees well with the assignment of that at 242 cm^{-1} to the Ag-S stretching in the argentothiosulphates (III-7). The vibrational spectra of other polythionic species, ($S_3O_6^{2-}$, $S_5O_6^{2-}$ and $S_6O_6^{2-}$), could be assigned in a similar way.

III-9. The structure of the dithionite, $S_2O_4^{2-}$, ion:-

The vibrational spectra of a nearly saturated aqueous sodium dithionite solution and of the solid salt are contained in Table III-10.

The dithionite ion in the crystalline state has approximate C_{2v} symmetry and occupies a C_2 site[66]. Raman and infrared measurements on crystalline sodium dithionite[67,68] are consistent with the X-ray results[66].

Although some of the vibrational bands of the dithionite ion in solution are closely related to those in the crystal, the emergence of the 585cm^{-1} band and the 97cm^{-1} shift in the S-S stretching frequency upon dissolution cannot be explained unless structural modifications are taken into account. The spectral changes below 300cm^{-1} can be related to the solid state spectra and are very similar to those observed on the disulphite ion, (see III-2), which in spite of similar changes was found to be largely maintaining the solid state symmetry. Thus, they cannot necessarily be taken as a criterion for any geometrical modification.

The staggered and the planar structures proposed for the dithionite ion in aqueous solution[68-70] are primarily based upon the occurrence of six bands in the Raman and upon their polarisation properties. However, the evidence can be disputed because quantitative measurements of the intensities of the bands as a function of the dithionite concentration have indicated that all of the polarised and most of the observed depolarised bands in the high frequency region are associated with species other than dithionite. They change their intensities independently to those of all other bands. The same conclusion was derived by inspection of standing aqueous dithionite solutions. Qualitative analysis shows that the band

reported by Simon and Kuchker[69], Takahashi et al.[68] and Peter and Meyer[70] at 998, 1000 and 997cm^{-1} respectively is in fact associated with the thiosulphate ion. Those observed at 1030 and 1052cm^{-1} are associated with the HO-SO_2^- isomer of the bisulphite ion and with the disulphite and the H-SO_3^- tautomer respectively. Some of these species are known products of the dithionite ion in aqueous solutions generated by a disproportionation process proceeding via a free radical mechanism[84-87]. Furthermore, the S-O stretching vibrations are closely related to those in the crystal and have similar frequencies in both states. Although not stated, the infrared spectra reported by Takahshi et al.[68] containing these vibrations in common in both states reveal the same point. Based upon these observations and upon the prediction that the ion should display no coincidences between the Raman and the infrared activities under the C_{2h} and D_{2h} group symmetries both the trans and the planar structures previously suggested[68-70] have been excluded. The bands associated with the S-O stretching modes are very weak and their observations in the Raman require a very high amplification. Since the existence of the dithionite ion is characterised by the S-S bond then the corresponding band should always be present. Hence the assignment of the band at 234cm^{-1} to the S-S stretching mode[68] has been discounted because of its early disappearance, ($\leqslant$0.1M), upon dilution. Assignment of the band at 585cm^{-1} to such a mode has been excluded also on the same ground. As a result the band at 463cm^{-1} has been assigned to the S-S stretching mode. A comparison with its frequency in the solid phase, (366cm^{-1}), reveals the considerable shift occurred upon dissolution. Thus, the C_2-gauche

symmetry has been assigned to the dithionite ion in aqueous solution on the basis of the above arguments and in order to account for the shift in the S-S stretching frequency and the emergence of the $585cm^{-1}$ band upon dissolution.

III-10. The fate of the dithionite ion in aqueous solutions:-

On passing into solution the dithionite ion, in addition to structural modification, immediately starts conversion into some other species as indicated by the independent behaviour of most of the S-O stretching bands. It has been shown[84-87] that such changes occur via free radical intermediates, the SO_2^- radical ion and its protonated forms playing a major role. Chemical analysis of the end products[84,85] revealed the presence of thiosulphate in small but measurable quantities. A secondary reaction involving thermal decomposition and occurring simultaneously with the oxidation was suggested in order to explain its formation[85].

Thus, although a large amount of work has been done regarding the dithionite ion in aqueous solutions the mode of thiosulphate formation is not yet clear. To seek an answer to this question employing spectroscopic methods, the present work is described below:

III-11. The presence of thiosulphate in aqueous dithionite solutions:-

Besides its own bands, (Table III-11), aqueous dithionite solution

exhibits a set of weak bands in the high frequency region, which upon dilution appears to behave as if they are associated with species other than dithionite. When left to stand, and as displayed in Fig.III-4, the following changes have been observed: (i) the weak bands became much more intense, (ii) those associated with the dithionite ion completely disappeared, and (iii) another set has emerged in different regions of the spectrum associated with various other species identified as thiosulphate, bisulphite, disulphite, sulphite, sulphate and dithionate. In alkaline solutions the rate is much reduced, the formation of the sulphide ion becomes more pronounced, and sulphite dominates over the di and bisulphite ions. On further standing sulphur separates out, possibly due to the decomposition of tetrathionate ions formed by slow oxidation of the thiosulphate species, a reaction which is accelerated by thiosulphate itself[6].

The behaviour of dilute solutions has been spectrophotometrically investigated, and the presence of some other species in aqueous dithionite solutions immediately upon dissolution has been clearly demonstrated. Examinations of de-aerated neutral and alkaline systems containing the dithionite ion have shown that while the ion displays an intense, characteristic and well-defined absorption band at 315 nm in the latter system a broad band occurring at 348 nm characterises the same species in neutral solutions. The rate of disappearance is strongly pH dependent. In 1.00M alkaline solutions containing 10^{-3} moles of dithionite the characteristic band at 315nm survives for more than 5 days.

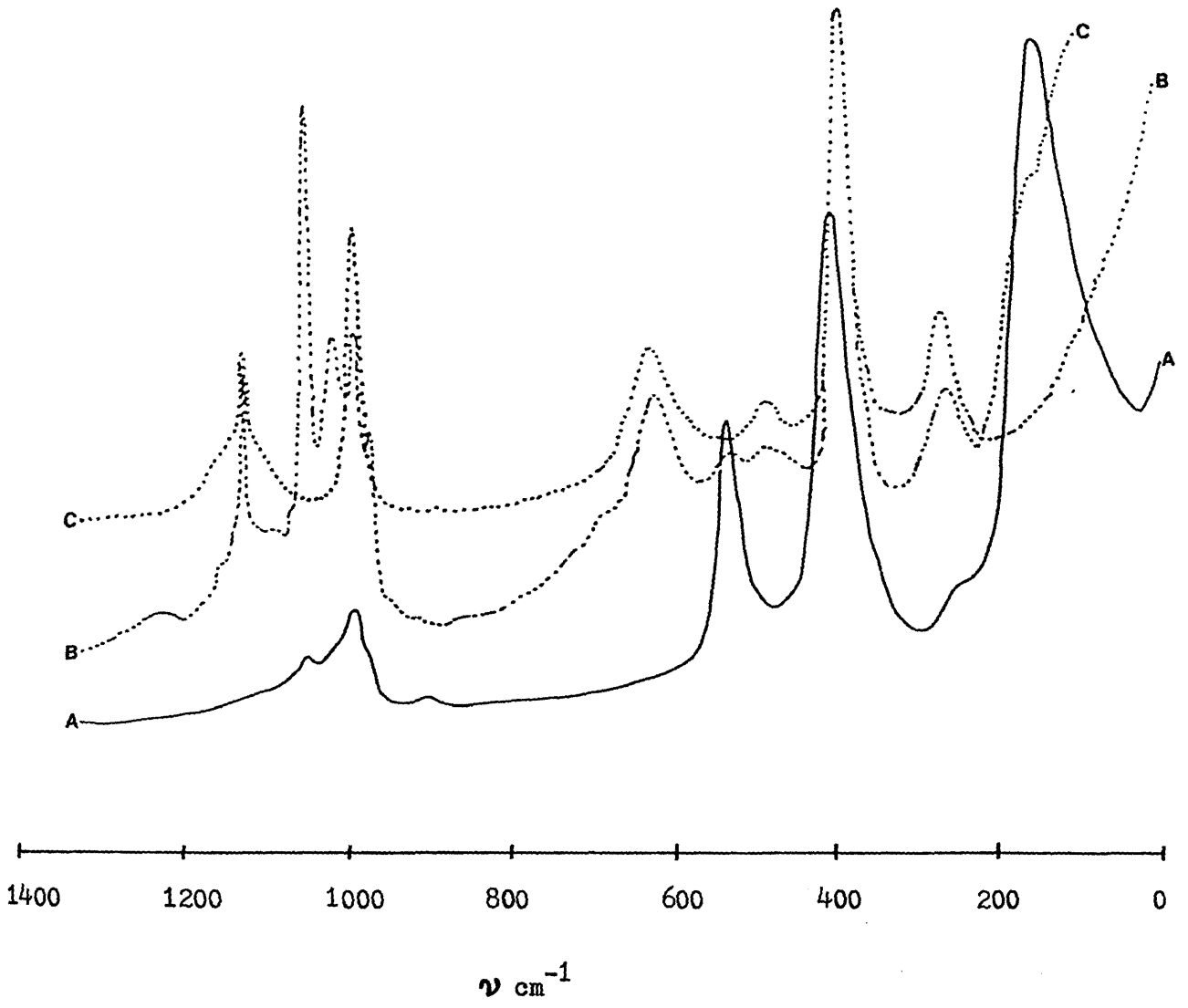

Fig. III-4. Raman spectra of:
A = Fresh aqueous dithionite solution
B = Standing aqueous dithionite solution
C = Thiosulphate solution

Apart from its own absorption band at 348nm the ultra-violet spectrum of a fresh 3×10^{-3} M aqueous dithionite solution exhibits three absorption maxima at 275, 214 and 200nm. A 7×10^{-4} M thiosulphate solution displays two bands at 214 and 192nm. Three absorption maxima associated with the disulphite ion and the $H\text{-}SO_3^-$ and $HO\text{-}SO_2^-$ tautomers of bisulphite species respectively have been identified in a 3×10^{-2} M aqueous disulphite solution at 256, 210 and 200nm. It is clear that thiosulphate, disulphite and both of the bisulphite isomers are present in fresh dithionite solutions. Conversion was almost instantaneous in non-de-aerated systems.. The absorption maxima are either shifted, or overlapped, the latter effect showing the limitation of the uv spectroscopy for qualitative and quantitative analyses.

Iodometric titrations of dithionite solutions after standing have indicated the formation of tetrathionate ions, (detected spectroscopically), suggesting the presence of thiosulphate in aqueous dithionite solutions. However, it was found that the addition of small amounts of the triiodide solution to freshly prepared dithionite samples generates the thiosulphate and the other non-dithionite species immediately. A highly exthothermic reaction occurred when freshly precipitated (from alkaline solution) dithionite was exposed to air to generate sulphate, disulphite, bisulphite and dithionate. Since the addition of triiodide solution implies oxidation also, then it seems more likely therefore that the energy required to cause the rupture of the sulphur-oxygen bond in the dithionite ion in order to yield thiosulphate and sulphide

species originates from an auto-oxidation process involving the free radicals and proceeding at a low rate. The formation of these species partially accounts for the reducing nature of the resultant solutions.

The disproportionation of the dithionite ion has been extensively investigated[84,85,88-93]. In order to account for the major presence of the thiosulphate ion in non-oxidised systems Rinker et al.[84,85] have postulated a thermal decomposition path. Its non-occurrence in oxidised systems has been indicated by the following reaction[88-93]:

$$Na_2S_2O_4 + H_2O + O_2 = NaHSO_3 + NaHSO_4$$

However, it was found in the present investigations that thiosulphate is present in all aqueous dithionite systems. The disproportionation is greatly enhanced by heat, H^+ and by the addition or the presence of oxidants.

Kinetic studies of the thermal decomposition of the dithionite ion in buffered and in unbuffered aqueous systems[84] have revealed that it is half order with respect to the hydrogen ion and three-halves order with respect to the dithionite ion. Based upon these observations the following mechanism was suggested[84]:

$$H^+ + S_2O_4^{2-} = HS_2O_4^-$$

$$H^+ + HS_2O_4^- = 2HSO_2^{\bullet}$$

$$HSO_2^{\bullet} + HS_2O_4^- = HSO_3^{\bullet} + HS_2O_3^-$$

$$HSO_2^{\bullet} + HSO_3^{\bullet} + H_2O = 2HSO_3^- + 2H^+$$

The hydrogen ion seems to be playing mainly a catalytic role. Its concentration being very small in neutral and alkaline solutions accounts for the rate retardation in those systems. The bisulphite ions undergo dimerisation [72,94] and establish a rapid equilibrium with the disulphite ions in aqueous solution:

$$2HSO_3^- = S_2O_5^{2-} + H_2O$$

Because the chemical behaviour of the disulphite ion is believed to be that of the bisulphite species, (see III-2), its detection in the dithionite systems will not affect the above scheme. However, the incorporation of some additional equations illustrating the formation of sulphate and the low presence of the dithionate ion is necessary. Acceleration of the decomposition by oxidation, protonation and by heating suggests: (i) the radical generating step is reversible and the equilbrium lies well over to the left:

$$S_2O_4^{2-} = 2SO_2^{\bullet}$$

The removal of the radical by the above reagents pulls the reaction in the forward direction:

$$SO_2^{\bullet} + O_2 = \text{products}$$

$$SO_2^{\bullet} + H = HSO_2^{\bullet} = \text{products}$$

(ii) the S-S bond in the dithionite ion is rather strong and heating

enhances its rupture and subsequently the generation of the reactive radical. It also provides the activation energies of the radical reactions, given in the above scheme (mechanism).

The behaviour of the dithionite ion in dilute acidic aqueous solutions has been extensively re-investigated [95-99], and the role of the various non-dithionite species, identified, in the kinetic stability of dithionite systems has been polarographically determined. In addition to a comprehensive mathematical model consistent with a two-step cyclic mechanism, a rather different sequence of reactions has been postulated by Cermak and Smutek[96,97] to illustrate the total path of the decomposition. The active sulphur generated at the very beginning of the induction period from a reaction involving the sulphoxylic acid, (H_2SO_2), and the dithionite ion initiates the decomposition chain. The appearance of some other active species, thiosulphurous acid and hydrogen sulphide, after a while commences the fast, auto-catalysed phase. The parallel and the consecutive secondary reactions prevailing in the latter phase, however, determine the yield of the final decomposition products. A full description can be found elsewhere[96,97].

Although the absence of the thiosulphate ion in the very early stages of the decomposition has been accounted for by suggesting some other reactions in which the thiosulphate ion has been consumed[96], its detection in the presence of excess HSO_3^- ions has been taken as a criterion for being a product of a consecutive

reaction involving the bisulphite ion and the active sulphur initially generated[96]. However, this postulation is discounted because the vibrational spectra of aqueous dithionite solutions, (Table III-11), have indicated the presence of the thiosulphate species immediately upon dissolution. Furthermore, a parallel increase in the yield of thiosulphate, bisulphite and of the other non-dithionite species occurs upon standing, (Table III-11 and Fig. III-4).

The relative stability of the dithionite solutions in the presence of the In^{3+}, Cd^{2+} and Zn^{2+} ions has been rationalised by Lem and Wayman[95] in terms of catalytic sulphide ions being partially removed by these cations. This interpretation is discounted also because it was found that the ion survives much longer in alkaline solutions in spite of the pronounced yield of the sulphide ion in those systems. In addition, the removal of any product should pull the reaction further according to the Le Chatelier's principle.

Table III-1. The vibrational spectra of the dithionate ion

$Na_2S_2O_6$ (crystal, R.)		$Na_2S_2O_6.2H_2O$ (crystal, R.)		$Na_2S_2O_6$ (solution, R.)		$Na_2S_2O_6$ (crystal, I.R.)		$Na_2S_2O_6.2H_2O$ (crystal, I.R.)		$Na_2S_2O_6$ (solution, I.R.)		Assignment
165	vw	147	vw									$\nu_4 A_1$;SO_3tor-
180	vw	176	vw									
216	vw	211	w									
244	vw	238	w					241	m			
311	vs	293	vs	282	vs			290	vw			$\nu_3 A_1$;S-S str.
335	s	327	s	320	m	335	w	336	w			$\nu_{11} E$;SO_3 rock.
								422	s			
								450	s			
466	vw	466	vw									
								509	s			
						525	vs sp	527	m	518	w	$\nu_8 A_2$;S-O def.
		544	m									
555	s	558	m	550	w	558	s	553	m	550	w	$\nu_{10} E$;S-O def.
						577	vs			575	w	$\nu_7 A_2$;S-O def.
								602	s			
								637	s			
726	s	708	s	710	s							$\nu_2 A_1$;S-O def.

continued

Table III-1 continued

$Na_2S_2O_6$ (crystal, R.)		$Na_2S_2O_6.2H_2O$ (crystal, R.)		$Na_2S_2O_6$ (solution, R.)		$Na_2S_2O_6$ (crystal, I.R.)		$Na_2S_2O_6.2H_2O$ (crystal, I.R.)		$Na_2S_2O_6$ (solution, I.R.)		Assignment
						995	s	995	s	993	ssp	$\nu_6 A_2$;S-O str.
						1000	ssh	1000	ssh			
						1080	vw					$\nu_7 + \nu_9$
1101	vs	1101	vs	1093	vs	1100	vw	1100	vw			$\nu_1 A_1$;S-O str.
1211	m	1216	m	1210	wbr	1210	sh	1212	sh	1210	sh	$\nu_9 E$;S-O str.
1224	m					1224	sh	1228	ssh			
						1241	vs	1247	s	1245	vs	$\nu_5 A_2$;S-O str.
						1258	sh					
1276	vw					1275	sh	1270	sh			$\nu_2 + \nu_9$

The abbreviations used have the following significance: R = Raman, I.R. = infrared, v = very, s = strong, m = medium, w = weak, sh = shoulder, sp = sharp, br = broad.

Table III-2. The vibrational spectra of the di and bisulphite ions

$Na_2S_2O_5$ (crystal, R.)		$Na_2S_2O_5$ (solution, R.)		$Na_2S_2O_5$ (crystal, I.R.)		$Na_2S_2O_5$ (in D_2O, I.R.)		Assignment
184	m	170	sh					
204	m	200	sh					
				221	m			
230	m	235	vs	239	m			$\nu_8 A'(S_2O_5^{2-})$; SO_2^- wag.
263	sh			261	w			
276	vs			274	w			
				285	w			
320	m	310	m	312	w			$\nu_{13} A''(S_2O_5^{2-})$; SO_2^- twist.
		400	w					$\nu_5 A' + \nu_9 A''(HO-SO_2^-)$; sym. + asym. S-(OH) def.
434	s	427	s	445	s	427	w	$\nu_7 A'(S_2O_5^{2-})$; S-S str.
		460	m					$\nu_4 A'(HO-SO_2^-)$; sym. S-O def.
				498	w			
516	w	516	w	511	s	511	w	$\nu_{12} A''(S_2O_5^{2-}).\nu_{12} A''(S_2O_5^{2-}) + \nu_6 E(H-SO_3^-)$ in aq state
535	w	531	m					spec.; asym. S-O def. of the SO_3^- gps.
556	w	558	w	564	s	558	w	$\nu_6 A' + \nu_{11} A''(S_2O_5^{2-})$; S-O def. of the SO_2^- gp. +
569	w							asym. S-O def. of the $(SO_3^- + SO_2^-O)$gp.

continued

Table III-2 continued

$Na_2S_2O_5$ (crystal, R.)		$Na_2S_2O_5$ (solution, R.)		$Na_2S_2O_5$ (crystal, I.R.)		$Na_2S_2O_5$ (in D_2O, I.R.)		Assignment
				588	vw			
		589	w			590	w	$\nu_8 A''(HO\text{-}SO_2^-)$; asym. S-O def.
				621	m			
				628	sh			
		635	w	633	m	634	m	$\nu_5 A'(S_2O_5^{2-}).\nu_5 A'(S_2O_5^{2-}) + \nu_3 A_1(H\text{-}SO_3^-)$ in aq.
				640	m			state spec.; sym. S-O def. of the SO_3^- gps.
				653	sh			
661	s	659	s	661	s	659	m	$\nu_4 A'(S_2O_5^{2-})$; sym. S-O def. of the $(SO_3^- + SO_2^-)$ gp.
		711	wbr			711	mbr	$\nu_3 A'(HO\text{-}SO_2^-)$; S-(OH) str.
						837	vw	$\nu_5 E(H\text{-}SO_3^-)$; H-S def.
980	w	970	w	975	vs	966	vs	$\nu_3 A'(S_2O_5^{2-})$; sym. S-O str. of the $(SO_3^- + SO_2^-)$ gp.
		984	w					$\nu_1 A_1(SO_4^{2-})$.
				995	sh			
		1025	s			1036	s	$\nu_2 A'(HO\text{-}SO_2^-)$; S-O str. of the S-O(-H) gp.
1064	s	1055	vs	1055	vs	1055	vs	$\nu_2 A'(S_2O_5^{2-}).\nu_2 A'(S_2O_5^{2-}) + \nu_2 A_1(H\text{-}SO_3^-)$ in aq.
1072	w			1070	s			state spec.; sym. S-O str. of the SO_3^- gps.

continued

Table III-2 continued

$Na_2S_2O_5$ (crystal, R.)		$Na_2S_2O_5$ (solution, R.)		$Na_2S_2O_5$ (crystal, I.R.)		$Na_2S_2O_5$ (in D_2O, I.R.)		Assignment
1087	w			1084	s	1080	vs	$\nu_1A'(S_2O_5^{2-}).\nu_1A'(S_2O_5^{2-}) + \nu_1A'(HO\text{-}SO_2^-)$ in aq. state spec.; sym. S-O str. of the SO_2^- gps.
		1093	w					$\nu_1A_1(S_2O_6^{2-})$.
				1122	s			
		1125	w					$\nu_5E(H\text{-}SO_3^-)$; H-S def.
				1148	ssh			
				1160	ssh			
1172	w	1175	w	1170	vs	1170	vs	$\nu_{10}A''(S_2O_5^{2-})$; asym. S-O str. of the $(SO_3^-+SO_2^-)$ gp.
1180	w			1180	sh			
1204	w	1200	w	1200	vs	1206	vs	$\nu_9A''(S_2O_5^{2-})$. $\nu_9A''(S_2O_5^{2-}) + \nu_4E(H\text{-}SO_3^-) + \nu_7A''(HO\text{-}SO_2^-)$ in aq. state spec.; asym. S-O str.
				1235	s			
				1265	s	1260	w	$\nu_6A''(HO\text{-}SO_2^-)$ in aq. state spec.; S-O-H def.
2561 *	m	2536	w					$\nu_1A_1(H\text{-}SO_3^-)$; H-S str.

* (see text)

Table III-3. The vibrational spectra of the Sulphite ion

Na_2SO_3 (crystal, R.)		Na_2SO_3 (solution, R.)		Na_2SO_3 (crystal, I.R.)		Na_2SO_3 (solution, I.R.)		Assignment
		448	w					
498	m	475	m	496	s			$\nu_4 E$; asym. S-O def.
639	w	620	w	630	s	624	w	$\nu_2 A_1$; sym. S-O def.
		900	w					$2\nu_4$.
950	s	936	m	952	ssh	940	s	$\nu_3 E$; asym. S-O str.
		955	sh					
987	vs	968	vs	970	sbr	960	sh	$\nu_1 A_1$; sym. S-O str.
				1005	ssh			
				1120	w			$\nu_2 + \nu_4$.
				1135	m			
				1214	w			$2\nu_2$.

Table III-4. The vibrational spectra of the Sulphate ion

Na_2SO_4 (crystal, R.)		Na_2SO_4 (solution, R.)		Na_2SO_4 (crystal, I.R.)		Na_2SO_4 (solution, I.R.)		Assignment
452	w	450	w					ν_2E; sym. S-O def.
467	w							
622	w	620	w	613	s	620	w	ν_4F_2; asym. S-O def.
635	w			635	m			
649	w							
994	vs	984	vs	1010	sh	982	vw	ν_1A_1; sym. S-O str.
1104	w	1105	wbr	1102	sbr	1105	sbr	ν_3F_2; asym. S-O str.
1134	w			1130	s			
1154	w							

Table III-5. The vibrational spectra of the bisulphate ion

$NaHSO_4$ (crystal, R.)		$NaHSO_4.H_2$) (crystal, R.)		$NaHSO_4$ (solution, R.)		$NaHSO_4$ (solution, I.R.)		Assignment
414	m	414	m					
424	m	420	sh					
447	m	437	m	430	mbr	450	mbr	$\nu_6 A' + \nu_{10} A''$; sym. + asym. S - (OH) def.
464	sh							
467	m	466	w					
565	w							
588	m	576	m					
602	m	606	m	596	sbr	590	s	$\nu_4 A' + \nu_5 A' + \nu_9 A''$; sym. + asym. S-O def.
610	w							
630	w							
		862	m					
870	s	880	m	896	mbr	881	s	$\nu_3 A'$; S-(OH) str.
918	w							
				984	vs	982	vw	$\nu_1 A_1 (SO_4^{2-})$.
1000	sh							
1008	s							
1018	sh							
1060	sh	1042	vs					

continued

Table III-5 continued

$NaHSO_4$ (crystal, R.)		$NaHSO_4.H_2O$ (crystal, R.)		$NaHSO_4$ (solution, R.)		$NaHSO_4$ (solution, I.R.)		Assignment
1066	vs	1054	sh	1054	vs	1054	s	$\nu_2 A'$; S-O str. of the S-O(-H) gp.
						1131	m	
						1148	sh	
1162	w	1180	w	1206	wbr	1206	sbr	$\nu_8 A''$; asym. S-O str.
1248	w	1248	w			1232	sh	$\nu_1 A'$; sym. S-O str. of the $S\bar{O}_3$ gp.
						1330	mbr	$\nu_7 A''$; S-O-H def.

Table III-6. The vibrational spectra of a fresh and of a standing aqueous sulphur dioxide solution

SO_2 (fresh, R.)		SO_2 (standing, R.)		SO_2 (fresh, I.R.)		SO_2 (standing, I.R.)		Assignment
		403	m					$\nu_5A'+\nu_9A''(HO\text{-}SO\text{-}OH) + \nu_6A' + \nu_{11}A''(H\text{-}SO_2\text{-}OH) + \nu_5A' + \nu_9A''(HO\text{-}SO_2^-)$; sym. + asym. S-(OH) def.
		460	m					$\nu_4A'(HO\text{-}SO_2^-)$.
		510	w			510	vw	$\nu_6E(H\text{-}SO_3^-)$.
527	w	527	w	527	w	527	w	$\nu_2A_1(SO_2)$; S-O def.
		550	m			550	w	$\nu_8A''(HO\text{-}SO\text{-}OH)+\nu_{10}A''(H\text{-}SO_2\text{-}OH)$; asym. S-O def.
		569	m					$\nu_4A'(HO\text{-}SO\text{-}OH)+\nu_5A'(H\text{-}SO_2\text{-}OH)$; sym. S-O def.
		600	m			595	vw	$\nu_8A''(HO\text{-}SO_2^-)+\nu_4A'+\nu_5A'+\nu_9A''(HSO_4^-)$.
		625	m			625	w	$\nu_3A_1(H\text{-}SO_3^-)$.
		710	wbr			710	vw	$\nu_3A'(HO\text{-}SO_2^-)$.
		790	s			790	vw	$\nu_3A'(HO\text{-}SO_2\text{-}OH)+\nu_4A'(H\text{-}SO_2\text{-}OH)$; S-(OH) str.
		896	w			880	vw	$\nu_3A'(HSO_4^-)$.
		966	m			940	w	$\nu_1A_1(SO_3^{2-})$.
		980	w					$\nu_1A_1(SO_4^{2-})$.
						1015	m	
1025	w	1025	s	1025	vw	1023	sh	$\nu_2A'(HO\text{-}SO_2^-)$.
1055	w	1055	s	1052	vw	1052	m	$\nu_2A'(HO\text{-}SO_2\text{-}OH)+\nu_3A'(H\text{-}SO_2\text{-}OH)$;S-O str. of the S-O(-H) gp.

continued

Table III-6 continued

SO_2 (fresh, R.)		SO_2 (standing, R.)		SO_2 (fresh, I.R.)		SO_2 (standing, I.R.)		Assignment
								$\nu_2 A'(HO\text{-}SO_2\text{-}OH)+\nu_3 A'(H\text{-}SO_2\text{-}OH)+\nu_2 A_1(H\text{-}SO_3^-)+\nu_2 A'(HSO_4^-)$.
						1078	vw	$\nu_1 A'(HO\text{-}SO_2^-)$.
		1091	vw					$\nu_1 A_1(S_2O_6^{2-})$.
1125	w	1125	s			1115	w	$\nu_1 A'(HO\text{-}SO_2\text{-}OH)+\nu_2 A'(H\text{-}SO_2\text{-}OH)$; sym.S-O str.
								$\nu_1 A'(HO\text{-}SO\text{-}OH)+\nu_2 A'(H\text{-}SO_2\text{-}OH)+\nu_9 A''(H\text{-}SO_2\text{-}OH)$
								$+\nu_5 E(H\text{-}SO_3^-)$ in Raman spec.; S-O str.+H-S def.
1151	vs	1151	vs	1151	m	1151	m	$\nu_1 A_1(SO_2)$; sym. S-O str.
		1210	wbr			1210	mbr	$\nu_7 A''(HO\text{-}SO\text{-}OH)+\nu_8 A''(H\text{-}SO_2\text{-}OH)+\nu_7 A''(HO\text{-}SO_2^-)$
								$+\nu_4 E\ (H\text{-}SO_3^-)+\nu_8 A''(HSO_4^-)$; asym. S-O str.
						1260	w	$\nu_6 A''(HO\text{-}SO\text{-}OH)+\nu_7 A''(H\text{-}SO_2\text{-}OH)+\nu_6 A''(HO\text{-}SO_2^-)$;
								S-O-H def.
1331	w	1331	w	1331	s	1331	s	$\nu_3 B_1(SO_2)$; asym. S-O str.
		2532	w					$\nu_1 A_1(H\text{-}SO_3^-)$.
		2608	w					$\nu_1 A'(H\text{-}SO_2\text{-}OH)$; H-S str.

Table III-7. The vibrational spectra of the thiosulphate ion

$Na_2S_2O_3$ (crystal, R.)		$Na_2S_2O_3 \cdot 5H_2O$ (crystal, R.)		$Na_2S_2O_3$ (solution, R.)		$Na_2S_2O_3$ (crystal, I.R.)		$Na_2S_2O_3$ (solution, I.R.)		Assignment
329	w	327	w			327	w			
		348	w	337	w	340	w			$\nu_6 E$; SO_3 rock.
368	w					369	w			
454	vs	437	vs	450	vs	455	w			$\nu_3 A_1$; S-S str.
540	w	548	w	536	w	536	s	536	w	$\nu_5 E$; asym. S-O def.
560	w					560	s			
		630	w							
674	s	675	w	669	m	674	s	669	m	$\nu_2 A_1$; sym. S-O def.
						907	vw			$\nu_5 + \nu_6$.
1004	s	1021	m	1000	s	1004	s	1000	s	$\nu_1 A_1$; sym. S-O str.
1139	w	1122	w	1122	mbr	1130	s	1122	vs	$\nu_4 E$; asym. S-O str.
1159	m	1168	w			1160	s			

Table III-8. The vibrational spectra of the argentothiosulphate complexes

$NaAgS_2O_3$[a] (cry., I.R.)		$AgTS^-$ (sol., I.R.)		$AgTS^-$ (sol., R.)		$Na_4Ag_2(S_2O_3)_3$[b] (cry., I.R.)		$Ag_2TS_3^{-4}$ (sol., I.R.)		$Ag_2TS_3^{-4}$ (sol., R.)		$Na_3Ag(S_2O_3)_2$[c] (cry., I.R.)		$AgTS_2^{-3}$ (sol., I.R.)		$AgTS_2^{-3}$ (sol., R)		Assignment
				242	w					242	w					242	vw	ν_4A_1;Ag-S str.
				340	w					340	w					340	w	$\nu_7E+\nu_7B_1$;SO_3 rock
				360	vw					360	vw					360	w	
419	w			420	s	420	w			420	s	420	w			430	s	ν_3A_1; S-S str.
533	m	531	w	531	w													ν_6E;asym.S-O def.
542	s					538	s					540	s					
						550	s	545	w	545	w	548	sh	545	w	545	w	ν_6B_1;asym.S-O def.
619	sh																	
632	vs	632	m	632	w	634	vs					635	sh					ν_2A_1;sym.S-O def.
						659	vs											
						670	sh	670		666	m	655	vs	665	w	665	w	ν_2A_1;sym.S-O def.
1008	vs	1000	s			1020	vs	999	s			1015	vs	999	vs			ν_1A_1;sym.S-O str.($S_2O_3^{2-}$-1+II).
										1020	m					1020	s	ν_1A_1($S_2O_3^{2-}$-II).
		1032	w			1036	sh	1030	m					1032	m			ν_1A_1($S_2O_3^{2-}$-I).
		1050	w	1050	vs					1050	s					1050	s	ν_1A_1($S_2O_3^{2-}$-I).
								1120	sh	1125	m			1118	sh			
1153	vs	1151	s	1160	w	1160	vs	1146	s	1160	w	1150	vsbr	1144	vs	1145	w	$\nu_5E+\nu_5B_1$;asym. S-Ostr.

continued

Table III-8 continued

$NaAgS_2O_3$[a] (cry.,I.R.)	$AgTS^-$ (sol.,I.R.)	$AgTS^-$ (sol.,R.)	$Na_4Ag_2(S_2O_3)_3$[b] (cry., I.R.)	$Ag_2TS_3^{-4}$ (sol.,I.R.)	$Ag_2TS_3^{-4}$ (sol.,R.)	$Na_3Ag(S_2O_3)_2$[c] (cry., I.R.)	$AgTS_2^{-3}$ (sol.,I.R.)	$AgTS_2^{-3}$ (sol.,R.)	Assignment
			1182 sh	1175 sh			1173 sh		
1210 vs									
1234 s			1227 sh			1225 sh			
	1370 vsbr			1370 sbr			1370 sbr		NO_3^-.

a = partially dehydrated at 65 C.

b,c = partially dehydrated at 120 C.

$S_2O_3^{2-}$-I = firmly bonded thiosulphate group.

$S_2O_3^{2-}$-II= loosely bonded, additional thiosulphate unit.

TS = thiosulphate.

Table III-9. The vibrational spectra of the tetrathionate ion

$Na_2S_4O_6$ (crystal, R.)		$Na_2S_4O_6$ (solution, R.)		$Na_2S_4O_6$ (crystal, I.R.)		$Na_2S_4O_6$ (solution, I.R.)		Assignment
138	m							
148	m	139	s					ν_5A; $SO_3 \cdot S.S_2O_3^{2-}$ def.
160	m							
184	w							
274	m	262	s					ν_4A; $S-S_2O_3^-$ str.
				298	m			
312	m	312	m	314	s	314	w	ν_8B; SO_3 rock.
398	vs	393	vs	395	s	393	w	ν_3A; $S-SO_3$ str.
				441	s			
526	sh							
533	m	530	m	527	s	535	m	ν_7B; asym. S-O def.
		547	wsh					
				600	s			
				632	s	617	w	
669	m	654	m			640	m	ν_2A; sym. S-O def.
		1025	w	1030	s	1020	s	

continued

Table III-9 continued

$Na_2S_4O_6$ (crystal, R.)		$Na_2S_4O_6$ (solution, R.)		$Na_2S_4O_6$ (crystal, I.R.)		$Na_2S_4O_6$ (solution, I.R.)		Assignment
1056	s	1046	vs	1052	s	1042	s	ν_1A; sym. S-O str.
				1116	w			
				1133	w			
				1155	w			
				1190	m			
1220	w	1225	wbr	1220	m	1225	sbr	ν_6B; asym. S-O str.
1241	w			1240	m			
1262	w							

Table III-10. The vibrational spectra of the dithionite ion

$Na_2S_2O_4$ (crystal, R.)		$Na_2S_2O_4$ (solution, R.)		$Na_2S_2O_4$ (crystal, I.R.)		$Na_2S_2O_4$ (solution, I.R.)		Assignment
70	m							
89	w							
101	s							
116	w							
139	m							
164	w							
175	sh							
185	s	180	sh					
259	vs	234	vs					ν_4A; SO_2 wag.
300	w							
345	w	330	w					ν_7B; SO_2 twist.
366	vs			367	vw			S-S str.
				426	s			
439	vw			444	ssh			
		463	s					ν_3A; S-S str.
509	vw			510	s	502	vw	ν_6B; asym. S-O def.
				524	sh			

continued

Table III-10 continued

$Na_2S_2O_4$ (crystal, R.)		$Na_2S_2O_4$ (solution, R.)		$Na_2S_2O_4$ (crystal, I.R.)		$Na_2S_2O_4$ (solution, I.R.)		Assignment
				542	s			
				553	s			
		585	m					ν_2A; sym. S-O def.
				622	sh			
				631	m			
662	vw			656	s			
				670	s			
910	vw	920	vw	920	s	920	s	ν_1A; sym. S-O str.
				997	w			
1023	vw			1017	m			
1034	w			1030	s			
1046	w			1045	m			
1064	vw							
1070	vw	1070	vw	1060	s	1059	s	ν_5B; asym. S-O str.

Table III-11. The vibrational spectra of a fresh and of a standing aqueous dithionite solution

$Na_2S_2O_4$ (fresh, R.)		$Na_2S_2O_4$ (standing, R.)		$Na_2S_2O_4$ (fresh, I.R.)		$Na_2S_2O_4$ (standing, I.R.)		Assignment
180	sh							
234	vs							$\nu_4 A(S_2O_4^{2-})$.
		235	m					$\nu_8 A'(S_2O_5^{2-})$.
330	w							$\nu_7 B(S_2O_4^{2-})$.
		336	w					$\nu_6 E(S_2O_3^{2-})$.
		400	w					$\nu_5 A' + \nu_9 A''(HO\text{-}S\bar{O}_2)$.
		430	w			427	w	$\nu_7 A'(S_2O_5^{2-})$.
		450	vs					$\nu_3 A_1(S_2O_3^{2-})$.
		460	sh					$\nu_4 A'(HO\text{-}S\bar{O}_2)$.
463	s							$\nu_3 A(S_2O_4^{2-})$.
				502	vw			$\nu_6 B(S_2O_4^{2-})$.
		510	w			510	w	$\nu_{12} A''(S_2O_5^{2-}) + \nu_6 E(H\text{-}S\bar{O}_3)$.

continued

Table III-11 continued

$Na_2S_2O_4$ (fresh, R.)		$Na_2S_2O_4$ (standing, R.)		$Na_2S_2O_4$ (fresh, I.R.)		$Na_2S_2O_4$ (standing, I.R.)		Assignment
		537	w			536	w	$\nu_5 E(S_2O_3^{2-})$.
585	m							$\nu_2 A(S_2O_4^{2-})$.
		587	w			586	w	$\nu_8 A''(HO\text{-}S\bar{O}_2)$.
		635	w			634	w	$\nu_5 A'(S_2O_5^{2-}) + \nu_3 A_1(H\text{-}S\bar{O}_3)$.
		657	wsh			657	wsh	$\nu_4 A'(S_2O_5^{2-})$.
		670	m			669	m	$\nu_2 A'(S_2O_3^{2-})$.
		715	w			771	w	$\nu_3 A'(HO\text{-}S\bar{O}_2)$.
920	vw			920	s			$\nu_1 A(S_2O_4^{2-})$.
		965	w			940	w	$\nu_1 A_1 + \nu_3 E(SO_3^{2-})$.
						966	m	$\nu_3 A'(S_2O_5^{2-})$.
984	vw	984	m					$\nu_1 A_1(SO_4^{2-})$.
1000	w	1000	s	1000	w	1000	s	$\nu_1 A_1(S_2O_3^{2-})$.
						1015	sh	

continued

Table III-11 continued

$Na_2S_2O_4$ (fresh, R.)		$Na_2S_2O_4$ (standing, R.)		$Na_2S_2O_4$ (fresh, I.R.)		$Na_2S_2O_4$ (standing, I.R.)		Assignment
1025	w	1025	s	1030	vw	1025	m	$\nu_2 A'(HO\text{-}SO_2)$.
1052	w	1055	vs	1052	vw	1054	m	$\nu_2 A'(S_2O_5^{2-}) + \nu_2 A_1(H\text{-}S\bar{O}_3)$.
1070	vw			1059	s			$\nu_5 B(S_2O_4^{2-})$.
						1081	m	$\nu_1 A'(S_2O_5^{2-}) + \nu_1 A'(HO\text{-}S\bar{O}_2)$.
		1093	w					$\nu_1 A_1(S_2O_6^{2-})$.
						1104	sh	$\nu_3 F_2(SO_4^{2-})$.
		1125	m			1115	s	$\nu_4 E(S_2O_3^{2-}).\nu_4 E(S_2O_3^{2-}) + \nu_5 E(H\text{-}S\bar{O}_3)$ in Roman Spec.
						1170	m	$\nu_{10} A''(S_2O_5^{2-})$.
		1210	wbr			1217	sbr	$\nu_9 A''(S_2O_5^{2-}) + \nu_4 E(H\text{-}S\bar{O}_3) + \nu_7 A''(HO\text{-}S\bar{O}_2)$.
						1245	w	$\nu_4 A_2(S_2O_6^{2-})$.
						1260	w	$\nu_6 A''(HO\text{-}S\bar{O}_2)$.
		2535	w					$\nu_1 A_1(H\text{-}S\bar{O}_3)$.

Table III-12. Detection limits

anion	ν,R. / Cm^{-1}	C / M	anion	ν,R. / Cm^{-1}	C / M	anion	ν,R. / Cm^{-1}	C / M
$S_2O_6^{2-}$	282,1093	0.01	SO_3^{2-}	968	0.03	$S_2O_3^{2-}$	450	0.02
$S_2O_5^{2-}$	427,1055	0.02	SO_4^{2-}	984	0.01	$S_4O_6^{2-}$	393,1046	0.01
$H\text{-}S\bar{O}_3$	1055	0.02	$HS\bar{O}_4$	1054	0.04	$S_2O_4^{2-}$	463	0.04
$HO\text{-}S\bar{O}_2$	1025	0.01						

R = Raman, C = Concentration, M = $moldcm^{-3}$.

Chapter IV

Results and Discussion

(calorimetric)

IV. Results and Discussion (calorimetric)

IV-A. Elucidation of the argentothiosulphate, $[Ag_m(S_2O_3)_n]^{-2n+m}$, complexes:-

In terms of the molar ratios of the reactants involved, the formation of distinct products should be indicated as inflection points on profiles relating composition to some measureable physical properties. Among other techniques, calorimetry seemed to be promising since effective stirring and precise control of the stoichiometry of the reactants are crucial. Furthermore, the heating effects of the reactions involved are considerable and can be precisely determined.

Based upon the above points, and in order to identify the species involved in photographic fixation, the reactions between silver and thiosulphate ions have been calorimetrically investigated. The associated heat effects are displayed in Tables IV-1, IV-3, IV-4, IV-7 and IV-8. The data contained in Tables IV-3 and IV-7 have been derived from thermo-titrimetric graphs. Those determined using ampoule-mode calorimetry are given in Tables IV-1 and IV-4, and are graphically displayed in Figs. IV-1 and IV-3. The ampoule-mode calorimetry has been used for selected molar ratios, and the thermo-titrimetry which follows all processes in a single run has been employed in order to elucidate the proper mechanism.

As the ampoule calorimetry results in Fig. IV-1 illustrate, the

additions of silver ions to aqueous thiosulphate solutions reveal three discontinuities at $S_2O_3^{2-}$: Ag^+ molar ratios of 2:1, 1:1 and 0.5:1 indicating the existence of $[Ag(S_2O_3)_2]^{-3}$, $AgS_2O_3^-$ and of the $Ag_2S_2O_3$ species respectively. The same conclusions have been derived by inspection of the corresponding thermo-titrimetric curve presented in Fig. IV-2.

Tables IV-4 and IV-7 display the results of the reverse procedure, in which thiosulphate ions are added to silver nitrate solutions. As Fig. IV-3 illustrates, and by revealing an additional inflection point at $S_2O_3^{2-}$: Ag^+ molar ratio of 1.5:1, the ampoule-mode calorimetry has indicated the existence of a fourth, $[Ag_2(S_2O_3)_3]^{-4}$, species. In the corresponding thermal titrimetry, and prior to a well-defined break at the 0.5:1 molar ratio a number of poorly-defined inflection points are indicated as shown in Fig. IV-4. As a consequence, a number of 'double formula intermediates' defined as $Ag_2S_2O_3 \cdot xAgNO_3$ have been suggested on the basis of the molar ratios involved. The value of x decreases progressively as titration proceeds, producing eventually the $Ag_2S_2O_3$ species as the well-defined inflection point at the 0.5:1 $S_2O_3^{2-}$: Ag^+ molar ratio indicates. Since the silver ion is in excess upon initial mixing, then the reaction sequence in the reverse titration can be summarised by the following equations:

$$S_2O_3^{2-} + (2 + x)Ag^+ = Ag_2S_2O_3 \cdot xAgNO_3 \text{ (aq)}$$

$$x/_2 S_2O_3^{2-} + Ag_2S_2O_3 \cdot xAgNO_3(aq) = (1 + x/_2)Ag_2S_2O_3(aq) + xNO_3^-$$

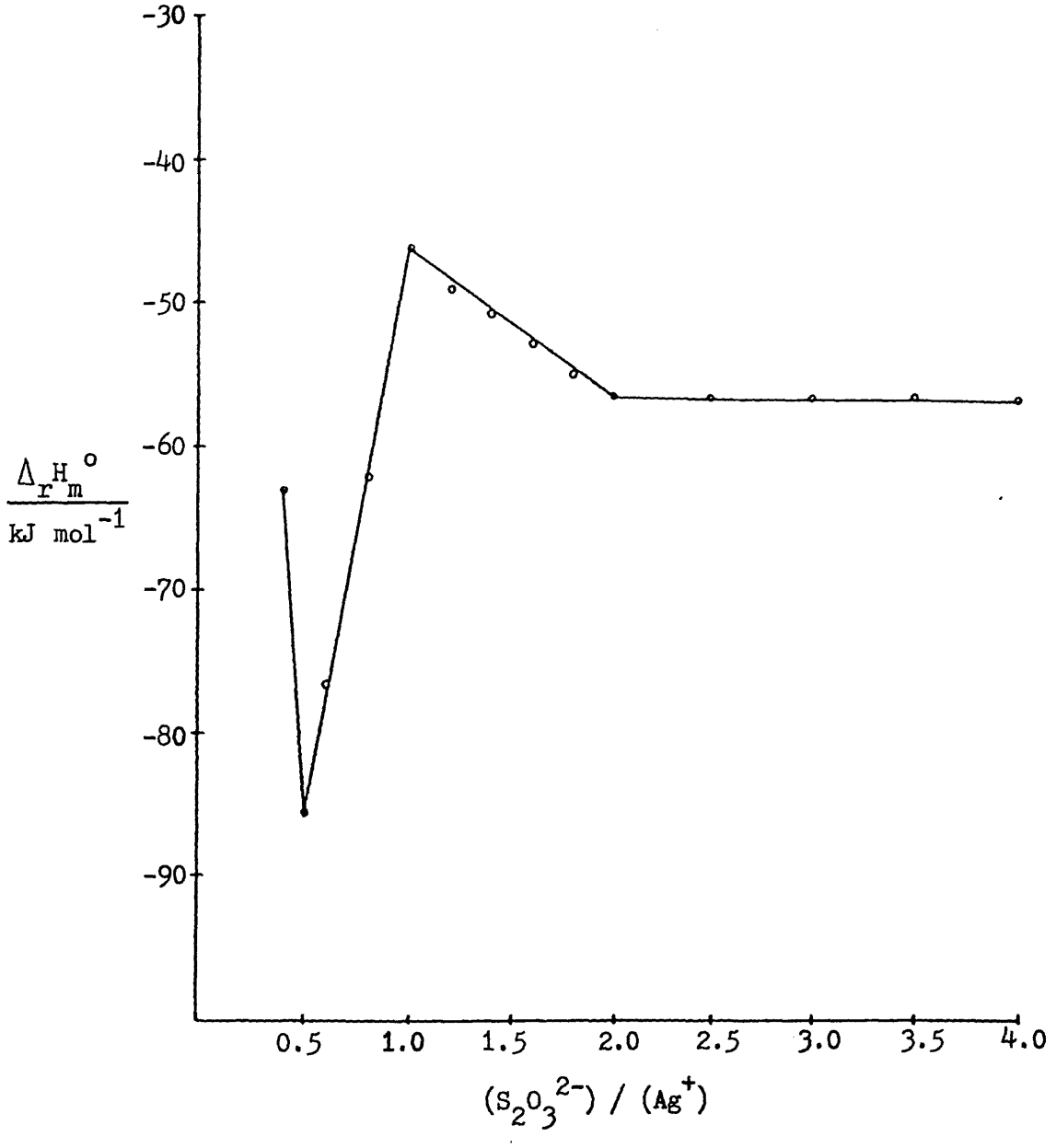

Fig. IV-1. $\Delta_r H_m^o$ vs $(S_2O_3^{2-})$ / (Ag^+) plot for the $Ag^+/S_2O_3^{2-}$ reactions (direct)

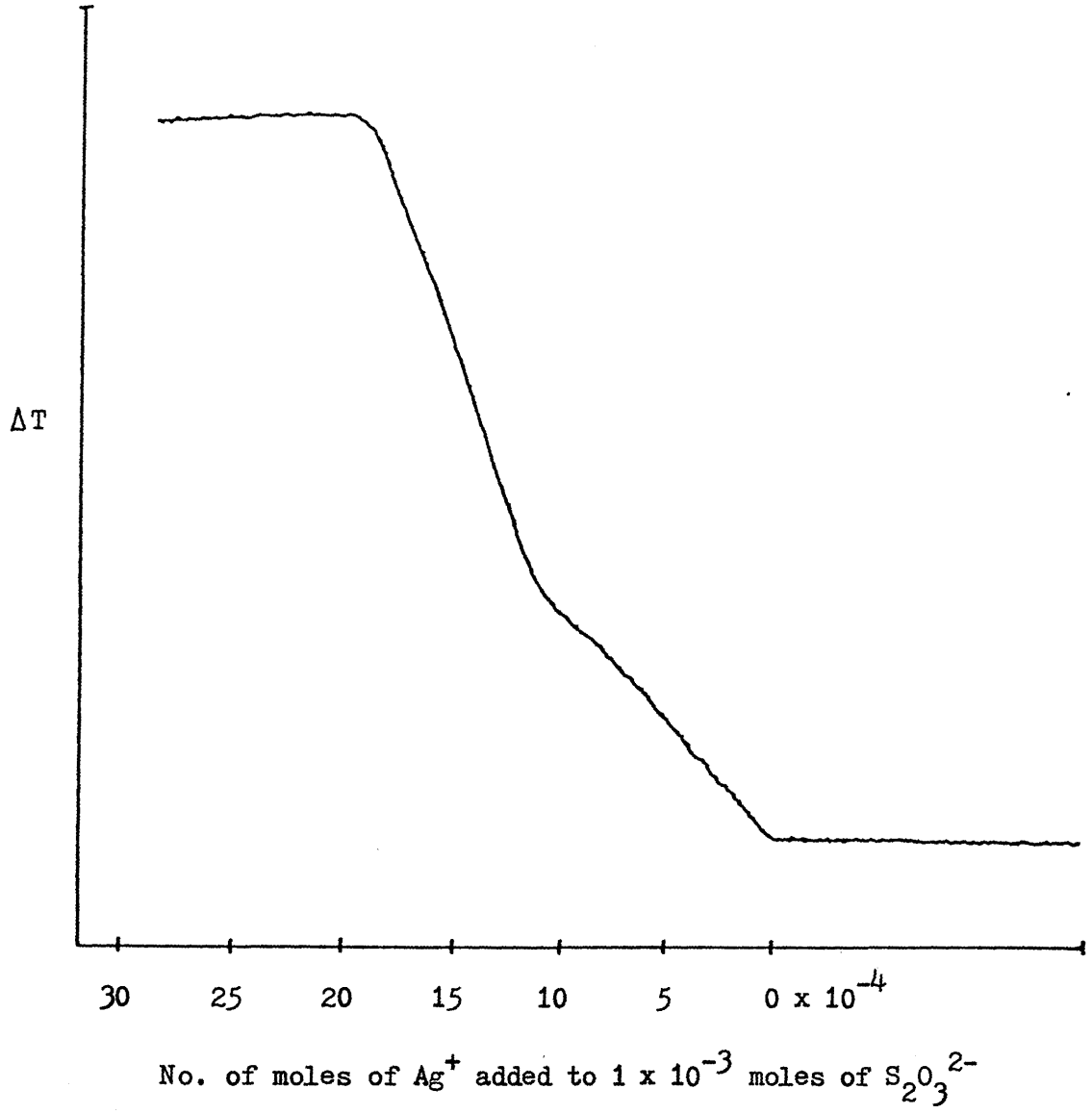

Fig. IV-2. Thermometric titration of $Ag^+/S_2O_3^{2-}$ (direct)

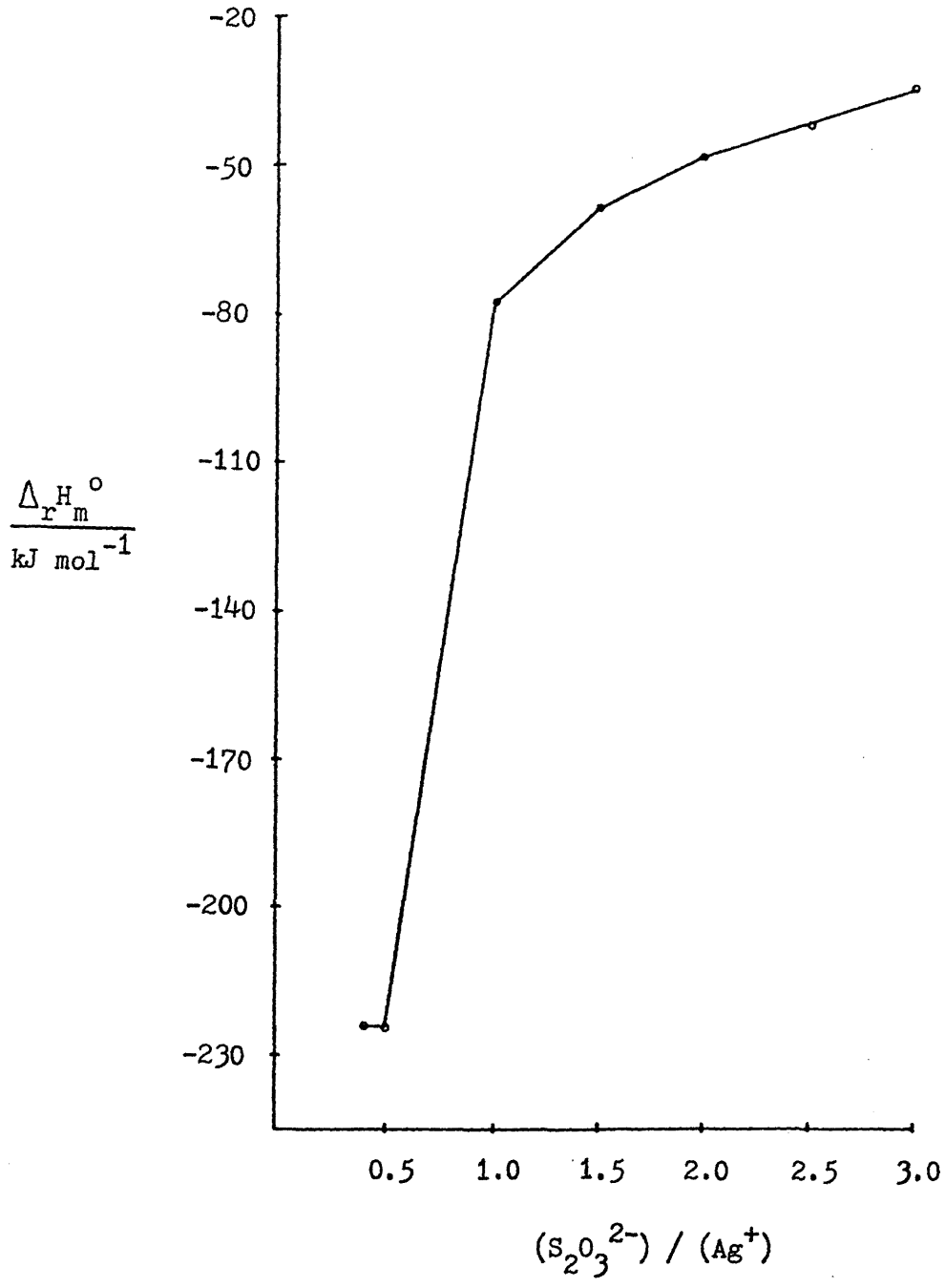

Fig. IV-3. $\Delta_r H_m^o$ vs $(S_2O_3^{2-})$ / (Ag^+) plot of the $S_2O_3^{2-}/Ag^+$ reactions (reverse)

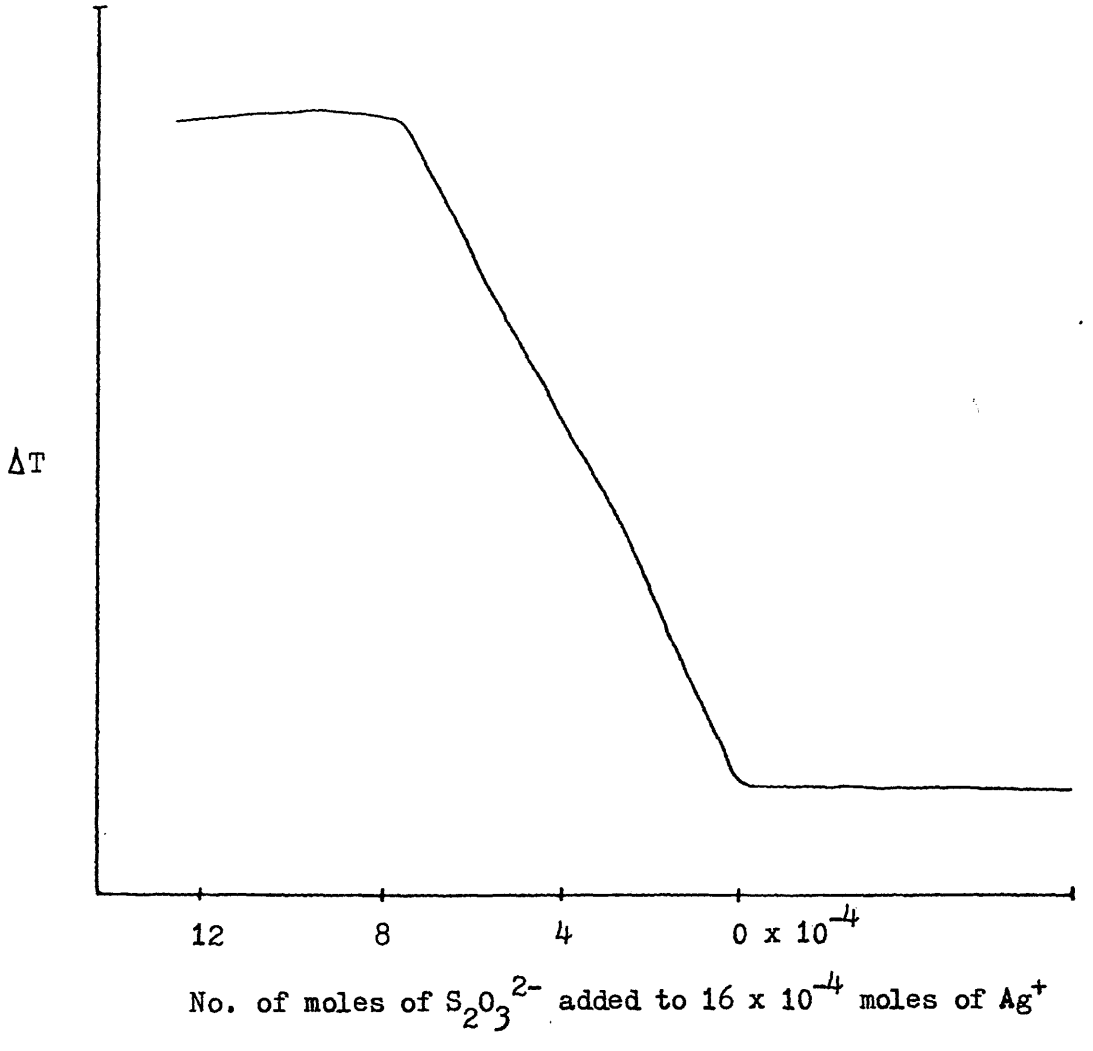

Fig. IV-4. Thermometric titration of $S_2O_3^{2-}/Ag^+$ (reverse)

$$Ag_2S_2O_3(aq) + H_2O = Ag_2S(c) + SO_4^{2-} + 2H^+$$

Based upon the above identifications and upon the sequential nature of the process involved, the following mechanism has been derived:

$$Ag^+ + 2S_2O_3^{2-} = [Ag(S_2O_3)_2]^{-3}$$

$$Ag^+ + S_2O_3^{2-} + [Ag(S_2O_3)_2]^{-3} = [Ag_2(S_2O_3)_3]^{-4}$$

$$Ag^+ + [Ag_2(S_2O_3)_3]^{-4} = 3AgS_2O_3^-$$

$$Ag^+ + AgS_2O_3^- = Ag_2S_2O_3\ (aq)$$

$$Ag_2S_2O_3(aq) + H_2O = Ag_2S(c) + SO_4^{2-} + 2H^+$$

With thorough stirring and excess of Ag^+, the overall process is very fast and irreversible. Poor stirring always results in instantaneous formation of the black Ag_2S precipitate. The sequence of the colour changes observed, (colourless → yellow → dark), during these reactions is in accordance with the formation of the above intermediates and not with the formation of the $Ag_2S_2O_3$ compound only as stated in almost all textbooks. Thus, the formation of a particular species is dependant upon the stoichiometry of the reactants and the efficiency of stirring. Although identifications of the $[Ag(S_2O_3)_2]^{-3}$, $AgS_2O_3^-$ and $Ag_2S_2O_3$ are consistent with some previous work[55-60], detection of species other than $Ag_2S_2O_3$ and its 'double formula intermediates' in the reverse

titration[59,60] has been ruled out on the basis of the above points.

In this work, the first three of the above intermediates have been isolated in the solid phase. Based upon their vibrational spectra, (see III-7), C_{3v} group symmetry has been assigned to the $AgS_2O_3^-$ compound and C_{2v} group to both $[Ag(S_2O_3)_2]^{-3}$ and $[Ag_2(S_2O_3)_3]^{-4}$ species. The short-lived compound $Ag_2S_2O_3$ has been described in terms of C_{2v} symmetry also, in which the constituent Ag_2S and SO_3 units are loosely held together by a very weak S-S bond. The rupture of this bond is believed to occur almost immediately when the $Ag^+:S_2O_3^{2-}$ molar ratio exceeds 2:1. As discussed in III-7, the rupture occurs as a result of continuous drifting of the electron-density of the S-S bond by the second Ag^+ ion in order to form the second Ag-S bond in $Ag_2S_2O_3$ as the following process illustrates:

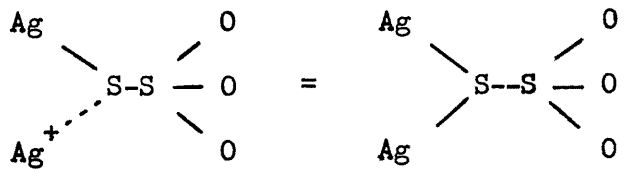

$= Ag_2S(c)+SO_3(g)$

(i) (ii) (iii)

It appears to be synchronising with the completion of the second Ag-S bond formation, the duration of which is believed to be the lifetime of the $Ag_2S_2O_3$ species. No evidence, (a break or an inflection point), for the S-S bond scission has been revealed by the enthalpy-composition curves, Figs. IV-1-4, and hence it is believed to be an athermal process. At $Ag^+:S_2O_3^{2-}$

molar ratios greater than 2:1 and less than 0.5:1, Figs. IV-1 and IV-3 describe the enthalpies of solution of the unreacted $AgNO_3$ and $Na_2S_2O_3$ crystals respectively. The enthalpy changes at these points being quantitatively in agreement with those experimentally measured, Tables IV-2 and IV-5, confirm the non-existence of stoichiometries other than those considered above. The non-occurrence of analogous features on the corresponding thermo-titrimetric graphs, Figs. IV-2 and IV-4, is due to the negligible values (45×10^{-4} kJ mol^{-1}) of the appropriate dilution processes.

Qualitative analyses of the decomposition products for the overall reaction have revealed the formation of the SO_4^{2-} and of the H^+ species. The former has been quantitatively confirmed via precipitation of $BaSO_4$ under standard gravimetric conditions. The latter was confirmed by standard titrimetry. Thus, the aqueous thiosulphate ion is rapidly, easily and quantitatively convertible into the sulphate species.

<u>IV-B. Validation of the reaction: $S_2O_3^{2-} + 2Ag^+ + H_2O = Ag_2S(c) + SO_4^{2-} + 2H^+$:-</u>

Validation of this equation was fully established by duplicate quantitative determinations of Ag_2S, SO_4^{2-} and of H^+ as follows:

Solutions of known compositions, (0.15M), were prepared by dissolving known masses of $Na_2S_2O_3 \cdot 5H_2O$ in definite volumes of de-aerated, deionised distilled water. While being thoroughly stirred, to each

solution 0.10M silver nitrate was added in drops from a burette up to the decomposition point. A slight excess of Ag^+ ions was always added in order to ensure complete conversion of all thiosulphate species. The supernatant liquid was then filtered off via a weighed silica filtering crucible of porosity 4. After being washed several times with de-aerated, deionised distilled water, the crucible and its contents were dried at 140°C, cooled to room temperature in a desiccator and then weighed. The process of drying, cooling and weighing was repeated until constant weight was attained. The weights of the Ag_2S precipitate so obtained are displayed in Table IV-9.

A slight excess of Cl^- ions from a barium-free solution was added to the filtrate in order to remove excess Ag^+. The second supernatant liquid so obtained was then filtered through another silica filtering crucible. The crucible and its contents were thoroughly washed, and the precipitated AgCl discarded. The filtrate was then gently heated to reduce volume, and a slight excess of 0.20M barium chloride solution was added in order to precipitate sulphate ions. The resultant supernatant liquid was filtered off via a silica filtering crucible of a known mass, and after being washed thoroughly the crucible and its contents were dried at 500°C, cooled in a desiccator and then weighed. The sequence of drying, cooling and weighing was repeatedly performed until constant weight was attained. The filtrate was then collected into a 250 cm^3 volumetric flask, diluted up to the mark, and, after shaking, 25.00 cm^3 aliquots were pipetted for titrations with 0.10M NaOH

solution in the presence of two drops of phenolphthalein indicator. Results, together with those of $BaSO_4$, are given in Table IV-9. The following set of equations is hence derived in order to illustrate the process of thiosulphate conversion:

$$2Ag^+ + S_2O_3^{2-} = Ag_2S_2O_3\ (aq) \qquad (1)$$

$$Ag_2S_2O_3(aq) = Ag_2S(c) + SO_3(aq) \qquad (2)$$

$$SO_3(aq) + H_2O = SO_4^{2-} + 2H^+ \qquad (3)$$

With the second and third steps occurring almost concurrently.

IV-C-1. The standard molar enthalpy of formation of aqueous sodium thiosulphate:-

In order to re-evaluate this because of the undefined uncertainty in the recommended value (-1125.50 kJ mol^{-1})[103], a novel experimental method based upon the reaction: $S_2O_3^{2-} + 2Ag^+ + H_2O = Ag_2S(c) + SO_4^{2-} + 2H^+$ is employed. The standard molar enthalpy of reaction, $\Delta_r H_m^\circ$, associated with equation (1) is determined.

$$2AgNO_3(c) + Na_2S_2O_3(aq) + H_2O(liq) = Ag_2S(c) + H_2SO_4(aq) + 2Na_2NO_3(aq) \qquad (1)$$

Hence equation (2) is obtained:

$$\Delta_f H_m^\circ\ Na_2S_2O_3(aq) = \Delta_f H_m^\circ\ Ag_2S(c) + \Delta_f H_m^\circ\ H_2SO_4(aq) + 2\Delta_f H_m^\circ\ NaNO_3(aq) - 2\Delta_f H_m^\circ\ AgNO_3(c) - \Delta_f H_m^\circ\ H_2O(liq) - \Delta_r H_m^\circ \qquad (2)$$

Conversion of thiosulphate into sulphate in this reaction is a two-step process:

$$2AgNO_3(c) + Na_2S_2O_3(aq) = Ag_2S_2O_3(aq) + 2NaNO_3(aq) \quad (3)$$

$$Ag_2S_2O_3(aq) + H_2O(liq) = Ag_2S(c) + H_2SO_4(aq) \quad (4)$$

Since hydrolysis of $Ag_2S_2O_3(aq)$ is believed to be athermal, (see IV-A), then the enthalpy of the overall reaction is equivalent to that of reaction (3).

Perrott and Fletcher[113] have reported the existence of Ag_2S in three different crystal modifications identified as α, β and γ. Being stable at ordinary temperatures[113], the β-phase is taken to be that involved in the calorimetric reaction. Using differential scanning calorimetry Ghosh and Nag[114] have determined the enthalpy changes of the $\beta \rightarrow \alpha$ and of the reverse transition.

Using appropriate ancillary data given in Table IV-10 together with the standard molar enthalpy of the reaction involved (1), contained in Table IV-1, the standard molar enthalpy of formation of aqueous sodium thiosulphate is calculated, using equation (2), to be:

$$\Delta_f H^\circ_m \, Na_2S_2O_3(aq) = -29.41 \pm 0.25 - 909.27 \pm 0.17 + 2(-447.15 \pm 0.41)$$

$$- 2(-124.39 \pm 0.25) - (-285.830 \pm 0.042) - 2(-85.41 \pm 0.16) =$$

$$- 1127.55 \pm 1.06 \text{ kJ mol}^{-1}.$$

Two similar values have been derived using thermo-titrimetric results given in Tables IV-3 and IV-7 together with the following equations:

$$2AgNO_3(aq) + Na_2S_2O_3(aq) + H_2O(liq) = Ag_2S(c) + H_2SO_4(aq) + 2NaNO_3(aq) \quad (1)$$

$$\Delta_f H_m^\circ\ Na_2S_2O_3(aq) = \Delta_f H_m^\circ\ Ag_2S(c) + \Delta_f H_m^\circ H_2SO_4(aq) + 2\Delta_f H_m^\circ\ NaNO_3(aq) - 2\Delta_f H_m^\circ\ AgNO_3(aq) - \Delta_f H_m^\circ\ H_2O(liq) - \Delta_r H_m^\circ \quad (2)$$

Substitution of $\Delta_r H_m^\circ$ contained in Table IV-3 in equation (2) gives:

$$\Delta_f H_m^\circ\ Na_2S_2O_3(aq) = -29.41 \pm 0.25 - 909.27 \pm 0.17 + 2(-447.15 \pm 0.41) - 2(-101.10 \pm 0.41) - (-285.830 \pm 0.042) - 2(-108.17 \pm 0.20) = -1128.61 \pm 1.26\ kJ\ mol^{-1}.$$

Substitution of $\Delta_r H_m^\circ$ given in Table IV-7 in the same equation yields:

$$\Delta_f H_m^\circ\ Na_2S_2O_3(aq) = -29.41 \pm 0.25 - 909.27 \pm 0.17 + 2(-447.15 \pm .41) - 2(-101.10 \pm 0.41) - (285.830 \pm 0.042) - (-216.37 \pm 0.15) = -1128.58 \pm 1.21\ kJ\ mol^{-1}.$$

The standard molar enthalpy of formation of $Na_2S_2O_3$ crystal is evaluated according to the following equations:

$$Na_2S_2O_3(c) + 2AgNO_3(aq) + H_2O(liq) = Ag_2S(c) + H_2SO_4(aq) + 2NaNO_3(aq)$$

$$\Delta_f H_m^\circ\ Na_2S_2O_3(c) = \Delta_f H_m^\circ\ Ag_2S(c) + \Delta_f H_m^\circ\ H_2SO_4(aq)$$

$$+ 2\Delta_f H_m^\circ\ NaNO_3(aq) - 2\Delta_f H_m^\circ\ AgNO_3(aq) - \Delta_f H_m^\circ\ H_2O(liq) - \Delta_r H_m^\circ.$$

Substitution of $\Delta_r H_m^\circ$ contained in Table IV-4 gives:

$$\Delta_f H_m^\circ\ Na_2S_2O_3(c) = 29.41\pm0.25 - 909.27\pm0.17 + 2(-447.15\pm0.41)$$

$$- 2(-101.10\pm0.41) - (-285.830\pm0.042) - (-224.18\pm0.19) =$$

$$-1120.77\pm1.21\ kJ\ mol^{-1}.$$

The literature values is -1117.13 kJ mol^{-1} [103].

Another value for the enthalpy of formation of aqueous sodium thiosulphate is derived by adding the enthalpy of solution of $Na_2S_2O_3(c)$ given in Table IV-5 to $\Delta_f H_m^\circ\ Na_2S_2O_3(c)$ calculated above as:

$$\Delta_f H_m^\circ\ Na_2S_2O_3(aq) = -1120.77\pm1.21 - 7.67\pm0.12 = -1128.44\pm1.22$$

$$kJ\ mol^{-1}.$$

The mean of the above four values, (-1128.30 ± 0.59kJ mol^{-1}), is calculated to be the standard molar enthalpy of formation of aqueous sodium thiosulphate in 1.00 molal solution. The literature value is -1125.50kJ mol^{-1} [103].

Using this value together with the standard molar enthalpy of formation of aqueous Na^+ ion given in Table IV-10 the standard molar

enthalpy of formation of the aqueous thiosulphate ion is evaluated according to the equation: $Na_2S_2O_3(aq)=2Na^+(aq)+S_2O_3^{2-}(aq)$ as:

$$-1128.30\pm0.59 = 2(-240.300\pm0.065) + \Delta_f H^\circ_m\ S_2O_3^{2-}(aq).$$

Hence:

$\Delta_f H^\circ_m\ S_2O_3^{2-}(aq) = -647.70\pm0.60$ kJ mol^{-1}. The literature value is -652.29 kJ mol^{-1} [102].

IV-C-2. The standard molar enthalpy of formation of sodium thiosulphate pentahydrate crystal:-

By assuming that thiosulphate behaves like sulphate, Zimmermann and Latimer[101] have estimated the enthalpy change associated with dilution by the water of crystallisation in $Na_2S_2O_3\cdot5H_2O$ as 130 cal (0.54 kJ). Applying this correction they evaluated the enthalpy of solution of $Na_2S_2O_3\cdot5H_2O(c)$ to be 46.74 ± 0.42kJ mol^{-1}. Applying the same correction to the experimental value given in Table IV-6 we get:

$$47.21\pm0.14 - 0.54 = 46.67\pm0.14 \text{ kJ mol}^{-1}.$$

Combination of this value with $\Delta_f H^\circ_m\ Na_2S_2O_3(aq)$ derived above yields the standard molar enthalpy of formation of $Na_2S_2O_3\cdot5H_2O(c)$:

$\Delta_f H^\circ_m\ Na_2S_2O_3\cdot5H_2O(c) = -1128.30\pm0.59 - 46.67\pm0.14 =$ -1174.97 ± 0.61 kJ mol^{-1}. The literature value is -2601.99 kJ mol^{-1} [103].

The enthalpies of formation of $Na_2S_2O_3(aq)$, $Na_2S_2O_3(c)$, $S_2O_3^{2-}(aq)$

and $Na_2S_2O_3 \cdot 5H_2O(c)$ derived in this work are more precise than those reported earlier[102,103]. The original data from which the recommended values[102,103] were derived are those measured by Bichowsky[100] and Zimmermann and Latimer[101]. The reactions used for the enthalpy determination were the acid hydrolyses of calcium thiosulphate and calcium sulphite dihydrate[100]. The overall process was summarised by the following equation:

$$S + CaSO_3 \cdot 2H_2O = CaS_2O_3(aq) + 2H_2O$$

Although this reaction is reversible and very slow at temperatures below 110°C[100] and as a consequence not suitable for calorimetric measurements, a fair agreement exists between the values derived herein and those previously reported[102,103]. To rationalise this on the basis of the actual determinations given by Bichowsky[100] the following set of equations is suggested:

$$S_2O_3^{2-} + 2H^+ = S + SO_2 + H_2O; \Delta_{r1}H_m^\circ \qquad (1)$$

$$SO_3^{2-} + 2H^+ = SO_2 + H_2O; \Delta_{r2}H_m^\circ \qquad (2)$$

$$S_2O_3^{2-} = S + SO_3^{2-}; \Delta_{r1}H_m^\circ - \Delta_{r2}H_m^\circ \qquad (3)$$

Both reactions (1) and (2) are irreversible and very fast. Thus they are potentially useful for thermochemical measurements. According to the above scheme, the enthalpy of reaction (3) and hence of that reported by Bichowsky[100] can only be indirectly measured. The literature value of $\Delta_f H_m^\circ Na_2S_2O_3 \cdot 5H_2O(c)$ was derived[103] according to the following equations:

$$Na_2S_2O_3 \cdot 5H_2O(c) + nH_2O(liq) = [Na_2S_2O_3(aq) + 5H_2O(liq)]_{(nH_2O,aq)}$$

$$\Delta_f H_m^\circ Na_2S_2O_3 \cdot 5H_2O(c) = \Delta_f H_m^\circ Na_2S_2O_3(aq) + 5\Delta_f H_m^\circ H_2O - \Delta H_s^\circ$$

where ΔH_s° is the enthalpy of solution of $Na_2S_2O_3 \cdot 5H_2O(c)$.

Gronvold and Meisingset[104] have investigated phase transitions in $Na_2S_2O_3 \cdot 5H_2O(c)$ and reported that it melts incongruently at 321.31K forming $Na_2S_2O_3 \cdot 2H_2O$ plus aqueous solution. Using the following equations,

$$Na_2S_2O_3 \cdot 5H_2O(c) = Na_2S_2O_3 \cdot 2H_2O(c) + 3H_2O(liq)$$

$$\Delta_f H_m^\circ Na_2S_2O_3 \cdot 2H_2O(c) = \Delta_f H_m^\circ Na_2S_2O_3 \cdot 5H_2O(c) - 3\Delta_f H_m^\circ H_2O(liq) + \Delta H_t^\circ$$

where ΔH_t° is the enthalpy of the transition,

together with the reported enthalpy change[104], the standard molar enthalpy of formation of $Na_2S_2O_3 \cdot 2H_2O(c)$ is tentatively calculated to be:

$$\Delta_f H_m^\circ Na_2S_2O_3 \cdot 2H_2O(c) = -1174.97 \pm 0.61 - 3(-285.830 \pm 0.042) + 48.8 \pm 0.6 = -268.68 \pm 0.86 \text{ kJ mol}^{-1}.$$

IV-D. The standard molar enthalpies of formation of the argentothiosulphate complexes:-

Four compounds, formulated as $Na_3Ag(S_2O_3)_2$, $Na_4Ag_2(S_2O_3)_3$,

$NaAgS_2O_3$ and $Ag_2S_2O_3$, have been identified by the enthalpy-composition curves, (Figs. IV-1-4), in this work. Among them, the enthalpy of formation of the complex ion $[Ag(S_2O_3)_2]^{-3}$ only is known[103,107,108]. However, its existence was not verified.

IV-D-1. The standard molar enthalpy of formation of aqueous $Na_3Ag(S_2O_3)_2$:-

Using the following equations,

$$AgNO_3(c) + 2Na_2S_2O_3(aq) = Na_3Ag(S_2O_3)_2(aq) + NaNO_3(aq)$$

$$\Delta_f H^\circ_m\ Na_3Ag(S_2O_3)_2(aq) = \Delta_f H^\circ_m\ AgNO_3(c) + 2\Delta_f H^\circ_m\ Na_2S_2O_3(aq) + \Delta_r H^\circ_m - \Delta_f H^\circ_m\ NaNO_3(aq),$$

together with appropriate data from Tables IV-1 and IV-10, the standard molar enthalpy of formation of $Na_3Ag(S_2O_3)_2(aq)$ is evaluated as:

$$\Delta_f H^\circ_m\ Na_3Ag(S_2O_3)_2(aq) = -124.39\pm0.25 + 2(-1128.30+0.59) + (-55.95\pm0.19) - (-447.15\pm0.41) = -1989.79\pm1.29\ kJ\ mol^{-1}.$$

$$\Delta_f H^\circ_m\ Na_3Ag(S_2O_3)_2(aq) = -124.39\pm0.25 + 2(-1128.30\pm0.59) + (-55.94\pm0.18) - (-447.15\pm0.41) = -1989.78\pm1.29\ kJ\ mol^{-1}.$$

$$\Delta_f H^\circ_m\ Na_3Ag(S_2O_3)_2(aq) = -124.39\pm0.25 + 2(-1128.30\pm0.59) + (-56.01\pm0.17) - (-447.15\pm0.41) = -1989.85\pm1.29\ kJ\ mol^{-1}.$$

Using the thermo-titrimetric result given in Table IV-3 together with the following equations,

$$AgNO_3(aq) + 2Na_2S_2O_3(aq) = Na_3Ag(S_2O_3)_2(aq) + NaNO_3(aq)$$

$$\Delta_f H_m^\circ\ Na_3Ag(S_2O_3)_2(aq) = \Delta_f H_m^\circ\ AgNO_3(aq) + 2\Delta_f H_m^\circ\ Na_2S_2O_3(aq) + \Delta_r H_m^\circ - \Delta_f H_m^\circ\ NaNO_3(aq),$$

a similar value is derived as:

$$\Delta_f H_m^\circ\ NaAg(S_2O_3)_2(aq) = -101.10 \pm 0.41 + 2(-1128.30 \pm 0.59) + (-78.89 \pm 0.19) - (-447.15 \pm 0.41) = -1989.44 \pm 1.33\ kJ\ mol^{-1}.$$

Another value is calculated using the result of the reverse addition, contained in Table IV-4, together with the following equations,

$$2Na_2S_2O_3(c) + AgNO_3(aq) = Na_3Ag(S_2O_3)_2(aq) + NaNO_3(aq)$$

$$\Delta_f H_m^\circ\ Na_3Ag(S_2O_3)_2(aq) = 2\Delta_f H_m^\circ\ Na_2S_2O_3(c) + \Delta_f H_m^\circ\ AgNO_3(aq) + 2\Delta_r H_m^\circ - \Delta_f H_m^\circ\ NaNO_3(aq),$$

$$\Delta_f H_m^\circ\ Na_3Ag(S_2O_3)_2(aq) = 2(-1120.77 \pm 1.21) + (-101.10 \pm 0.41) + 2(-46.97 \pm 0.15) - (-447.15 \pm 0.41) = -1989.43 \pm 2.51\ kJ\ mol^{-1}.$$

The mean of the above five values, (-1989.66 ± 0.72 kJ mol^{-1}), is calculated to be the standard molar enthalpy of formation of aqueous $Na_3Ag(S_2O_3)_2$ in 1.00 molal solution.

Eastman and Milner[107] have measured the heats of solution of AgCl and AgBr crystals in a thiosulphate solution. Based upon their data, the standard molar enthalpy of formation of $[Ag(S_2O_3)_2]^{-3}$ was evaluated to be -1285.74 kJ mol^{-1} [103,108]. Addition of the enthalpy of formation of 3 moles of Na^+ ion to this value yields:

$$\Delta_f H^\circ_m \; Na_3Ag(S_2O_3)_2(aq) \quad = \quad -1285.74 \pm 2.51 + 3(240.300 \pm 0.065)$$

$$= \quad -2006.64 \pm 2.52 \text{ kJ mol}^{-1}.$$

Although this value differs significantly from that derived above, it agrees well with some of those given in Table IV-8. The values contained in this Table are derived using the following equations,

$$AgX(c) + 2Na_2S_2O_3(aq) \quad = \quad Na_3Ag(S_2O_3)_2(aq) + NaX(aq),$$

$$\Delta_f H^\circ_m \; Na_3Ag(S_2O_3)_2(aq) \quad = \quad \Delta_f H^\circ_m \; AgX(c) + 2\Delta_f H^\circ_m \; Na_3S_2O_3(aq) +$$

$$\Delta_r H^\circ_m \; - \Delta_f H^\circ_m \; NaX(aq) \qquad (\text{where } X = Cl^-, Br^-, I^-),$$

together with appropriate enthalpies ($\Delta_r H^\circ_m$) and relevant ancillary data given in Tables IV-8 and IV-10 respectively.

The data contained in Table IV-8 demonstrate clearly that the enthalpy change of a specific reaction is dependent upon the concentration of the reaction medium. Reactions in concentrated solutions are more exothermic than those in dilute solutions. In order to eliminate this effect, the reactions involved in the present evaluations have been performed in very dilute systems (0.001-0.01M). At these compositions the reactions involving silver halides are unmeasurable. From the concentrations and the masses

used it is clear that $AgX/S_2O_3^{2-}$ reactions involve the formation of the $Na_3Ag(S_2O_3)_2$ species only. The additional covalent character in Ag-X bond arose from the polarising ability and the polarisability of the silver and halide ions respectively accounts for the relative slowness of these reactions. The AgI crystal is known to exist in a number of modifications[115,116]. Being stable at ordinary temperatures[115,116], the metastable cubic γ-phase is taken to be that involved in the calorimetric reaction.

De Marco et al.[109,110] have postulated the existence of the $[Ag(S_2O_3)_2]^{-3}$ species and determined potentiometrically the free energy, the enthalpy and the entropy changes associated with the reaction: $2S_2O_3^{2-} + Ag^+ = [Ag(S_2O_3)_2]^{-3}$ as -70.66 ± 1.6, -73.04 ± 6.4 kJ mol^{-1}, and -8 ± 20 J mol^{-1}T^{-1} respectively. However, the enthalpy of the reaction is considerably lower than that given in Table IV-3, viz -78.89 ± 0.19 kJ mol^{-1}.

IV-D-2. The standard molar enthalpy of formation of aqueous $Na_4Ag_2(S_2O_3)_3$:-

Using the following equations,

$$3Na_2S_2O_3(c) + 2AgNO_3(aq) = Na_4Ag_2(S_2O_3)_3(aq) + 2NaNO_3(aq)$$

$$\Delta_fH^\circ_m\ Na_4Ag_2(S_2O_3)_3(aq) = 3\Delta_fH^\circ_m Na_2S_2O_3(c) + 2\Delta_fH^\circ_m\ AgNO_3(aq)$$

$$+ 3\Delta_rH^\circ_m - 2\Delta_fH^\circ_m\ NaNO_3(aq),$$

together with appropriate data from Tables IV-4 and IV-10, the standard molar enthalpy of formation of aqueous $Na_4Ag_2(S_2O_3)_3$ is

calculated to be:

$$\Delta_f H^\circ_m \; Na_4Ag_2(S_2O_3)(aq) = 3(-1120.77\pm1.21) + 2(-101.10\pm0.41)$$

$$+ 3(-57.93\pm0.20) - 2(-447.15\pm0.41) = -2844.00\pm3.86 \text{ kJ mol}^{-1}$$

in 1.00 molal solution.

IV-D-3. The standard molar enthalpy of formation of aqueous $NaAgS_2O_3$:-

Using the following equations,

$$AgNO_3(c) + Na_2S_2O_3(aq) = NaAgS_2O_3(aq) + NaNO_3(aq)$$

$$\Delta_f H^\circ_m \; NaAgS_2O_3(aq) = \Delta_f H^\circ_m \; AgNO_3(c) + \Delta_f H^\circ_m \; Na_2S_2O_3(aq)$$

$$+ \Delta_r H^\circ_m - {}_fH_m \; NaNO_3(aq),$$

together with the relevant $\Delta_r H^\circ_m$ contained in Table IV-1, the standard molar enthalpy of formation of $NaAgS_2O_3(aq)$ is calculated to be:

$$\Delta_f H^\circ_m \; NaAgS_2O_3(aq) = -124.39\pm0.25 + (-1128.30\pm0.59) +$$

$$(-46.16\pm0.15) - (-447.15\pm0.41) = -851.70\pm0.78 \text{ kJ mol}^{-1}.$$

A similar value is derived using the thermo-titrimetric result given in Table IV-3 together with the following equations,

$$AgNO_3(aq) + Na_2S_2O_3(aq) = NaAgS_2O_3(aq) + NaNO_3(aq)$$

$$\Delta_f H^\circ_m \; NaAgS_2O_3(aq) = \Delta_f H^\circ_m \; AgNO_3(aq) + \Delta_f H^\circ_m \; Na_2S_2O_3(aq)$$

$$+ \Delta_r H^\circ_m - \Delta_f H^\circ_m \; NaNO_3(aq), \text{ as:}$$

$$\Delta_f H_m^\circ \, NaAgS_2O_3(aq) = -101.10 \pm 0.41 + (-1128.30 \pm 0.59) + (-69.13 \pm 0.18) - (-447.15 \pm 0.41) = -851.38 \pm 0.85 \text{ kJ mol}^{-1}.$$

Using the following equations,

$$Na_2S_2O_3(c) + AgNO_3(aq) = NaAgS_2O_3(aq) + NaNO_3(aq)$$

$$\Delta_f H_m^\circ \, NaAgS_2O_3(aq) = \Delta_f H_m^\circ \, Na_2S_2O_3(c) + \Delta_f H_m^\circ \, AgNO_3(aq) + \Delta_r H_m^\circ - \Delta_f H_m^\circ \, NaNO_3(aq)$$

together with the relevant $\Delta_r H_m^\circ$ contained in Table IV-4 another value is calculated as:

$$\Delta_f H_m^\circ \, NaAgS_2O_3(aq) = -1120.77 \pm 1.21 + (-101.10 \pm 0.41) + (-77.56 \pm 0.18) - (-447.15 \pm 0.41) = -852.28 \pm 1.35 \text{ kJ mol}^{-1}.$$

The mean of the above three values, (-851.79 ± 0.59 kJ mol^{-1}), is calculated to be the standard molar enthalpy of formation of aqueous $NaAgS_2O_3$ in 1.00 molal solution.

De Marco et al.[109-110] have postulated the existence of the $AgS_2O_3^-$ species and measured potentiometrically the free energy, the enthalpy and the entropy changes associated with the reaction: $S_2O_3^{2-} + Ag^+ = AgS_2O_3^-$ as -51.90 ± 2.0, -60.78 ± 20 kJ mol^{-1} and -29.7 ± 50 J mol^{-1}T^{-1} respectively. However, the enthalpy of the reaction is significantly lower than that given in Table IV-3, viz -69.13 ± 0.18 kJ mol^{-1}.

IV-D-4. The standard molar enthalpy of formation of aqueous $Ag_2S_2O_3$:-

As the following scheme illustrates, conversion of thiosulphate into sulphate is a two-step process:

$$2AgNO_3(c) + Na_2S_2O_3(aq) = Ag_2S_2O_3(aq) + 2NaNO_3(aq) \quad (1)$$

$$Ag_2S_2O_3(aq) + H_2O(liq) = Ag_2S(c) + H_2SO_4(aq) \quad (2)$$

Since hydrolysis of $Ag_2S_2O_3$ (aq) is believed to be athermal, (see IV-A), then using reaction (2) the following thermochemical equation can be derived:

$$\Delta_f H^\circ_m\ Ag_2S_2O_3(aq) = \Delta_f H^\circ_m\ Ag_2S(c) + \Delta_f H^\circ_m\ H_2SO_4(aq) - \Delta_f H^\circ_m\ H_2O(liq) - \Delta_r H^\circ_m \quad (3)$$

Substitution of appropriate ancillary data from Table IV-10 yields:

$$\Delta_f H^\circ_m\ Ag_2S_2O_3(aq) = -29.41 \pm 0.25 + (-909.27 \pm 0.17) - (-285.830 \pm 0.042) - (0) = -652.85 \pm 0.31\ kJ\ mol^{-1}$$

in 1.00 molal solution.

Table IV-1. Calorimetric investigations of the $Ag^+/S_2O_3^{2-}$ reactions (direct)

$m(AgNO_3)$	$C(Na_2S_2O_3)$	$\Delta_r H_m^\circ$	$\Delta_r H_m^\circ$ (mean)	$[S_2O_3]^{2-}/[Ag^+]$	$Na_{2n-m}Ag_m(S_2O_3)_n$	$\Delta_f H_m^\circ$ $Na_{2n-m}Ag_m(S_2O_3)_n(aq)$
g	M	kJ mol^{-1}	kJ mol^{-1}			kJ mol^{-1}
0.04275	0.001	-63.07	-62.99±0.18	0.4		
0.04287		-62.96				
0.04302		-62.93				
0.03331		-85.35	-85.41±0.16	0.5	$Ag_2S_2O_3$	-652.85±0.31
0.03340		-85.26				
0.03356		-85.44				
0.03371		-85.69				
0.03389		-85.57				
0.03402		-85.36				
0.03425		-85.18				
0.05645	0.002	-76.49	-76.46±0.17	0.6		
0.05711		-76.51				
0.05716		-76.38				
0.04242		-61.89	-61.96±0.17	0.8		
0.04252		-61.97				
0.04269		-62.03				
0.04931	0.003	-46.36	-46.16±0.15	1.0	$NaAgS_2O_3$	-851.70±0.78
0.04987		-46.30				
0.05019		-46.23				
0.05071		-45.93				
0.05098		-46.16				
0.05106		-46.31				
0.05113		-45.89				
0.05124		-46.10				

continued

Table IV-1 continued

$m(AgNO_3)$ / g	$C(Na_2S_2O_3)$ / M	$\Delta_r H^\circ_m$ / kJ mol^{-1}	$\Delta_r H^\circ_m$ (mean) / kJ mol^{-1}	$[S_2O_3]^{2-}/[Ag^+]$	$Na_{2n-m}Ag_m(S_2O_3)_n$	$\Delta_f H^\circ_m$ $Na_{2n-m}Ag_m(S_2O_3)_n(aq)$ / kJ mol^{-1}
0.04238		-48.53	-48.62±0.19	1.2		
0.04247		-48.65				
0.04268		-48.67				
0.03628		-50.39	-50.31±0.20	1.4		
0.03635		-50.31				
0.03647		-50.23				
0.05331	0.005	-52.53	-52.45±0.20	1.6		
0.05346		-52.44				
0.05369		-52.37				
0.04708		-54.73	-54.79±0.18	1.8		
0.04723		-54.87				
0.04736		-54.76				
0.03383		-56.36	-55.95±0.19	2.5	$Na_3Ag(S_2O_3)_2$	-1989.79±1.29
0.03404		-55.96				
0.03646		-55.79		2.3		
0.03709		-55.85				
0.03863		-56.03		2.2		
0.04204		-55.76		2.0		
0.04473		-55.89		1.9		
0.05680	0.01	-56.25	-55.94±0.18	3.0	$Na_3Ag(S_2O_3)_2$	-1989.78±1.29
0.05795		-55.86		2.9		
0.06281		-55.93		2.7		
0.06650		-55.78		2.6		
0.07069		-56.18		2.4		

continued

Table IV-1 continued

$m(AgNO_3)$ / g	$C(Na_2S_2O_3)$ / M	$\Delta_rH^\circ_m$ / kJ mol^{-1}	$\Delta_rH^\circ_m$ (mean) / kJ mol^{-1}	$[S_2O_3]^{2-}/[Ag^+]$	$Na_{2n-m}Ag_m(S_2O_3)_n$	$\Delta_fH^\circ_m$ $Na_{2n-m}Ag_m(S_2O_3)_n(aq)$ / kJ mol^{-1}
0 08120		-55.79		2.1		
0.08555		-55.82		2.0		
0.04261		-56.17	-56.01±0.17	4.0	$Na_3Ag(S_2O_3)_2$	-1989.85±1.29
0.04374		-55.95		3.9		
0.04710		-55.89		3.6		
0.04900		-55.86		3.5		
0.05123		-56.31		3.3		
0.05353		-56.09		3.2		
0.05610		-55.83		3.0		

The abbreviations used have the following significance: m=mass, C=concentration, M=mol dcm^{-3}, $\Delta_rH^\circ_m$ = the standard molar enthalpy of the reaction, $\Delta_fH^\circ_m$ = the standard molar enthalpy of formation. The molar mass of $AgNO_3$ was taken to be 169.89g mol^{-1}. In each experiment 100.00cm^3 of solution was used.

Table IV-2. The enthalpy of solution of $AgNO_3$[a]

$m(AgNO_3)$ / g	ΔH_s° / kJ mol^{-1}	ΔH_s° (mean) / kJ mol^{-1}
0.08728	23.14	22.96±0.11
0.09821	22.85	
0.10461	22.93	
0.11712	22.99	
0.14066	22.87	
0.15170	23.00	

[a] $AgNO_3(c)+nH_2O(liq) = [Ag^+ + NO_3^-]_{(nH_2O,aq)}$

Table IV-3. Thermo-titrimetric investigations of the $Ag^+/S_2O_3^{2-}$ reactions (direct)

$C(AgNO_3)$ / M	$V(AgNO_3)$ / $cm^3 min^{-1}$	$C(Na_2S_2O_3)$ / M	$V(Na_2S_2O_3)$ / cm^3	t_{r1} / min	$\Delta_{r1}H_m^\circ$ / $kJ mol^{-1}$	$\Delta_{r1}H_m^\circ$(mean) / $kJ\ mol^{-1}$	$[S_2O_3]^{2-}/[Ag^+]$	$Na_{2n-m}Ag_m(S_2O_3)_n$	$\Delta_f H_m^\circ Na_{2n-m}Ag_m(S_2O_3)_n(aq)$ / $kJ\ mol^{-1}$
1.00	0.33	0.004	200.00	1.2	-78.93	-78.89±0.19	2.0	$Na_3Ag(S_2O_3)_2$	-1989.44±1.33
		0.004		1.2	-78.66				
		0.004		1.2	-79.28				
		0.005		1.5	-78.84				
		0.005		1.5	-78.73				
		0.005		1.5	-78.98				
		0.005		1.5	-78.78				

$C(AgNO_3)$ / M	$V(AgNO_3)$ / $cm^3 min^{-1}$	$C(Na_2S_2O_3)$ / M	$V(Na_2S_2O_3)$ / cm^3	t_{r2} / min	$\Delta_{r2}H_m^\circ$ / $kJ mol^{-1}$	$\Delta_{r2}H_m^\circ$(mean) / $kJ\ mol^{-1}$	$[S_2O_3]^{2-}/[Ag^+]$	$Na_{2n-m}Ag_m(S_2O_3)_n$	$\Delta_f H_m^\circ Na_{2n-m}Ag_m(S_2O_3)_n(aq)$ / $kJ\ mol^{-1}$
1.00	0.33	0.004	200.00	2.4	-69.19	-69.13±0.18	1.0	$NaAgS_2O_3$	-851.38±0.85
		0.004		2.4	-69.31				
		0.004		2.4	-68.98				
		0.005		3.0	-69.11				
		0.005		3.0	-69.46				
		0.005		3.0	-68.93				
		0.005		3.0	-68.96				

continued

Table IV-3 continued

$C(AgNO_3)$ M	$V(AgNO_3)$ $cm^3 min^{-1}$	$C(Na_2S_2O_3)$ M	$V(Na_2S_2O_3)$ cm^3	t_{r3} min	$\Delta_{r3}H^\circ_m$ $kJ mol^{-1}$	$\Delta_{r3}H^\circ_m$(mean) $kJ\ mol^{-1}$	$[S_2O_3]^{2-}/[Ag^+]$	$Na_{2n-m}Ag_m(S_2O_3)_n$	$\Delta_f H^\circ_m Na_{2n-m}Ag_m(S_2O_3)_n(aq)$ $kJ\ mol^{-1}$
1.00	0.33	0.004	200.00	4.8	-107.87	-108.17±0.20	0.5	$Ag_2S_2O_3$	-652.85±0.31
		0.004		4.8	-108.13				
		0.004		4.8	-108.45				
		0.005		6.0	-108.28				
		0.005		6.0	-107.93				
		0.005		6.0	-108.19				
		0.005		6.0	-108.36				

v = volume, t_r = time of reactions,

$r_1 = Ag^+ + 2S_2O_3^{2-} = [Ag(S_2O_3)_2]^{-3}$,

$r_2 = Ag^+ + Ag(S_2O_3)_2^{-3} = 2AgS_2O_3^-$,

$r_3 = Ag^+ + AgS_2O_3^- = Ag_2S_2O_3$

$r_4 = Ag_2S_2O_3 + H_2O = Ag_2S(c) + SO_4^{2-} + 2H^+$.

Table IV-4. Calorimetric investigations of the $S_2O_3^{2-}/Ag^+$ reactions (reverse)

$m(Na_2S_2O_3)$ / g	$C(AgNO_3)$ / M	$\Delta_r H_m^\circ$ / kJ mol^{-1}	$\Delta_r H_m^\circ$ (mean) / kJ mol^{-1}	$[S_2O_3]^{2-}/[Ag^+]$	$Na_{2n-m}Ag_m(S_2O_3)_n$	$\Delta_f H_m^\circ$ $Na_{2n-m}Ag_m(S_2O_3)_n(aq)$ / kJ mol^{-1}
0.03158	0.005	-223.95	-224.02±0.21	0.4		
0.03160		-223.99				
0.03166		-224.11				
0.02979	0.004	-224.33	-224.18±0.19	0.5	$Ag_2S_2O_3$	-652.85±0.31
0.03090		-224.98				
0.03158		-224.08				
0.03158		-224.20				
0.03159		-224.36				
0.03160		-224.42				
0.03166		-223.91				
0.06315		-77.59	-77.56±0.18	1.0	$NaAgS_2O_3$	-852.28±1.35
0.06316		-77.86				
0.06316		-77.28				
0.06317		-77.35				
0.06319		-77.69				
0.06325		-77.51				
0.06340		-77.64				
0.09473		-58.06	-57.93±0.20	1.5	$Na_4Ag_2(S_2O_3)_3$	-2844.00±3.86
0.09478		-57.66				
0.09484		-57.68				
0.09490		-58.23				
0.09490		-58.10				
0.09492		-57.67				
0.09492		-58.17				
0.09517		-57.87				

continued

Table IV-4 continued

$m(Na_2S_2O_3)$ / g	$C(AgNO_3)$ / M	$\Delta_r H_m^\circ$ / kJ mol^{-1}	$\Delta_r H_m^\circ$ (mean) / kJ mol^{-1}	$[S_2O_3]^{2-}/[Ag^+]$	$Na_{2n-m}Ag_m(S_2O_3)_n$	$\Delta_f H_m^\circ$ $Na_{2n-m}Ag_m(S_2O_3)_n(aq)$ / kJ mol^{-1}
0.12632		-47.08	-46.97±0.15	2.0	$Na_3Ag(S_2O_3)_2$	-1989.43±2.51
0.12640		-46.89				
0.12640		-46.67				
0.12647		-47.01				
0.12653		-46.93				
0.12657		-47.02				
0.12660		-47.18				
0.07906	0.002	-39.98	-40.01±0.20	2.5		
0.07906		-40.10				
0.07921		-39.95				
0.09480		-33.60	-33.52±0.18	3.0		
0.09511		-33.51				
0.09520		-33.46				

Table IV-5. The enthalpy of solution of $Na_2S_2O_3$[a]

$m(Na_2S_2O_3)$ / g	ΔH_s° / kJ mol^{-1}	ΔH_s° (mean) / kJ mol^{-1}
0.21103	-7.51	-7.67±0.12
0.21888	-7.74	
0.21957	-7.80	
0.22147	-7.59	
0.23182	-7.76	
0.26557	-7.62	

[a] $Na_2S_2O_3(c)+nH_2O(liq) = [2Na^+ + S_2O_3^{2-}](nH_2O,aq)$.

The molar mass of $Na_2S_2O_3$ was taken to be 158.12 g mol^{-1}.

Table IV-6. The enthalpy of solution of $Na_2S_2O_3 \cdot 5H_2O$[a]

$m(Na_2S_2O_3 \cdot 5H_2O)$ / g	ΔH_s° / kJ mol^{-1}	ΔH_s° (mean) / kJ mol^{-1}
0.14503	47.26	47.21±0.14
0.15080	47.39	
0.15763	47.11	
0.17214	47.02	
0.17646	47.31	
0.20376	47.19	

a $Na_2S_2O_3 \cdot 5H_2O(c) + nH_2O(liq) = [2Na^+ + S_2O_3^{2-}]_{(n+5H_2O,aq)}$.

The molar mass of $Na_2S_2O_3 \cdot 5H_2O$ was taken to be 248.19 g mol^{-1}.

Table IV-7. Thermo-titrimetric investigations of the $S_2O_3^{2-}/Ag^+$ reactions (reverse)

$C(Na_2S_2O_3)$ / M	$V(Na_2S_2O_3)$ / $cm^3 min^{-1}$	$C(AgNO_3)$ / M	$V(AgNO_3)$ / cm^3	t_{r1} / min	$\Delta_{r1}H^\circ_m$ / kJ mol^{-1}	$\Delta_{r1}H^\circ_m$(mean) / kJ mol^{-1}	$[S_2O_3]^{2-}/[Ag^+]$	$Ag_2S_2O_3 \cdot xAgNO_3$	$\Delta_f H^\circ_m Ag_2S_2O_3 \cdot xAgNO_3(aq)$ / kJ mol^{-1}
1.00	0.33	0.005	200.00	0.5	-238.67	-238.61±0.76	0.165	$Ag_2S_2O_3 \cdot 4AgNO_3$	-1079.21±2.77
		0.005		0.5	-238.55		0.165		
		0.007		0.5	-236.31	-236.24±0.96	0.118	$Ag_2S_2O_3 \cdot 6AgNO_3$	-1279.04±3.56
		0.007		0.5	-236.16		0.118		
		0.008		0.5	-214.82	-214.77±0.70	0.103	$Ag_2S_2O_3 \cdot 8AgNO_3$	-1459.77±4.28
		0.008		0.5	-214.71		0.103		
		0.01		0.5	-224.37	-224.27±1.27	0.083	$Ag_2S_2O_3 \cdot 10AgNO_3$	-1671.47±5.18
		0.01		0.5	-224.17		0.083		

$C(Na_2S_2O_3)$ / M	$V(Na_2S_2O_3)$ / $cm^3 min^{-1}$	$C(AgNO_3)$ / M	$V(AgNO_3)$ / cm^3	t_{r2} / min	$\Delta_{r2}H^\circ_m$ / kJmol^{-1}	$\Delta_{r2}H^\circ_m$(mean) / kJ mol^{-1}	$[S_2O_3]^{2-}/[Ag^+]$	$Ag_2S_2O_3 \cdot xAgNO_3$	$\Delta_f H^\circ_m Ag_2S_2O_3 \cdot xAgNO_3(aq)$ / kJ mol^{-1}
1.00	0.33	0.005	200.00	0.75	-228.40	-228.32±1.08	0.248	$Ag_2S_2O_3 \cdot 2AgNO_3$	-867.72±2.22
		0.005		0.75	-228.23		0.248		
		0.007		0.75	-238.76	-238.56±0.23	0.177	$Ag_2S_2O_3 \cdot 4AgNO_3$	-1079.16±2.67
		0.007		0.75	-238.49		0.177		
		0.008		0.75	-238.43		0.155		
		0.008		0.75	-238.54		0.155		
		0.01		0.75	-236.18	-236.05±1.65	0.124	$Ag_2S_2O_3 \cdot 6AgNO_3$	-1278.85±3.81
		0.01		0.75	-235.92		0.124		

continued

Table IV-7 continued

$C(Na_2S_2O_3)$ / M	$V(Na_2S_2O_3)$ / $cm^3 min^{-1}$	$C(AgNO_3)$ / M	$V(AgNO_3)$ / cm^3	t_{r3} / min	$\Delta_{r3}H^\circ_m$ / $kJ mol^{-1}$	$\Delta_{r3}H^\circ_m$(mean) / $kJ\ mol^{-1}$	$[S_2O_3]^{2-}/[Ag^+]$	$Ag_2S_2O_3 \cdot xAgNO_3$	$\Delta_f H^\circ_m Ag_2S_2O_3 \cdot xAgNO_3(aq)$ / $kJ\ mol^{-1}$
1.00	0.33	0.005	200.00	1.0	-212.65	-212.58±0.89	0.330	$Ag_2S_2O_3 \cdot AgNO_3$	-749.88±1.82
		0.005		1.0	-212.51		0.330		
		0.007		1.0	-228.34	-228.13±0.28	0.236	$Ag_2S_2O_3 \cdot 2AgNO_3$	-866.53±1.95
		0.007		1.0	-227.96		0.236		
		0.008		1.2	-228.01		0.248		
		0.008		1.2	-228.19		0.248		
		0.01		1.2	-241.10	-241.21±1.34	0.198	$Ag_2S_2O_3 \cdot 3AgNO_3$	-980.71±2.65
		0.01		1.2	-241.31		0.198		

$C(Na_2S_2O_3)$ / M	$V(Na_2S_2O_3)$ / $cm^3 min^{-1}$	$C(AgNO_3)$ / M	$V(AgNO_3)$ / cm^3	t_{r4} / min	$\Delta_{r4}H^\circ_m$ / $kJ mol^{-1}$	$\Delta_{r4}H^\circ_m$(mean) / $kJ\ mol^{-1}$	$[S_2O_3]^{2-}/[Ag^+]$	$Ag_2S_2O_3 \cdot xAgNO_3$	$\Delta_f H^\circ_m Ag_2S_2O_3 \cdot xAgNO_3(aq)$ / $kJ\ mol^{-1}$
1.00	0.33	0.005	200.00	1.5	-216.59	-216.37±0.15	0.5	$Ag_2S_2O_3$	-652.85±0.31
		0.005		1.5	-216.25		0.5		
		0.007		2.1	-216.43		0.5		
		0.007		2.1	-216.56		0.5		
		0.008		2.4	-216.31		0.5		
		0.008		2.4	-216.22		0.5		
		0.01		3.0	-216.50		0.5		
		0.01		3.0	-216.11		0.5		

$r_1 = S_2O_3^{2-} + (2+x)Ag^+ = Ag_2S_2O_3.xAg^+$, $r_4 = x/2 S_2O_3^{2-} + Ag_2S_2O_3.xAg^+ = (1+x/2)\ Ag_2S_2O_3$, $r_5 = Ag_2S_2O_3 + H_2O = Ag_2S(c) + SO_4^{2-} + 2H^+$, i=1,2,3.

Table IV-8. Calorimetric investigations of the $AgX/S_2O_3^{2-}$ reactions

AgX	m(AgX) / g	$C(Na_2S_2O_3)$ / M	$\Delta_r H_m^\circ$ / k mol^{-1}	$\Delta_r H_m^\circ$ (mean) / kJ mol^{-1}	$Na_{2n-m}Ag_m(S_2O_3)_n$	$\Delta_f H_m^\circ$ $Na_{2n-m}Ag_m(S_2O_3)_n(aq)$ / kJ mol^{-1}
AgCl	0.04509	0.5	-19.38	-19.41±0.19	$Na_3Ag(S_2O_3)_2$	-1995.70±1.20
	0.05303		-19.69			
	0.06407		-19.49			
	0.07015		-19.34			
	0.08902		-19.41			
	0.10519		-19.14			
	0.04512	1.0	-25.87	-25.70±0.22		-2001.99±1.21
	0.05324		-25.54			
	0.06830		-25.68			
	0.07828		-25.99			
	0.08482		-25.41			
	0.09104		-25.73			
	0.04325	1.5	-29.37	-29.36±0.19		-2005.65±1.20
	0.05536		-29.45			
	0.06315		-29.66			
	0.07826		-29.33			
	0.08707		-29.16			
	0.09527		-29.21			
	0.06654	2.0	-30.53	-30.54±0.18		-2006.83±1.20
	0.07609		-30.37			
	0.08363		-30.41			
	0.09242		-30.66			
	0.11558		-30.83			
	0.15494		-30.46			
	0.06309	2.5	-30.49	-30.59±0.19		-2006.88±1.20
	0.07703		-30.76			
	0.08518		-30.70			

continued

Table IV-8 continued

AgX	m(AgX) / g	$C(Na_2S_2O_3)$ / M	$\Delta_r H_m^\circ$ / kJ mol^{-1}	$\Delta_r H_m^\circ$ (mean) / kJ mol^{-1}	$Na_{2n-m}Ag_m(S_2O_3)_n$	$\Delta_f H_m^\circ$ $Na_{2n-m}Ag_m(S_2O_3)_n(aq)$ / kJ mol^{-1}
	0.10644		-30.38			
	0.11327		-30.42			
	0.12604		-30.81			
AgBr	0.75168	0.5	0.39	0.55±0.17	$Na_3Ag(S_2O_3)_2$	-1994.62±1.42
	0.78294		0.45			
	0.81650		0.43			
	0.82256		0.71			
	0.83712		0.53			
	0.84246		0.79			
	0.19564	2.5	-12.18	-11.94±0.18		
	0.20226		-11.95			-2007.11±1.42
	0.21619		-11.77			
	0.23586		-11.90			
	0.24630		-12.08			
	0.25869		-11.73			
AgI	0.15781	0.5	25.27	25.13±0.20	$Na_3Ag(S_2O_3)_2$	-1996.23±1.37
	0.16235		25.13			
	0.17196		24.97			
	0.18265		25.18			
	0.19567		25.38			
	0.20268		24.86			
	0.15673	2.5	14.49	14.34±0.13		-2007.02±1.37
	0.16553		14.43			
	0.17489		14.34			
	0.18635		14.37			
	0.19356		14.16			
	0.20489		14.23			

The molar masses of AgCl, AgBr and of AgI were taken to be 143.34, 187.80 and 234.79 g mol^{-1} respectively.

Table IV-9. Gravimetric and titrimetric investigations of the reaction:

$$S_2O_3^{2-} + 2Ag^+ + H_2O = Ag_2S(c) + SO_4^{2-} + 2H^+$$

$m(Na_2S_2O_3 \cdot 5H_2O)$ g	$m_1(BaSO_4)$ g	$m_2(BaSO_4)$ g	$m_1 x10^2\%$ m_2	$m_1(Ag_2S)$ g	$m_2(Ag_2S)$ g	$m_1 x10^2\%$ m_2	C(NaOH) M	$V(H^+)$ cm^3	V(NaOH) cm^3	$C_1(H^+)x10^{-3}$ M	$C_2(H^+)x10^{-3}$ M	$C_1 x10^2\%$ C_2
0.3000	0.2807	0.2821	99.50				0.10	25.00	2.40	2.40	2.42	99.17
0.3079	0.2876	0.2896	99.50						2.44	2.44	2.48	98.39
0.2877				0.2849	0.2875	99.10						
0.3391				0.3400	0.3385	100.44						

m_1, C_1 = practical determinations,
m_2, C_2 = calculated values,
v = volume of the aliquots titrated.

The molar masses of Ba^{2+}, Ag^+, SO_4^{2-}, S and of $Na_2S_2O_3 \cdot 5H_2O$ were taken to be 137.36, 107.88, 96.07, 32.07 and 248.19 g mol^{-1} respectively.

Table IV-10. Ancillary thermochemical data

M^+/X^-	state	$\Delta_f H_m^\circ$ / kJ mol^{-1}	ref.	Mx	state	$\Delta_f H_m^\circ$ / kJ mol^{-1}	ref.
Na^+	aq	-240.300±0.065	112	$AgNO_3$	C	-124.39 ±0.25*	108
K^+	aq	-252.17 ±0.10	112	AgCl	C	-127.070±0.085	112
Ag^+	aq	105.750±0.085	112	AgBr	C	-100.37 ±0.75*	108
Cl^-	aq	-167.080±0.088	112	AgI	C	-61.84 ±0.67*	108
Br^-	aq	-121.50 ±0.15	112	β-Ag_2S	C	-29.41 ±0.25*	108
I^-	aq	-56.785±0.071	117	H_2O	L	-285.830±0.042	112
NO_3^-	aq	-206.85 ±0.40	118	H_2SO_4	aq	-909.27 ±0.17*	102

* Uncertainty = ± 2 units of the last quoted figure[102,108].

Chapter V

Results and Discussion

(Solubility)

V. Results and Discussion (solubility)

V-1. The differential heat of solution of sodium dithionate dihydrate from the temperature coefficient of solubility:-

The solubility of polar-covalent and ionic solutes in polar solvents has been attributed to electrostatic interactions between the solvent molecules and the solute particles. As the following thermochemical cycle illustrates,

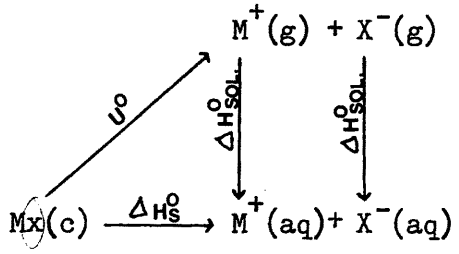

(where U^o, ΔH^o_s and $\Delta H^o_{solv.}$ are the lattice energy and the enthalpies of solution and of solvation respectively), the process of dissolution of an ionic crystal can be formally divided into two steps: (i) the lattice collapse and the subsequent release of the existing ions in the gaseous phase, and (ii) the solvation of the gaseous ions furnished. However, dissolution occurs only when the energy of solvation is greater than that required to rupture the crystal lattice. With increase in the charge of either ions the lattice energy increases more rapidly than the enthalpy of solvation, and as the result a parallel decrease in solubility occurs. The polarisability of the anion is also of significant importance since the tendency to be more readily polarised than

the solvent molecules results in the increase of the lattice energy, and as a consequence solubility decreases. On the other hand, solubility is enhanced by the reduction of interionic attractions in the crystal when solvents of high polarity and dielectric constants are employed.

When a concentrated solution is cooled, the slope of the cooling curve changes at the temperature at which the solute crystallises out. The change in the slope is due to release of heat by the process of crystallisation, the commencement of which indicates the attainment of saturation. In sodium dithionate dihydrate solution, the state of dynamic equilibrium reached at the saturation point can be illustrated as:

$$Na_2S_2O_6 \cdot 2H_2O(c) + nH_2O(liq) = \left[2Na^+ + S_2O_6^{2-}\right](n+2H_2O,aq)$$

Thermodynamic functions of such state are summarised and interrelated by the following equations:

$$\Delta G^o = \Delta H^o - T\Delta S^o \qquad (1)$$

$$\Delta G^o = -RT \ln K \qquad (2)$$

where ΔG^o, ΔH^o, ΔS^o are the standard free energy, enthalpy and entropy changes, and R, T and K are the gas content, the absolute temperature and the equilibrium constant (=solubility) respectively. Combination of equations (1) and (2) gives the familiar result of the van't Hoff isochore:

$$\ln K = \frac{\Delta H^o}{RT} + \frac{\Delta S^o}{R} \qquad (3)$$

Ignoring the temperature-dependence of ΔH^o over the range investigated, equation (3) has been regarded as a linear equation. Hence a plot of ln K versus $1/T$ should yield a straight line, the slope and the intercept of which should be equivalent to $-\Delta H^o/R$ and $\Delta S^o/R$ respectively.

Several procedures have been adopted to investigate the solubility of a particular species in a specific solvent as a function of temperature. While some utilise chemical methods of analysis of aliquots withdrawn at fixed temperature intervals from the solution while cooling, others employ physical techniques, e.g., spectrophotometry. While the physical methods have the advantage of being rapid, chemical analysis reveals the absolute values of compositions. A rapid and simple physical technique known as dynamic precipitation has been used in this work. It is essentially based upon the van't Hoff isochore, which describes the enthalpy and entropy changes in systems at equilibrium in terms of the equilibrium constants. The temperature at which crystallisation commences is the physical property to be measured, and the variation of this with the composition of the solution is the working principle of this technique.

Solubility measurements, using the above method, on a saturated solution of sodium dithionate dihydrate are given in Table V-1, and are graphically displayed in Fig. V-1. From the graph, the slope ($=\Delta H^o/R$) and the intercept ($=\Delta S^o/R$) were found to be 1981.8 and 6.67 respectively. Multiplication of these values by R yields:

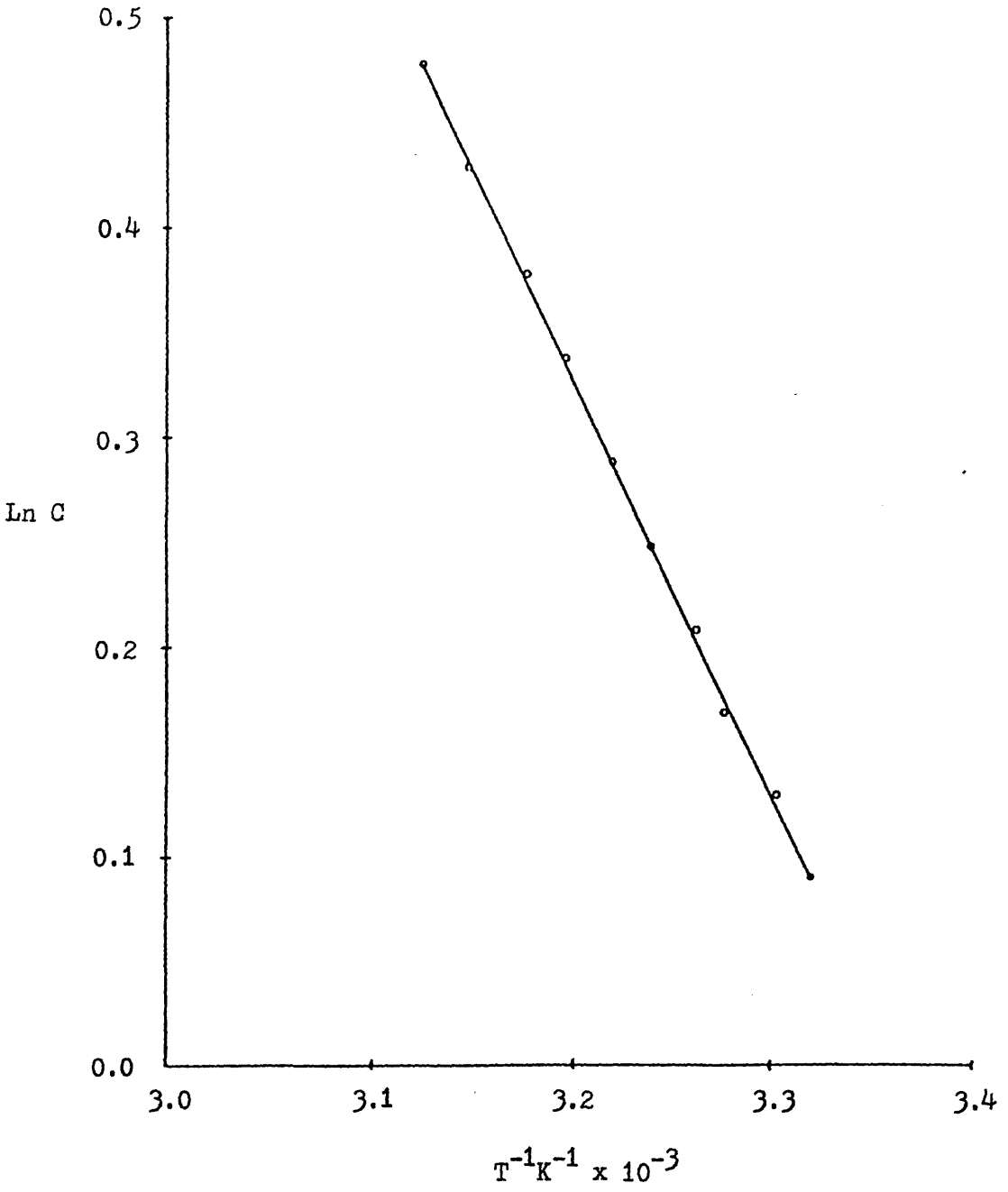

Fig. V-1. LnC vs 1/T plot for sodium dithionate dihydrate crystals

$$\Delta H^{o} = 1981.8 \times 8.314 \times 10^{-3} = 16.48 \text{ kJ mol}^{-1}$$

$$\Delta S^{o} = 6.67 \times 8.314 = 55.45 \text{ J mol}^{-1} \text{ T}^{-1}$$

Substitution of these values in equation (1) gives:

$$\Delta G^{o} = 16.48 - 298.15 \times 55.45 \times 10^{-3} = -0.05 \text{ kJ mol}^{-1} \text{ at } 25^{\circ}\text{C}.$$

This value is in fair agreement with the fact that the free energy change in a system at equilibrium is zero at the standard state. For more precise computation, evaluations of ionic activities and activity coefficients are necessary as the Williamson[119] equation states. As illustrated below, the equation has been derived in order to calculate the differential heats of solutions for perfect and imperfect systems in equilibrium with hydrated and unhydrated solutes of any kind in terms of mean ionic activities, activity coefficients and molalities:

$$\Delta H_{sol.} = \nu RT^{2}(dm/dt)_{sat.} \cdot [(\delta \ln \gamma / \delta m)_{T} + (1/m)_{sat}]$$

$\Delta H_{sol.}$ is the heat absorbed per mole of solute dissolved in the nearly saturated solution, or the heat released per mole upon crystallisation. m is the molality of the saturated solution, ν is the total number of ions released by one molecule of the solute and has a value of unity in non-electrolytes, and γ is the mean ionic activity coefficient.

V-2. Suggestions for future work:-

(i) Sulphur dioxide reacts extremely fast with the hydroxide ion.

Hence it might react with other strong nucleophiles and Lewis bases under suitable conditions to form coordinated species:

$$Nu: + SO_2 \quad = \quad Nu^{+} \rightarrow SO_2$$

Other reactions could involve amines, e.g. alkaloids.

(ii) The nature of gold and copper-thiosulphate complexing is also worth investigating.

Table V-1. Solubility of $Na_2S_2O_6 \cdot 2H_2O$[a]

$w(Na_2S_2O_6 \cdot 2H_2O)$ / g	$C(Na_2S_2O_6 \cdot 2H_2O)$ / M	C	T / °C	T / K	$T^{-1} \times 10^{-3}$ / K^{-1}	m	c	r	$\Delta H^o_{sol.}$ / kJ mol^{-1}	$\Delta S^o_{sol.}$ / J $mol^{-1} T^{-1}$
7.45	1.62	0.48	46.8 46.9	320.00	3.125	-1981.8	6.67	0.99	16.48	55.45
	1.54	0.43	44.5 44.5	317.65	3.148					
	1.47	0.38	41.8 41.9	315.00	3.175					
	1.40	0.34	39.7 39.7	312.85	3.196					
	1.34	0.29	37.5 37.6	310.70	3.219					
	1.28	0.25	35.3 35.4	308.50	3.241					
	1.23	0.21	33.1 33.2	306.30	3.265					
	1.18	0.17	32.1 32.1	305.25	3.276					
	1.14	0.13	29.5 29.6	302.70	3.304					
	1.10	0.09	28.1 28.2	310.30	3.319					

[a] $Na_2S_2O_6 \cdot 2H_2O(c) + nH_2O(liq) = [2Na^+ S_2O_6^{2-}]_{(n+2H_2O,aq)}$.

w = weight, C = concentration (=solubility), M = mol dcm^{-3}, T = temperature, m = slope, c = intercept, r = correlation coefficient, $\Delta H^o_{sol.}$ = enthalpy of solution at saturation, $\Delta S^o_{sol.}$ = entropy of solution at saturation.

Chapter VI

Experimental methods

VI. Experimental methods

VI-A. Spectroscopic techniques:-

VI-A-1. Raman Spectra:-

These were measured on a Coderg PH1 monochromator Raman spectrophotometer with a Coherent Radiation argon laser using the 19434cm^{-1} (514.5nm) argon line as the exciting frequency at a power of ≃ 500 mw and a low noise, Peltier cooled, photomultiplier detector. Solid state spectra were taken on samples contained in sealed capillaries. The slit widths were 2 and 4 cm^{-1} for measurements in crystals and in solutions respectively.

VI-A-2. Infrared spectra:-

These were obtained on a Perkin-Elmer 983 infrared spectrometer equipped with a Data Station. Solid state spectra were investigated either as nujol mulls or as caesium iodide discs, in the region below 1500 cm^{-1}. Aqueous state spectra were measured as thin films of nearly saturated solutions firmly held between two KRS-5 plates. Due to strong absorption by water, bands in the region below 900 cm^{-1} are inevitably weak.

VI-A-3. Ultraviolet spectra:-

These were obtained on a Perkin-Elmer 550S uv/vis spectrophotometer using silica cells of 1 cm path length. All measurements were

conducted at room temperature and the band frequencies are accurate to $\pm$ 2 cm^{-1}.

VI-A-4. Reagents:-

Commercial grade compounds supplied by B.D.H and May and Baker Co. were re-crystallised once and then used to prepare nearly saturated solutions. Due to the possibility of oxidation of sulphite, bisulphite, thiosulphate and dithionite solutions, precautions were taken to minimise the presence of oxygen in these systems. Deionised water was first boiled and then allowed to cool while passing a current of nitrogen gas through it. An aqueous sulphur dioxide solution was prepared by bubbling sulphur dioxide at a low rate through cooled, de-aerated deionised water. The solution so obtained was then sealed in a number of evacuated glass tubes kept at zero and 25°C.

VI-B. Thermochemical techniques:-

VI-B-1. Ampoule and titration-mode calorimeters:-

The present thermochemical investigations have been executed in isoperibol, differential solution calorimeters constructed in this laboratory[120]. The essential components of both ampoule and titration modes are the same. A slight modification in the design of the reaction chamber is made in order to allow for the entry of a capillary delivery tip from the titrant reservoir to accommodate the titration mode. Two different capacity flasks of the conventional

Dewar type were available. The 100 cm^3 capacity twin vessels were employed in the ampoule-mode calorimetry and the 200 cm^3 capacity ones were used in thermo-titrimetric determinations. In addition to the typical components of the reference unit, an ampoule confining a definite mass of the second reactant was suspended in the reaction chamber as Fig. VI-1 illustrates.

In thermo-titrimetry, the titrant was delivered into the reaction chamber by means of a constant-speed syringe burette, the plunger of which was attached to a bar driven by a cam in the synchronous motor drive. The delivery rate was evaluated by weighing the amount of water delivered over a known period of time. Of the different flow rates readily obtainable with the aid of interchangeable precision-machined gears, the 0.33 cm^3 min^{-1} was selected and has been exclusively used in the present determinations. Fitted with a capillary delivery tip, a two metres long polyvinyl chloride tube filled with the titrant and constituting the reservoir was connected to the syringe burette and immersed under the surface of the solution to be titrated. While the capillary delivery tip was allowed to enter into the titration chamber via the inlet specially built for, the thermistor, the calibration heater and the glass stirrer (operated by a synchronous rotator) were inserted through the appropriate bushes screwed into the aluminium lid. The stirring rod is connected to the constant speed motor by means of narrow bore rubber tubing which slides onto a brass fitting on the motor shaft. Both of the twin vessels have their own constant speed motors (Electrocraft Corp. Motomatic Model E55DMG with E550-M

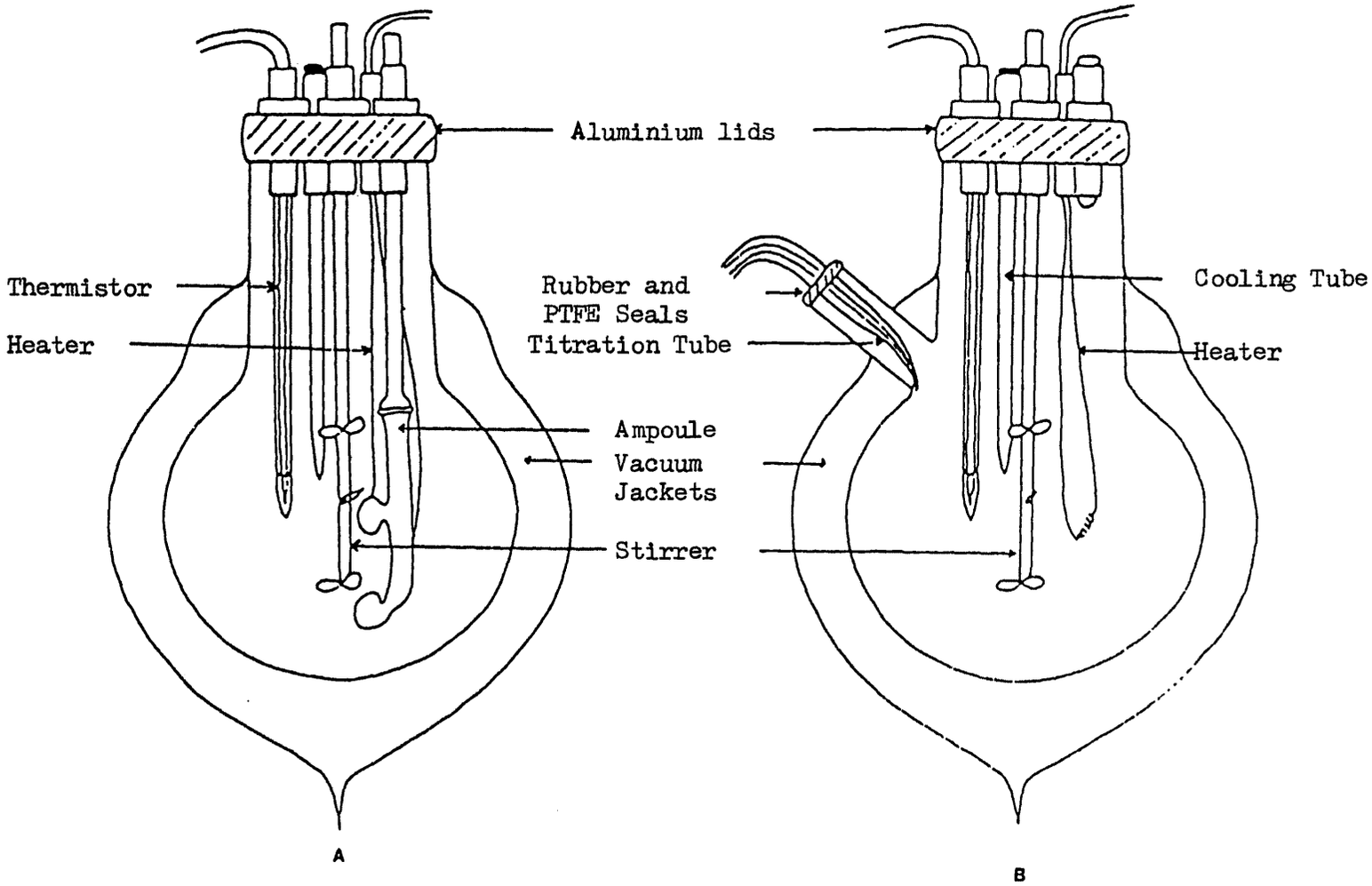

Fig. VI-1. Calorimetric vessels: A = Ampoule-mode reaction chamber
B = Titration-mode reaction chamber

controllers). By varying the speeds of the rotators desirable stirring rates were adjusted. By stirring the twin vessels at identical rates the heating effect of the stirring process was almost eliminated. This illustrates the superiority of these calorimeters over the LKB, and reveals their advantage in precipitation reactions where effective stirring is crucial. To the lower part of the stirring rod a spike and a couple of paddles were attached. In order to achieve effective mixing and a better heat distribution, the paddles were arranged so that while the top pair force downwards the bottom ones force upwards.

Crystalline materials were ground in an agate mortar. Using a microbalance samples were then weighed into ampoules blown from B5 sockets. Each ampoule bears two thin bulbs on one side, one at the lower end and the other about halfway along the length of the ampoule tube. The two bulbs were broken against the lower pair of the paddles and the spike, when the reaction was to be initiated, respectively. This system provides thorough flushing of the ampoule contents.

The constant voltage source (Ether Ltd, type AA100) provides a stable voltage supply to the calibration circuit which consists of a standard 10 ohm resistor (Croydon Precision Instruments Co., type RSI), a 100 ohm chip resistor (Tronac Inc., type R24) and an on-off switch, all in series. While the standard resistor allows the evaluation of the current flowing through the circuit by measuring the voltage, the 100 ohm resistor supplies energy to the

reaction chamber during the calibration run. A pair of leads were connected to either side of the resistor in order to allow for the measurement of the voltage while the current is on. The leads and the resistor were encased in a PTFE sleeve. The switch triggers a timer simultaneously as the circuit is switched on and off, thus allowing for the duration of the energy input into the reaction chamber in the calibration run to be measured. Thermistors, (110k ohm, Swift-Sasco Ltd, type YSI 44011), sealed in thin tapered glass tubes containing few drops of silicone oil for better thermal conductance were used as the temperature sensing devices.

The twin vessels were immersed in a well-stirred thermostatic bath kept at 25.0°C using a proportional counter. Temperature changes during the reaction and the calibration runs were detected by an a.c. bridge to which the thermistors have been connected. The net differential temperature displacements were automatically recorded by means of a potentiometric recorder connected to the a.c. bridge. The contents of the twin vessels were stirred for ca. 30 minutes prior to, and after, the initiation of the reaction. The two flasks were allowed to attain thermal equilibria with the surroundings overnight. All determinations were carried out at 25.0 ± 0.1°C. A full description of the construction and operation of these calorimeters is available elsewhere[120].

To perform calorimetric evaluations, the energy equivalence, Σ, of the reaction chamber and its contents was first determined in terms of the corrected temperature displacement measured, ΔT_c, and

the electric energy added during the calibration experiment according to the following formula:

$$\Sigma = \frac{v \times I \times t}{\Delta T_c \times 10^3} \text{ kJ } T^{-1}$$

where v and I are the voltage (in volts) and the current (in amperes), respectively, across the heater and t is the calibration time in seconds. Multiplication of the above expression by the corrected[121-123] temperature change during the reaction period ΔT_r, and subsequent division by the number of moles, n, of the appropriate reactant gives the molar enthalpy of the reaction, $\Delta_r H_m{}^o$, as the following equation illustrates:

$$\Delta_r H_m{}^o = \frac{\Sigma \times \Delta T_r}{n} = \frac{v \times I \times t \times \Delta T_r \times M}{\Delta T_c \times m \times 10^3} \text{ kJ mol}^{-1}$$

where M and m are the molecular weight and the mass of the selected reactant respectively.

VI-B-2. Tests reactions:-

The performance of the ampoule-mode calorimeter was checked periodically using the standard test method of neutralisation of tris (hydroxymethyl) amino methane with 0.1M HCl. That of the titration mode was checked using the $Ag^+/(Br^- + Cl^-)$ reaction. Results together with the accepted values[108,111,112] are given in Tables VI-1 and VI-2.

As Fig. VI-2 illustrates, the thermo-titrimetry of the silver ion into an aqueous solution containing bromide and chloride ions displays two inflection points at $Ag^+ : x^-$ molar ratios of 1:1 and 1:1 suggesting two sequential reactions. This is confirmed by calibration of the ordinate axis in terms of energy, showing that AgBr and then AgCl were quantitatively and sequentially precipitated:

$$Ag^+ + (Br^- + Cl^-) = AgBr(c) + Cl^- \quad (1)$$

$$Ag^+ + Cl^- = AgCl(c) \quad (2)$$

This validates the calorimetric system, and discounts an earlier report[107] suggesting the formation of a solid solution of the bromide and chloride of silver when silver nitrate is added to a mixed halide solution.

VI-B-3. Reagents:-

Analar grade $AgNO_3$ and $Na_2S_2O_3.5H_2O$ compounds (of purity>99.5%) were used without further purification. Solutions of known compositions were prepared by direct weighing of definite masses into the proper volumes of de-aerated deionised distilled water. An anhydrous $Na_2S_2O_3$ sample was obtained by alcoholic precipitation from a concentrated thiosulphate pentahydrate solution and then dehydrating to constant mass at 140°C for 30 hours. Its crystal composition was iodometrically assessed prior to, and after, the calorimetric measurements in which it was involved. Because of the

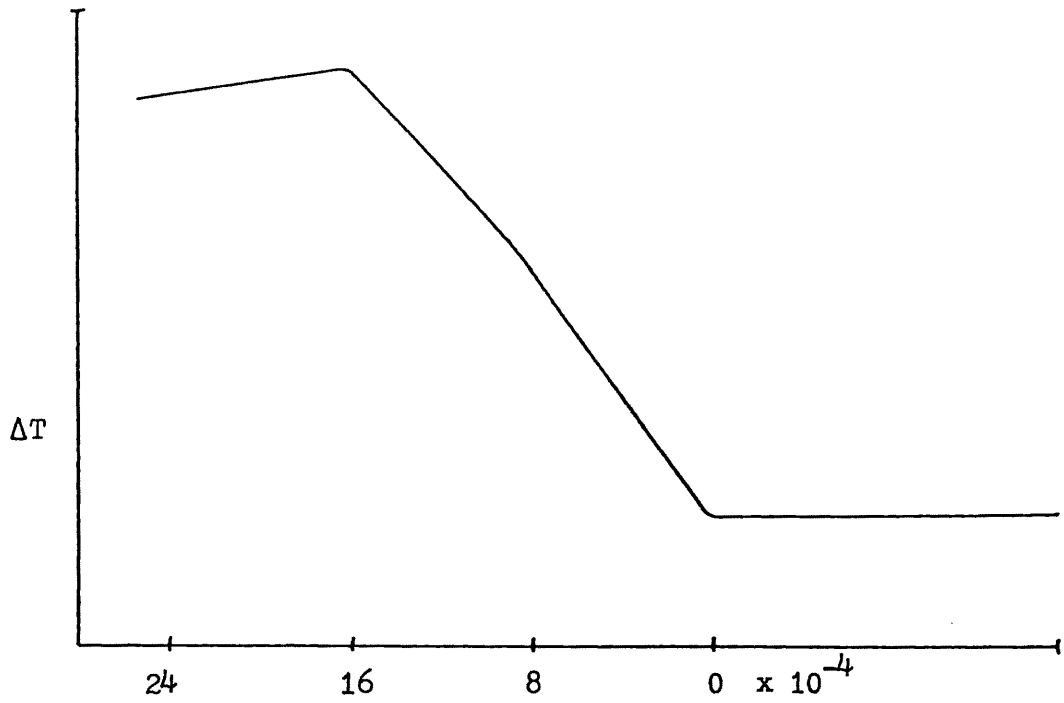

No. of moles of Ag^+ added to 2 x 8 x 10^{-4} moles of (Br^- + Cl^-)

Fig. VI-2. Thermometric titration of $Ag^+/(Br^- + Cl^-)$

efflorescent nature of the $Na_2S_2O_3 \cdot 5H_2O$ crystal, its composition was analysed also. The results are contained in Table IV-3.

Fresh AgCl, AgBr and AgI crystals were metathetically precipitated by adding solutions of appropriate, high grade sodium halides to silver nitrate. The AgX crystals were then washed repeatedly with de-ionised distilled water and dried by heating at 120°C for 24 hours to constant mass. Special precautions were taken to prevent exposure to light while precipitating, drying and weighing into the ampoules.

VI-C. Solubility measurements:-

A known mass of analar grade $Na_2S_2O_6 \cdot 2H_2O$ crystals was weighed into a glass bulb and a solution of known composition was then prepared by adding a definite volume of de-ionised distilled water from a microburette. The bulb with its contents was gently heated in a hot water bath to effect dissolution, and while being clamped inside a transparent enclosure to exclude draughts was then allowed to cool. A calibrated mercury thermometer graduated into 0.1°C and passing through the lid of the bulb was used to monitor the temperature at which crystallisation commences. The re-appearance of the crystals and the corresponding temperature mark the saturation point. A known volume of deionised water was added each time, and each individual measurement was repeated until concordant results ($\pm$ 0.1°C) were obtained. In order to achieve uniform distribution of heat, the solution was thoroughly stirred throughout the whole operation.

Table VI-1. The enthalpy of neutralisation of Tris[a] with 0.10M HCl

m(Tris) / g	$\Delta_r H_m^\circ$ / kJ mol^{-1}	$\Delta_r H_m^\circ$ (mean) / kJ mol^{-1}	$\Delta_r H_m$ (lit.[111]) / kJ mol^{-1}
0.06950	-29.83	-29.89±0.11	-29.862±0.028
0.07354	-29.89		
0.09526	-30.04		
0.10180	-29.84		
0.12114	-29.75		
0.16242	-29.96		

[a] Tris = tris (hydroxy methyl) aminomethane = $(HOCH_2)_3\ CNH_2$.

Its molar mass was taken to be 121.14 g mol^{-1}.

Table VI-2. Thermo-titrimetric investigations of the $Ag^+/(Br^- + Cl^-)$ reactions

$C(AgNO_3)$ / M	$V(AgNO_3)$ / $cm^3 min^{-1}$	C(KX) / M	V(KX) / cm^3	t_{r1} / min	$\Delta_{r1}H_m^\circ$ / kJ mol^{-1}	$\Delta_{r1}H_m^\circ$ (mean) / kJ mol^{-1}	$\Delta_f H_m^\circ$ (AgBr) / kJ mol^{-1}	$\Delta_f H_m^\circ$ (AgBr.lit.[100]) / kJ mol^{-1}
1.00	0.33	0.003	200.00	1.8	-84.62	-84.41±0.18	-100.16±0.63	-100.37±0.75
		0.003		1.8	-84.57			
		0.003		1.8	-84.14			
		0.004		2.4	-84.58			
		0.004		2.4	-84.21			
		0.004		2.4	-84.46			
		0.004		2.4	-84.30			

$C(AgNO_3)$ / M	$V(AgNO_3)$ / $cm^3 min^{-1}$	C(KX) / M	V(KX) / cm^3	t_{r2} / min	$\Delta_{r2}H_m^\circ$ / kJ mol^{-1}	$\Delta_{r2}H_m^\circ$ (mean) / kJ mol^{-1}	$\Delta_f H_m^\circ$ (AgCl) / kJ mol^{-1}	$\Delta_f H_m^\circ$ (AgCl.lit.[112]) / kJ mol^{-1}
1.00	0.33	0.003	200.00	1.8	-65.73	-65.50±0.20	-126.78±0.63	-127.070±0.085
		0.003		1.8	-65.28			
		0.003		1.8	-65.76			
		0.004		2.4	-65.33			
		0.004		2.4	-65.50			
		0.004		2.4	-65.24			
		0.004		2.4	-65.63			

$r_1 = Ag^+ + (Br^- + Cl^-) = AgBr(c) + Cl^-$, $r_2 = Ag^+ + Cl^- = AgCl(c)$.

Table VI-3. Iodometric* investigations of the $Na_2S_2O_3$ and $Na_2S_2O_3 \cdot 5H_2O$ crystal compositions

$m(Na_2S_2O_3)$ / g	$C(Na_2S_2O_3)$ / M	$m(Na_2S_2O_3 \cdot 5H_2O)$ / g	$C(Na_2S_2O_3)$ / M	$m(KIO_3)$ / g	$C(KIO_3)$ / M	$m(KI)$ / g	$C(KI)$ / M	$C(KI)/C(KIO_3)$	$V(2M\ H_2SO_4)$ / cm^3
15.8214	1.00			0.5356	0.025	2.1594	0.13	5.20	7.60
15.8301	1.00								
		24.8237	1.00						
		24.8289	1.00						

$C(H^+)$ / M	$C(H^+)/C(KIO_3)$	$C(I_2)$ / M	$V^*(I_2)$ / cm^3	$V_1(Na_2S_2O_3)$ / cm^3	$V_2(Na_2S_2O_3)$ / cm^3	$V_1/V_2 \times 10^2\%$	Water content / Moles
0.152	6.08	0.075	25.00	3.73	3.75	99.47	≃0
				3.73	3.75	99.47	≃0
				3.72	3.75	99.20	≃5
				3.73	3.75	99.47	≃5

* $IO_3^- + 5I^- + 6H = 3I_2 + 3H_2O$, $I_2 + 2S_2O_3^{2-} = S_4O_6^{2-} + 2I^-$,

v^* = volumes of the aliquots titrated,

v_1 = practical determinations,

v_2 = calculated values.

References (chapters II,III,IV,V and VI):-

1. Martinez, S., Garcia, S.B. and Rivoir, L., Acta Cryst., 9, 145, (1956).

2. Kirfel, A., Will, G. and Weiss, A., Acta Cryst., 36B, 223 (1980).

3. Stanley, E., Acta Cryst., 9, 897 (1956).

4. Liminga, R., Abrahams, S.C. and Bernstein, J.L., Chem. Phys., 73, 1432 (1980).

5. Duval, C. and Lecomte, J., Comp. Rend., 217, 42 (1943).

6. Gerding, H. and Eriks, K., Rec. Trav. Chim., 69, 724 (1950).

7. Palmer, W.G., J. Chem. Soc., 1552 (1961).

8. Buijs, K., J. Chem. Phys., 36, 861 (1962).

9. Dawson, P., Hargreave, M.M. and Wilkinson, G.R., Spectrochim. Acta, 31A, 1533 (1975).

10. Beattie, I.R., Gall, M.J. and Ozin, G.A., J. Chem. soc., 1001A (1969).

11. Loewenschuss, A. and Marcus, Y., Chem. Rev., 84(2), 89 (1984).

12. Zachariasen, W.H.,Phys. Rev., 40, 923 (1932).

13. Lindqvist, I. and Mortsell, M., Acta Cryst., 10, 406 (1957).

14. Baggio, S., Acta Cryst., 27B, 517 (1971).

15. Magnusson, A., Johansson, L.G. and Lindqvist, O., Acta Cryst., 39C, 819 (1983).

16. Simon, A., Waldmann, K. and Steger, E., Z. Anorg. Allgem. Chem., 288, 131 (1956).

17. Rocchiciolli, C., Comp. Rend., 250, 2347 (1960).

18. Buijs, K., J. Inorg. Nuc. Chem;, 24A, 229 (1962).

19. Herlinger, A.W. and Long, T.V., Inorg. Chem., 8, 1661 (1969).

20. Meyer, B., Peter, L. and Shaskey, C.R., Spoectrochim. Acta, 35A, 345 (1979).

21. David, S.J. and Ault, B.S., Inorg. Chem., 23, 1211 (1984).

22. Peter, L. and Meyer, B., Inorg. Chem., 24, 3071 (1985).

23. Brosche, F. and Schultz, N., Z., Physic. Chem., 110, 435 (1924).

24. Fadda, P., Nuovo Cim., 9, 227 (1932).

25. Simon, A. and Schmidt, W., Z. Elektrochem., 64, 737 (1960).

26. Golding, R.M., J. Chem. Soc., 3711 (1960).

27. Johansson, L.G., Lindqvist, O. and Vannerberg, N.G.,, Acta Cryst., 36B, 2523 (1980).

28. Zachariasen, W.H. and Buckley, H.E., Phys. Rev., 37, 1295 (1931).

29. Evans, J.C. and Bernstein, H.J., Can. J. Chem., 33, 1270 (1955).

30. Verma, V.P., Thermochimica Acta, 89, 363 (1985).

31. Zachariasen, W.H., Krist. Z., 82, 161 (1932).

32. Walrafen, G.E. and Dood, D.M., Trans. Far. Soc., 57, 1286 (1961).

33. Baran, E.J. and Aymonino, P.J.W., Spectrochim. Acta, 24A , 288 (1968).

34. Walrafen, G.E., Chem. Phys., 39, 1479 (1963).

35. Walrafen, G.E., Irish, D.E. and Young, T.F., J. Chem. Phys., 37, 662 (1962).

36. Cross, P.C. and Brockway, L.O., J. Chem. Phys., 3, 821 (1935).

37. Schomaker, V. and Stevenson, D.P., J. Am. Chem. Soc., 62(1), 1270 (1940).

38. Crable, G.F. and Smith, W.V., J. Chem. Phys., 19, 502 (1951).

39. Sirvetz, M.H., J. Chem. Phys., 19, 938 (1951).

40. Shelton, R.D., Nielsen, A.H. and Fletcher, W.H., J. Chem. Phys., 21, 2178 (1953).

41. Post, B., Schwartz, R.S. and Frankuchen, I., Acta Cryst., 5, 372 (1952).

42. Giguere, P.A. and Falk, M., Can. J. Chem., 34(2), 1833 (1956).

43. Anderson, A. and Savoie, R., Can. J. Chem., 43(2), 2271 (1965).

44. Barbe, A., Delahaigue, A. and Jouve, P., Spectrochim. Acta, 27A, 1439 (1971).

45. Anderson, A. and Campbell, M.C.W., J. Chem. Phys., 67(3), 4300 (1977).

46. Brooker, M.H. and Eysel, H.H., J. Raman Spectrosc., 11, 322 (1981).

47. Nord, L., J. Molec. Struct., 96, 19 (1982).

48. Brooker, M.H. and Eysel, H.H., J. Phys. Chem., 88, 6201 (1984).

49. Brooker, M.H., J. Molec. Struct., 112, 221 (1984).

50. Hayashi, S., Oobatake, M., Ooi, T. and Machida, K., Bull. Chem. Soc. Jpn, 58, 1105 (1985).

51. Taylor, P.G. and Beevers, C.A., Acta Cryst., 5, 341 (1952).

52. Sandor, E. and Csordas, L., Acta Cryst., 14, 237 (1961).

53. Siebert, H., Z. Anorg. Allgem. Chem., 275, 225 (1954).

54. Freedman, A.N. and Straughan, B.P., Spectrochim. Acta, 27A, 1455 (1971).

55. Baines, H., J. Chem. Soc., 2763 (1929).

56. Bassette. H. and Lemon, J. T., J. Chem. Soc., 1423 (1933).

57. Baines, H., J. Phot. Sci., 3, 175 (1955).

58. Chateau, H. and Pouradier, J., Sci. Ind., Phot., 24, 129 (1953).

59. Gaur, J.N. and Bhadraver, M.S., J. Ind. Chem. soc., 36(2), 108 (1959).

60. Bhadraver, M.S., Bull. Chem. Soc. Jpn, 35, 1939 (1962).

61. El-Hinnawi, M.A., Peter, L. and Meyer, B., J. Raman Spectrosc., 16(4), 272 (1985).

62. Foss, O., Furberg, S. and Zachariasen, W.H., Acta Chem. Scand., 8,459 (1954).

63. Foss, O. and Hordvik, A., Acta Chem. Scand., 12,1700 (1958).

64. Lecomte, J., Duval, C. and Franck, R., Comp. Rend., 257,326 (1963).

65. Meyer, B., Ospina, M. and Peter, L.B., Anal. Chim. Acta, 117, 301 (1980).

66. Dunitz, J.D., Acta. Cryst., 9, 579 (1956).

67. Duval, C. and Lecomte, J., Bull. Soc. Chim. France, 11, 376 (1944).

68. Takahashi, H., Kaneko, N. and Miwa, K., Spectrochim. Acta, 38A, 1147 (1982).

69. Simon, A. and Kuchler, H., Z. Anorg. Allgem. Chem., 260, 161 (1949).

70. Peter, L. and Meyer, B.J. Molec. Struct., 95, 131 (1982).

71. Adams, W.A., Gardner, C.L. and Fouchard, D.T., Conf. Int. Raman spectrosc., 7th, 202 (1980).

72. Connick, R.E., Tam, T.M. and Deuster, E.V., Inorg. Chem., 21, 103 (1982).

73. Littlejohn, D. and Chang, S.G., Environ. Sci. Tech., 18, 305 (1984).

74. Lecki, A.H., Trans. Far. Soc., 32, 1700 (1936).

75. Walrafen, G.E., J. Chem. Phys., 36,90 (1962).

76. Hidy, G.M., Hansen, D.A., Henry, R.C., Ganesan, K. and Collins,J., J. Air Pollu. Contr. Assoc., 34(4), 333 (1984).

77. Simon, A. and Waldmann, K., Z. Anorg. Allgem. Chem., 283, 359 (1956).

78. Gerding, H. and Nijveld, W.J., Nature, 137, 1070 (1936).

79. Rao, B.P., Proc. Ind. Acad. Sci., 20A, 292 (1944).

80. Jones, L.H. and McLaren, E., J. Chem. Phys., 28, 995 (1958).

81. Falk, M. and Giguere, P.A., Can. J. Chem., 36, 1121 (1958).

82. Rhec, J.S. and Dasgupta, P.K., J. Phys. Chem., 89, 1799 (1985).

83. Lyons, D. and Nickless, G., Inorg. Sulphur Chem., Nichless, G. ed., Elsevier, Amsterdam (1968).

84. Rinker, R.G., Lynn, S., Mason, D.M. and Corcoran, W.H., Ind. Eng. Chem. Fund., 4, 282 (1965).

85. Rinker, R.G., Gordon, T.P., Mason, D.M., Sakaida, R.R. and Corcoran, W.H., J. Phys. Chem., 64, 573 (1960).

86. Rinker, R.G., Gordon, T.P., Mason, D.M. and Corcoran, W.H., J. Phys. Chem., 63, 302 (1959).

87. Rinker, R.G. and Lynn, S.,J. Phys. Chem., 72, 4706 (1968).

88. Morello, J.A., Craw, M.R., Constantine, H.P. and Forster, R.E., J. Appl. physio., 19(3), 522 (1964).

89. Creutz, C. and Sutin, N., Inorg. Chem., 13, 2041 (1974).

90. Kawagoe, M. and Robinson, C.W., Can. J. Chem. Eng., 59(4), 471 (1981).

91. Singh. D.K., Sharma, R.N. and Srivastave, R.D., ALCHE J., 24(2), 232 (1978).

92. Watt, G.D. and Burns, A., Biochem. J., 152, 33 (1975).

93. Forlani, L., Ioppolo, C., Antonini, E., Martin, C.J. and Marini, M.A., J. Inorg. Chem., 20(2), 147 (1984).

94. Bourne, D.W.A., Higuchi, T. and Pitman, I.H., J. Pharm. Sci., 63, 865 (1974).

95. Lem, W.J. and Wayman, M., Can. J. Chem., 48(3), 2778 (1970).

96. Cermak, V. and Smutek, M., Collect. Czech. Chem. Commun., 40(11), 3241 (1975).

97. Smutek, M. and Cermak. V., Collect. Czech. Chem. Commun., 40(11), 3265 (1975).

98. Lem, W.J. and Wayman, M., Can. J. Chem., 48(1), 776 (1970).

99. Wayman, M. and Lem. W.J., Can. J. Chem., 48(1), 782 (1970).

100. Bichowsky, F.R., J. Am. Chem. Soc., 45, 2225 (1923).

101. Zimmermann, H.W. and Latimer, W.M., J. Am. Chem. Soc., 61, 1554 (1939).

102. Wagman, D.D., Evans, W.H., Parker, V.B., Halow, I., Bailey, S.M. and Schumm, R.H., "Selected Values of Chemical Thermodynamic Properties", NBS Technical Note 270-3, U.S. Dept. of Commerce, Washington DC (1968).

103. Rossini, F.D., Wagman, D.D., Evans, W.H., Levine, S. and Jaffe, I., "Selected Values of Chemical Thermodynamic Properties", NBS Circular 500, U.S. Dept. of Commerce, Washington DC (1952).

104. Gronvold, F. and Meisingset, K.K., J. Chem. Thermody., 1083 (1982).

105. Revision to Ref. 102 in Appendix of NBS Technical Note 270-8 (1981).

106. Murray, R.C. Jr. and Cubicciotti, D., J. Electrochem. Soc., 130(4), 866 (1983).

107. Eastman. E.D. and Milner, R.T., J. Chem. Phys., 1, 444 (1933).

108. Wagman, D.D., Evans, W.H., Parker, V.B., Halow, I., Bailey, S.M. and Schumm, R.H., "Selected Values of Chemical Thermodynamic Properties", NBS Technical Note 270-4, U.S. Dept. of Commerce, Washington DC (1969).

109. De Marco, D., Bellomo, A. and Roberts, A.D., J. Inorg. Nuc. Chem., 42, 599 (1980).

110. De Marco, D., Mauceri, G., Casale, A. and Marchese, A., Annali Di Chimica (Rome), 75 (9-10), 415 (1985).

111. Vanderzee, C.E., Waugh, D.H. and Hass, N.C., J. Chem. Thermody., 13, 1 (1981).

112. CODATA Recommended Key Values for Thermodynamics, 1975, CODATA Bulletin, 17 (1976).

113. Perrott, C.M. and Fletcher, N.H., J. Chem. Phys., 50, 2344 (1969).

114. Ghosh, B.P. and Nag, K., J. Thermal Analysis, 29(3), 433 (1984).

115. Perrott, C.M. and Fletcher, N.H., J. Chem. Phys., 48, 2143 (1968).

116. Quaranta, N.E. and Bazan, J.C., Solid State Ionics, 11(1), 71 (1983).

117. Johnson, G.K., J. Chem. Thermody., 9, 835 (1977).

118. CODATA Tentative Set of Key Values for Thermodynamics. Part VIII. Special Report. Paris. April (1980).

119. Williamson, A.T., Trans. Far. Soc., 40, 421 (1944).

120. Peake, S.J., Ph.D. Thesis, University of London (1976).

121. Wadso, I., Sci. Tools, 13(3), 33 (1966).

122. Gunn, S.R., J. Chem. Thermody., 3, 19 (1971).

123. Vanderzee, C.E., J. Chem. Thermody., 13, 1139 (1981).